Spectrum Sensing for Cognitive Radio

by

CAPTAIN KAMAL MANHARLAL
201321003

A Thesis Submitted in Partial Fulfilment of the Requirements for the Degree of

DOCTOR OF PHILOSOPHY
to

DHIRUBHAI AMBANI INSTITUTE OF INFORMATION AND COMMUNICATION TECHNOLOGY

January, 2019

Declaration

I hereby declare that

i) the thesis comprises of my original work towards the degree of Doctor of Philosophy at Dhirubhai Ambani Institute of Information and Communication Technology and has not been submitted elsewhere for a degree,

ii) due acknowledgment has been made in the text to all the reference material used.

Captain Kamal Manharlal

Certificate

This is to certify that the thesis work entitled SPECTRUM SENSING FOR COGNITIVE RADIO has been carried out by CAPTAIN KAMAL MANHARLAL for the degree of Doctor of Philosophy at *Dhirubhai Ambani Institute of Information and Communication Technology* under my supervision.

Prof. Manjunath V. Joshi
Thesis Supervisor

Acknowledgments

First and above all, I praise God, the almighty for providing me this opportunity and granting me the capability to proceed successfully. Although the work described here was performed independently, I never would have been able to complete it if not for the support of many wonderful people. I would like to offer my sincere thanks to them.

I would like begin by expressing my sincere gratitude to my supervisor Prof. Manjunath V. Joshi, with whom I have learned immensely and has had a strong influence in my development as a researcher. He has constantly encouraged me to ensure that I remain focused on achieving my goal. I am grateful to him for patiently supervising and directing my work, fruitful discussions, providing learning opportunities on a number of occasions, and helping me throughout all the different steps of my doctoral research endeavor for the past few years. Prof. Joshi's achievements, his work ethics, and his keen eye for every important detail have been an inspiration throughout all the years I have worked with him.

On a broader note, I wish to acknowledge all the professors of DA-IICT who have inspired me directly or indirectly. I would like to thank faculty members Prof. Hemant Patil and Prof. Deepak Ghodgaonkar who have shaped my thinking about this research direction during the thesis work. I express my gratitude to Prof. K. S. Dasgupta (Director), Mr. Soman Nair (Registrar), Prof. Sanjeev Gupta (former Dean-R&D), Prof. Laxminarayana Pillutla (Convener-ICT), Prof. Aditya Tatu (former Ph.D. Coordinator) and Prof. V. Sunitha (M.Tech. Coordinator) who have helped me throughout my time at DA-IICT. I would like to thank the administrative and technical staff members, Mr. Ramesh Prajapati, Mr. Rajendra Shah and help-desk of DA-IICT who have been kind enough to advise and

help me in their respective roles. My gratitude also extends to staff of DA-IICT resource-center.

I made a lot of new friends at DA-IICT, who helped me in many steps of my study. I thank all of them for everything that they did for me. I thankful to Krishna Gopal, Rishikant and Jignesh for helping me with the mathematical derivations. Thanks to Pramod (Eurecom, France), Tanvina (Cogknit Semantics, Bangalore), Zaki (IISc Bangalore), Avni (IISc Bangalore), other PhD students at DA-IICT Sumukh, Parth, Nirmesh, Hardik, Prashant, Madhu, Nupur and Vandana for their kind cooperation. I am also thankful to all my friends from SVNIT, MGITER and BM&BFWHS for their constant support and encouragement.

I am deeply thankful to my entire family for their love and support. Words can not express how grateful I am to my mother, father, brother, sister in law and my wife for all of the sacrifices that you have made on my behalf. Your prayer for me was what sustained me thus far. I acknowledge my entire family for providing me healthy educated atmosphere in our family.

Contents

Abstract

Due to the rapid growth of new wireless communication services and applications, need for radio frequency (RF) spectrum is continuously increasing. Most of the available RF spectrum is already been licensed to the existing wireless systems. On the other hand, it is found that spectrum is significantly underutilized due to the static frequency allocation to the dedicated users and hence the spectrum holes or spectrum opportunities arise. Considering the scarce RF spectrum, supporting new services and applications is a challenging task that requires innovative technologies capable of providing new ways of exploiting the available radio spectrum. Cognitive Radio (CR) has received immense research attention, both in the academia and industry, as it is considered a promising solution to the problem of spectrum scarcity by introducing the notion of opportunistic spectrum usage. A CR is a device that senses the spectrum of licensed users (also known as primary users) for spectrum opportunities, and transmits its data only when the spectrum is sensed to be not occupied. For the efficient utilization of the spectrum while limiting the interference to the licensed users, the CR should be able to sense the spectrum occupancy quickly as well as accurately. This makes spectrum sensing one of the main functionalities of the cognitive radio. Spectrum sensing is a hypothesis testing problem, where the goal is to test whether the primary user is inactive (the null or noise only hypothesis), or not (the alternate or signal present hypothesis). Spectrum sensing can be broadly classified into two types, namely, narrowband and wideband sensing. Narrowband sensing is used for finding the occupancy status of a single licensed band where as wideband sensing deals with the scenario where multiple licensed bands are sensed for spectrum opportunities.

In this thesis, our focus is on the analysis of the existing spectrum sensing algorithm considering practical scenarios and propose novel techniques for spectrum sensing. Energy detection (ED) also known as conventional energy detection (CED) based spectrum sensing is a very popular technique due to its simplicity and reduced computational complexity. In our first work, we analyze the ED based narrowband spectrum sensing over $\eta - \lambda - \mu$ fading channel model. It is a general model and includes other fading models as its special cases and can be used to study the performance of ED under practical scenarios. The performance improvement is shown using antenna diversity and cooperative sensing. The analysis is then extended to the case when there exists shadowing in addition to fading.

ED is generalized by changing the squaring operation while computing energy by an arbitrary positive number p which is known as generalized energy detector (GED). To decide the threshold for GED, the true value of the noise variance is required but in practice only its expected value is known. The true value of noise variance varies over time and location giving rise to noise uncertainty. Due to this there exist a phenomenon known as signal to noise radio (SNR) wall which says that in the presence of noise uncertainty below certain SNR value known as the SNR wall, it is not possible to detect the presence of signal even if very large number of samples are taken for detection. In our second work, we study the SNR wall for GED considering no diversity, diversity and cooperative sensing scenarios under noise uncertainty and fading. All the derived expressions are validated using Monte Carlo simulations.

In literature, the use of antenna diversity to improve the detection performance of narrowband spectrum sensing is extensively studied. In our next work, we propose new detection algorithms that make use of square law combining (SLC) and square law selection (SLS) diversities for wideband spectrum sensing. We provide complete theoretical analysis of the proposed algorithms and validate them using Monte Carlo simulations. The performance improvement is shown against the algorithm that do not use diversity. We also study the effects of different parameters on the performance of the proposed algorithms.

An alternative to antenna diversity is the cooperative spectrum sensing where multiple secondary users also known as cooperating secondary users collaborate by sharing their sensing information for the detection of the spectrum opportunities. Finally, in our last work, we propose novel detection algorithm for cooperative wideband spectrum sensing. We make use of hard combining for data fusion since it minimizes the bandwidth requirements of the control channel. We show that the proposed algorithm performs better than algorithm without cooperative sensing. Also, it performs better than our previously proposed algorithms that use antenna diversity by choosing appropriate number of cooperating secondary users. We also study the effects of different parameters on the performance.

Keywords:

Cognitive radio, spectrum sensing, narrowband spectrum sensing, wideband spectrum sensing, energy detection, generalized energy detection, noise uncertainty, SNR wall, diversity, cooperative wideband spectrum sensing, hard combining.

List of Tables

List of Figures

CHAPTER 1

Introduction

Wireless communication systems utilize the radio frequency (RF) spectrum as their propagation environment. The need for RF spectrum is increasing due to the rapid growth in users, applications and bandwidth of modern wireless communication systems. Most of the available RF spectrum has already been allocated to the existing wireless systems. However, only a small part of it can be licensed to new wireless applications. A study by the Spectrum Policy Task Force (SPTF) of the Federal Communications Commission (FCC) has showed that the RF spectrum is significantly underutilized due to the static spectrum allocation and dedicated access through licensing resulting in the wastage of the resources [41, 42]. Spectrum holes or spectrum opportunities arise due to the current static spectrum licensing scheme. Spectrum holes are defined as frequency bands which are allocated to the licensed users but are not utilized in some locations at some times and therefore can be used by the unlicensed users or cognitive users or secondary users (SUs) [56]. Cognitive Radio (CR) is a new paradigm of designing wireless communications systems which aims to maximize the utilization of the underutilized RF spectrum. The term cognitive radio was first introduced by Joseph Mitola III in his papers in 1999 [81, 82, 83]. Simon Haykin in [56] defines the cognitive radio, built on the the software defined radio, as an intelligent wireless communication system that is aware of its environment and uses the methodology of understanding-by-building to learn from the environment and adapt to statistical variations in the input stimuli, with two primary objectives in mind: (1) highly reliable communication whenever and wherever needed and (2) efficient utilization of radio spectrum. CR users, i.e., secondary users (SUs), are allowed to

access the licensed spectrum bands of primary users (PUs), i.e., licensed users, as long as they do not cause unacceptable interference to the PUs. CR is a promising solution to the continuously increasing RF spectrum demands and the spectrum scarcity caused by the fixed frequency allocations [41, 42]. This resulted in CR technology gaining increased attention and has been highlighted by both standards and regulatory bodies [31, 43, 95]. The main functions of cognitive radio to support intelligent and efficient dynamic spectrum access are as follows:

- Spectrum sensing: The goal of the spectrum sensing is to determine the occupancy status of the primary users in the licensed bands by periodically sensing the target frequency bands. In other words, CR detects the spectrum opportunities or spectrum holes and also determines the method of accessing it without causing interference to the licensed primary user.

- Spectrum analysis: The unlicensed secondary users make use of information obtained from spectrum sensing to schedule and plan spectrum access. In spectrum analysis, information obtained from spectrum sensing is analyzed to gain knowledge about the spectrum hole, i.e., interference estimation, duration of availability and the probability of collision with a PU due to miss detection.

- Spectrum access: The spectrum holes are accessed by the secondary users once a decision is made on spectrum access based on spectrum analysis. Spectrum access is performed based a cognitive media access control (MAC) protocol, which aims to avoid interference to the primary users and also with other secondary users. The CR transmitter is also required to perform negotiation with the CR receiver to synchronize the transmission so that the effective communication can be achieved successfully.

- Spectrum mobility: It is the function related to the change of frequency band of CR users. When a PU starts transmitting in the licensed band which is currently utilized by the secondary user, the secondary user can change to a spectrum band which is idle. This change in operating frequency band is referred to as spectrum handoff.

One of the main functionalities of CR is the spectrum sensing [19, 57]. In this dissertation, our main focus is on spectrum sensing. This thesis presents the study of existing narrowband spectrum sensing techniques for practical scenarios and also presents novel detection algorithms for wideband spectrum sensing to improve the detection performance. One of our approaches also uses cooperative spectrum sensing for wideband spectrum sensing. In what fallows, we provide quick introduction to the spectrum sensing where we discuss narrowband, wideband and cooperative spectrum sensing.

1.1 Spectrum Sensing

One of the crucial requirements of SU is to monitor the usage activity in the licensed spectrum to exploit underutilized spectrum (referred to as the spectrum opportunity or spectrum holes) without causing harmful interference to the PUs. Furthermore, PUs do not have any obligation to share and change their operating parameters for sharing spectrum with SUs. Hence, SU should be able to independently detect spectrum holes without any help from PUs; this ability is called spectrum sensing, which is considered as one of the critical components in cognitive radio networks [109]. Before utilizing the licensed spectrum, SUs need to identify whether the band is occupied by any PU. During the use of a particular licensed band, SUs need to continuously monitor whether any PU has become active in that band and if so, the SUs need to vacate that band. To achieve this, we need efficient spectrum sensing techniques that minimize interference to the PU and at the same time maximize the spectrum utilization. There are mainly two types of spectrum sensing, namely, narrowband and wideband sensing. Excellent survey on spectrum sensing can be found in [5]. In the following sections, we give brief introduction to both narrowband and wideband sensing.

1.1.1 Narrowband Spectrum Sensing

Narrowband spectrum sensing is used for finding the occupancy status of a single PU licensed band. The term narrowband implies that the bandwidth of the

signal is sufficiently small such that the channel frequency response can be considered flat. In other words, the bandwidth of our interest is smaller than the coherence bandwidth that represents the maximum bandwidth over which the channel response is flat. We now give a brief explanation on some of the narrowband spectrum sensing techniques. The detailed survey on narrowband spectrum sensing can be found in [74, 131].

Match Filter Detection

The matched filter (MF) [19, 62] based spectrum sensing is on optimal detection scheme since it maximizes the signal to noise ratio (SNR) in the presence of additive noise. This is a coherent detection technique in which the received signal is correlated with the template for detecting the presence of the known signal in the received signal. Here, the CR requires the prior knowledge about PUs. Also, it is required that CRs to be equipped with carrier synchronization and timing devices, leading to increased implementation complexity.

Cyclostationary Detection

Man-made signals are generally nonstationary. Some of them are cyclostationary, i.e., their statistics exhibit periodicity, which may be caused by modulation and coding or even be intentionally produced to aid channel estimation and synchronization or intentionally induced to assist spectrum sensing [76, 114, 115]. In cyclostationary detection [26, 27, 46, 63, 70, 98], such periodicity is utilized for detection of random signal with a particular modulation type in a background of noise and other modulated signals. This detection scheme is capable of differentiating the primary signal from the interference and noise. However, this scheme requires partial prior information about the primary signal and its computational cost is relatively high.

Covariance-Based Detection

The primary signal received at the SU is usually correlated due to the dispersive channel, use of multiple antennas, or even over sampling. Hence, the covariance

of the received signal when PU is transmitting is different from when it is not transmitting. This property is used to differentiate the case where the PU signal is present from the the case where it is absent [134, 136].

Eigenvalue Based Detection

In eigenvalue based detection [135, 137, 138], eigenvalues of the covariance matrix received at the secondary user are utilized for signal detection. Detection schemes based on covariance matrix and eigenvalues represent blind detection schemes and they do not require any information about the PU signal. These schemes performance better when the signals to be detected are highly correlated.

Energy Detection

Energy detection (ED) [37, 38, 65, 123] is a non-coherent detection method that do not require any prior knowledge about the PUs. The computational complexity of ED based spectrum sensing is relatively low. However, ED performs poor under low SNR scenario and when noise uncertainty is considered. Due to its simplicity and reduced computational complexity, ED represents a very popular spectrum sensing technique even though other techniques may exhibit better performance. Considering the advantages of ED, we adopt it for our study in this thesis and propose different algorithms based on the same.

1.1.2 Wideband Spectrum Sensing

In wideband spectrum sensing, multiple spectrum bands are sensed for spectrum opportunities. Ultimately, our aim is to sense a frequency bandwidth that exceeds the coherence bandwidth of a channel. To do this, one should note that narrowband sensing techniques cannot be directly used for wideband case. This is because these techniques make single binary decision for the whole spectrum and thus cannot identify individual spectrum holes that lie within the wide frequency spectrum. The wideband spectrum sensing can be broadly classified into two classes, i.e., Nyquist and sub-Nyquist wideband sensing. Detailed survey on wideband spectrum sensing can be found in [109].

Nyquist Wideband Spectrum Sensing

In Nyquist wideband spectrum sensing [40, 96, 97, 112, 117], we directly acquire the wideband signal using a standard analog to digital converter which samples the wideband signal at the Nyquist sampling rate. We then use signal processing techniques to detect the spectrum opportunities. The sampling rate required in this case is very high and hence practically unaffordable. Due to this reason, sensing the wideband at Nyquist rate poses significant challenge in terms of building the necessary hardware that operates at a sufficiently high sampling rate and in designing high speed signal processing algorithms.

Sub-Nyquist Wideband Spectrum Sensing

The problem of high sampling rate or high implementation complexity in Nyquist wideband spectrum sensing can be solved by using sub-Nyquist wideband spectrum sensing. In this type of sampling, we acquire the wideband signal at the sampling rates which are lower than the Nyquist rate and detect the spectrum opportunities using these partial measurements. There are mainly two types of sub-Nyquist wideband spectrum sensing which are compressive sensing based [51, 54, 118, 119, 121, 127] and multichannel sub-Nyquist wideband sensing [80, 108, 124].

1.1.3 Cooperative Spectrum Sensing

Spectrum sensing is an important functionality of CR to improve the spectrum utilization and at the same time limiting the harmful interference to the licensed users. However, the detection performance in practice is greatly affected by the effect of multipath fading and shadowing. To combat the effect of these issues, cooperative spectrum sensing (CSS) has been shown to be effective method to improve the detection performance by exploiting the spatial diversity. In CSS, multiple secondary users known as cooperating secondary users (CSUs) collaborate by sharing their information in order to detect the spectrum opportunities. The CSS can be used for both narrowband and wideband sensing. The detailed survey

on cooperative spectrum sensing can be found in [3] where issues of cooperation methods, cooperative gain and the cooperation overhead are discussed.

1.2 Thesis contribution

Having provided brief introduction to spectrum sensing, we now summarize the important contributions of this thesis, the details of which are discussed in the subsequent chapters.

The energy detection (ED) based spectrum sensing [37, 38, 65, 123] is a popular spectrum sensing technique due to its simplicity. However, the performance of ED degrades under low SNR, noise uncertainty, multipath fading and shadowing. Hence, it is necessary to study the performance of ED under different scenarios. The performance of ED for narrowband spectrum sensing is studied under different fading channels [11, 12, 37, 38, 102]. In our first work, we give the performance of ED under general fading model which includes other existing fading models as the special cases. We also show performance improvement using diversity and cooperative detection. This analysis is then extended to the case when there exists shadowing in addition to fading.

The ED is generalized by changing the squaring operation while computing energy by an arbitrary positive power p which is known as the generalized energy detector (GED). In our next work, we study SNR wall for GED considering narrowband spectrum sensing under no diversity, diversity and cooperative spectrum sensing in the presence of noise uncertainty and fading. First, the SNR wall expressions are obtained considering AWGN channel and the conclusions are drawn based on them. The effects of diversity on the SNR walls are discussed. The analysis is then extended to channel with Nakagami fading where the SNR walls are obtained numerically. The effect of fading on SNR wall is discussed. All the obtained for SNR walls are validated using Monte Carlo simulations.

In literature, the use of diversity for performance improvement is mostly limited to narrowband spectrum sensing. To this end, we propose the use of diversity for wideband spectrum sensing in our next work. We make use of square

law combining (SLC) and square law selection (SLS) diversity schemes in our proposed algorithms. The performance improvement is shown against the existing algorithm. Also in existing literature, the theoretical analysis for wideband spectrum sensing is limited to no fading. In our work, we give theoretical analysis considering Nakagami fading channel and also validate it using Monte Carlo simulations. The effects of different parameters on the performance of the proposed algorithms are also discussed.

Finally, in our last work, we propose novel detection algorithm for cooperative wideband spectrum sensing that make use of hard combining. We use hard combining because it incurs reduced cooperation overhead. We provide complete theoretical analysis of the proposed algorithm and validate it using Monte Carlo simulation. We show that the proposed algorithm outperforms the existing algorithm used without cooperation. Also, it performs better than our previously proposed algorithms that make use of diversity by choosing appropriate number of cooperating secondary users.

To summarize, in this thesis, we have addressed the problem of narrowband as well as wideband spectrum sensing. This includes our following works:

- Performance of energy detection (ED) based spectrum sensing for narrowband over $\eta - \lambda - \mu$ fading channel,
- Performance of generalized energy detector (GED) under diversity and cooperation by considering noise uncertainty and fading,
- Use of diversity for wideband spectrum sensing under fading,
- Detection algorithm for cooperative wideband spectrum sensing.

1.3 Thesis organization

The contents of this thesis are organized as follows. The literature review is presented in chapter 2. As already discussed, the performance of energy detector degrades under low SNR, fading and shadowing and hence it is important to study its performance under different fading scenarios. We analyze the performance of

energy detection based narrowband spectrum sensing for under $\eta - \lambda - \mu$ fading channel in chapter 3. It is a general fading model which includes other fading models as the special cases. Here, the expressions for average probability of false alarm and the average probability of detection are derived. We also show the performance improvement using diversity and collaborative detection. The analysis under only fading is then extended to the case when there exists shadowing in addition to fading.

Generally, it is assumed that the true noise variance is known. In practice, what is actually known is the expected value of the noise variance. The true value of the noise variance varies with time and location giving rise to what is known as noise uncertainty. The performance of GED is greatly affected by noise uncertainty and fading which gives rise to the phenomenon known as the SNR wall. In chapter 4, we analyze SNR wall for GED under diversity and cooperation in the presence of noise uncertainty and fading.

We next consider the case of wideband spectrum sensing. The use of diversity for performance improvement in narrowband spectrum sensing is well studied in the literature. We propose the use of diversity for wideband spectrum sensing in chapter 5. Two new detection algorithms are proposed and it is shown that the performance improves when compared to the no diversity case. The complete theoretical analysis for the proposed algorithms are given under Nakagami fading channel and validated using simulations.

In chapter 6, we propose novel detection algorithm that uses cooperative spectrum sensing with hard combining for wideband sensing. Hard combining is used for data fusion because it incurs reduced cooperation overhead. Complete theoretical analysis for the proposed algorithm is given and validated using simulation. Performance improvement is shown against no cooperation. Also, by choosing appropriate number of cooperating secondary users, the algorithm performs better than our algorithms that use diversity.

Finally, in chapter 7, we conclude the thesis by summarizing the main contributions and by listing out future research directions. Most of the material discussed in this thesis has been published in our works [20, 21, 22, 23, 24].

CHAPTER 2

Literature Review

In this Chapter, we provide a review of the literature for spectrum sensing highlighting the insights of current research status in these areas. We first review the literature on narrowband spectrum sensing in Section 2.1 followed by wideband spectrum sensing in Section 2.2 and cooperative spectrum sensing in Section 2.3.

2.1 Narrowband Spectrum Sensing

Various detection techniques for narrowband spectrum sensing have been investigated, namely, matched filtering based detection [19, 62], cyclostationary detection [26, 63, 70], covariance based detection [134, 136], eigenvalue based detection [135, 137, 138] and energy detection [37, 38, 65, 123]. The optimal way to detect the occupancy status of the PU signal under AWGN is the matched filter detection [19, 62], since it maximizes the received signal to noise ratio. However, a matched filter effectively requires demodulation of primary user signal. This means that cognitive radio has a priori knowledge of primary user signal at both PHY and MAC layers. The main advantage of matched filter is that it does not require significant amount of time to achieve high processing gain since only $O(1/SNR)$ samples are needed to meet a given probability of detection constraint [35]. However, the main drawback of a matched filter detection is that a CR would need a dedicated receiver for every PU class. Man-made signals are generally nonstationary. However, few of these signals are cyclostationary, i.e., their statistics exhibit periodicity, which may be caused due to the use of modulation and coding or even it may intentionally introduced to aid channel estimation and synchro-

nization. Such periodicity can be utilized for detecting a random signal with a particular modulation type in a background of noise and other modulated signals. This is called cyclostationary detection which was first introduced in [45]. The cyclostationary detection is realized by analyzing the cyclic autocorrelation function (CAF) [32] of the received signal, or, equivalently, its two-dimensional spectrum correlation function (SCF) [46], since the spectrum redundancy caused by periodicity in the modulated signal results in correlation between widely separated frequency components [46, 67]. In [26], the noise rejection property of the cyclostationary spectrum is used to perform spectrum sensing at very low signal to noise ratio (SNR). The spectrum sensing algorithm for IEEE 802.22 WRAN is developed. It is shown using simulation that for the probability of false alarm as 0.1, the probability of miss detection of 0.1 is achieved using the proposed algorithm at SNR$= -25\ dB$. The cycle frequency domain profile (CDP) is used for signal detection and preprocessing for signal classification in [63]. Signal features are extracted from CDP and a Hidden Markov Model (HMM) has been used for classification. It is shown that the CDP-based detector and the HMM-based classifier can detect and classify PU signals at low SNRs. A generalized likelihood ratio test (GLRT) for detecting the presence of cyclostationarity using multiple cyclic frequencies is proposed in [70] and the performance improvement is shown using simulations in low SNR regime. The cyclostationary detection can be used to differentiate the primary signal from the interference and noise. It works even in very low SNR region and its performance is independent of the noise uncertainty. But, the limitation of the cyclostationary detection is that, similar to matched filter, it also requires prior knowledge about the PU signal. Added to this, the computational complexity is also high when compared to energy detector. Researchers have also attempted to solve the spectrum sensing problem by using the covariance of the received signal. We know that the statistical covariance of the signal and noise are different and hence can be used to differentiate the case where the primary user's signal is present from the case where there is only noise. The spectrum sensing algorithms based on this idea are proposed in [134, 136] in which sample covariance matrix is calculated using the limited number of re-

ceived signal samples. Based on the eigenvalues of the sample covariance matrix, different spectrum sensing algorithms are proposed in [135, 137, 138]. Authors in [138] propose spectrum sensing method based on the maximum eigenvalue. The spectrum sensing method based on the ratio of the maximum eigenvalue to the minimum eigenvalue is proposed in [135, 137]. The detection scheme based on the ratio of the average eigenvalue to the minimum eigenvalue is also proposed by the authors in [137]. Spectrum sensing methods based on covariance matrix and its eigenvalues do not need any kind of knowledge about the signal, channel and the noise power. These methods performs better than ED when the received signal samples are correlated. Also, the computational complexity of these approaches are high. Energy Detection (ED) based spectrum sensing proposed in [37, 38, 65, 123] is the most popular technique due to its simplicity. ED is a non-coherent blind detection technique and it does not require any prior knowledge about the PU signal. It is simple to design and implement in practice. The computational complexity of ED is significantly less when compared to other techniques. Looking at the advantages of ED, we make use of ED in all our works.

In the literature, many studies have been dedicated to the analysis of ED based spectrum sensing by considering different communication scenarios. In [123], Urkowitz derive the probability of detection (P_D) and probability of false alarm (P_F) under additive white Gaussian noise (AWGN) channel. Kostylev in [65], revisited the problem of ED considering the fading conditions and obtained the expressions for P_D and P_F under Rayleigh, Rice and Nakagami fading channels. Closed form expressions for the average probability of detection ($\bar{P}_D$) for no diversity and with diversity under Rayleigh, Rician and Nakagami fading channels are derived in [37]. Authors in [58] derive the expressions for $\bar{P}_D$ for the no diversity case and the maximal ratio combining (MRC) diversity case considering Nakagami-m and Rician fading by using the moment generating function (MGF) method and probability density function (pdf) method. In [13], the detection performance of ED is investigated under very low SNR levels. The closed form expressions are derived for the average probability of missed detection considering Rayleigh and Nakagami$-m$ fading channels. The performance of ED over gen-

eralized $k-\mu$ and $k-\mu$ *extreme* fading channels have been investigated in [102] where the expressions for $\bar{P}_D$ are derived for no diversity case which are then subsequently extended to square law selection (SLS) diversity and for cooperative detection. The performance of ED over wireless channels with composite multipath fading and shadowing is studied in [12]. The performance of energy detector over $\eta-\mu$ fading channel is analyzed in [11]. The performance of ED over mixture gamma distribution is studied in [4] where the expressions for average probability of detection are derived. The analysis is then extended to square law selection and square law combining diversity schemes. Recently, in [14], the performance of ED is investigated over Nakagami$-q$/ Hoyt fading channel. Authors in [18], study the effects of RF impairments such as in-phase and quadrature-phase imbalance, low-noise amplifier nonlinearities, and phase noise on the performance of ED based spectrum sensing. Although in literature, ED based spectrum sensing is studied in different scenarios, there is still scope in analyzing the performance of ED under more general fading channel. In our work, we investigate the performance of ED under $\eta-\lambda-\mu$ fading model which is more general and includes other fading models as its special cases.

In ED, also known as conventional energy detector (CED), if the noise variance is known exactly, it is possible to detect the PU signal even at very low SNR if the sensing time is made sufficiently large [62]. In practice, the noise variance varies with time as well as location giving rise to noise uncertainty [116]. The effect of worst case noise uncertainty on CED is discussed in [104, 116]. In [116], a phenomenon called SNR wall is studied. The effect of uniformly distributed noise uncertainty on the performance of CED is studied in [52, 139]. The authors in [139] derive the the expression for SNR wall for CED assuming a uniform distribution for noise uncertainty. In [77], an asymptotic analysis of noise power estimation is performed for CED. The condition for existence of SNR wall is obtained and the effect of noise power estimation on the performance is studied. The SNR wall for cooperative spectrum sensing (CSS) assuming the same SNRs and the noise uncertainties for all the cooperating secondary users is discussed in [126, 133]. The CED is generalized by replacing the squaring operation of received signal

amplitude by an arbitrary positive power p, which is referred to as the generalized energy detector (GED) [59, 60] or the improved energy detector [28, 100, 101] or p-norm detector [16, 17] or the L_p-norm detector [84]. In [28, 101, 103], it is shown that performance of the CED can be improved by choosing a suitable value for p that depends on P_F, the average SNR as well as on the sample size. In [16, 17], different approximations for P_F and P_D are developed by considering different fading scenarios. Also, for antenna diversity reception, new detection schemes called $p-$law combining (pLC) and $p-$law selection (pLS) are proposed. In [59, 60], the performance of GED is studied under noise uncertainty where the authors in [59] show that under worst case of noise uncertainty the SNR wall is not dependent on the value of p. It is also shown that under the assumption of uniform distribution of noise uncertainty, the CED represents the optimum ED. The expression for SNR wall is obtained in [60] where the noise uncertainty is once again chosen as uniformly distributed. It is also shown that the SNR wall does not depend on the value of p. The study of the detection performance is then extended to noise uncertainty having log normal distribution and the SNR wall for the same is calculated numerically. Authors in [59, 60] have derived the SNR wall for GED under noise uncertainty considering no diversity.

2.2 Wideband Spectrum Sensing

A simple approach of wideband spectrum sensing (WSS) is to acquire the wideband signal by sampling at the corresponding Nyquist rate using standard analog to digital converter (ADC) and then apply digital signal processing techniques to detect the spectrum opportunities. Number of researchers have studied WSS based on Nyquist sampling. Authors in [96, 97] have proposed an optimal multiband joint detection scheme for WSS in which a bank of multiple narrowband detectors are jointly optimized to improve the aggregate opportunistic throughput of a CR system while limiting the interference to the PU system. This technique suffers from issues such as power consumption and non feasibility of ultra high sampling ADCs. As the extension of this, authors in [44] propose an adaptive

multiband spectrum sensing algorithm. The algorithm consists of two phases: the exploration phase, where substantial portion of the available channels are eliminated according to accumulated statistics and the detection phase, where multiple spectrum opportunities are finally identified among the remaining channels. A wavelet based spectrum sensing algorithm is proposed in [117] and [39] where the power spectral density (PSD) of the wideband spectrum is modeled as a series of consecutive frequency subbands, in which the PSD is smooth within each subband but exhibits discontinuities and irregularities on the border of two neighboring subbands. The wavelet transform is then used to locate the boundaries of the subbands and the occupancy status of the subbands are decided based on the PSD levels in each subband. Farhang-Boroujeny in [40] proposes a filter bank approach for wideband spectrum sensing where a bank of prototype filters is used to process the wideband signal. Here, the baseband is directly estimated by using a prototype filter and the other bands are obtained by modulating the prototype filter. In each band, the corresponding portion of the wideband is down converted to form a baseband version of that subband on which a narrowband sensing algorithm is applied. The drawback of this approach is that, due to the parallel structure of the filter bank, the implementation of this algorithm requires a large number of radio frequency (RF) components. The extension of this work can be found in [64, 69]. In general a SU may not be interested in finding all the spectrum opportunities, instead the interest lies in finding sufficient numbers of spectrum opportunity. This can be achieved if we consider only a part of the wideband spectrum for sensing. Keeping this into consideration, authors in [112] propose partial band Nyquist sampling (PBNS) which samples part of the wideband instead of entire wideband thus reducing the sampling rate. Since PBNS uses the traditional Nyquist sampling it represents the simplest wideband spectrum sensing scheme.

Due to the drawback of high sampling rate in Nyquist WSS, sub-Nyquist sensing is drawing more and more interest. Two important types of sub-Nyquist wideband sensing are compressive sensing-based and multichannel sub-Nyquist based wideband sensing. Compressive sensing based wideband spectrum sens-

ing was first introduced in [118] where fewer samples are used to perform wideband spectrum sensing. The number of samples closer to the information rate are used, rather than the inverse of the bandwidth. Here, the wideband spectrum is reconstructed and then wavelet based edge detection is used to detect the spectrum opportunities. To improve the robustness against noise uncertainty, a cyclic feature detection based compressive sensing algorithm for wideband spectrum sensing is proposed in [119]. Authors in [132] proposed a distributed compressive sensing based sensing algorithm for cooperative multihop cognitive radio networks in order to reduce the acquisition cost. To realize the analogue compressive sensing, an analogue-to-information converter (AIC), is proposed in [121]. A quadrature analogue-to-information converter is introduced in [129] to rapidly sense the spectrum of interest. Comparison of various architectures in compressive sensing are presented in [30]. In addition to this, number of wideband spectrum sensing techniques that make use of compressive sensing can also be found in [51, 54, 127]. Mishali and Eldar proposed a multichannel sub-Nyquist sampling approach known as modulated wideband converter (MWC) in [80] by modifying the AIC model. An alternative multichannel sub-Nyquist sampling approach is the multi-coset sampling. Multi-coset sampling is equivalent to choosing some samples from a uniform grid, which can be obtained using a sampling rate f_s higher than the Nyquist rate. The uniform grid is then divided into blocks of m consecutive samples and in each block v $(v < m)$ samples are retained. Thus, it is often implemented by using v sampling channels with sampling rate of f_s/m, with different sampling channels having different time offsets. To obtain a unique solution for the wideband spectrum from these partial measurements, the sampling pattern should be carefully designed. In [124], some sampling patterns were proved to be valid for unique signal reconstruction. The advantage of the multi-coset approach is that the sampling rate in each channel is m times lower than the Nyquist rate. One drawback of the multi-coset approach is that the channel synchronization should be met such that accurate time offsets between sampling channels are required to satisfy a specific sampling pattern for robust spectral reconstruction. To relax the multichannel synchronization requirement, an asyn-

chronous multirate wideband sensing approach was studied in [108]. The multicoset sub-Nyquist sampling has been carefully analyzed in [130]. The complexity and the power consumption of the presented implementation are considered in details.

2.3 Cooperative Spectrum Sensing

Cooperative spectrum sensing (CSS) has been shown to be an effective method to combat the adverse effects of multipath fading and shadowing by exploiting spatial diversity [48]. Traditionally, the cooperative spectrum sensing methods focused on narrowband sensing. Cooperative spectrum sensing can be classified as either centralized [48, 122, 125] or distributed [49, 68]. In centralized CSS, all the CSUs send their sensing information to a central entity called fusion center (FC). The FC combines the received local sensing information and then takes decision on the occupancy of the PU channel. Distributed cooperative sensing is another approach where instead of reporting them to a FC, the CSUs exchange sensing information with one another. Data fusion is a process of combining local sensing information for hypothesis testing. In general, the sensing results reported to the FC or shared with neighboring users can be combined in two different ways (i) Soft Combining [72, 73, 140]: CR users can transmit the entire local sensing samples or the complete local test statistics for soft decision, can utilize the conventional combining techniques such as equal gain combining (EGC) and maximal ratio combining (MRC). (ii) Hard combining [93, 141]: CSUs make a local decision and transmit the one bit information for hard combining. The three rules that are applied by hard decision combining are the OR, AND, and k out of M rule.

The performance of cooperative spectrum sensing scheme based on hard combining over Nakagami-m fading channel is studied in [29]. In [86], the performance using energy detection is investigated to improve the sensing performance in channels such as log-normal shadowing and Nakagami fading. Here, the hard decision combining rule is performed at fusion center (FC) to make the final deci-

sion on the ON/OFF status of PU. Comparison among data fusion rules has been investigated for a wide range of average SNR values is also studied in [86]. A similar analysis is done in [85] over Hoyt/Nakagami-q fading channel. The analysis for hard combining over Hoyt and Weibull fading channel is carried out in [88]. Authors in [87] study CSS using energy detection which uses soft combining. Here, the performance is studied under several soft data fusion schemes namely, square law selection (SLS), square law combining (SLC) and maximal ratio combining (MRC), that are implemented at fusion center (FC). The performance has been assessed under AWGN, log-normal shadowing, Rayleigh and Rician fading channels.

The performance of energy detection based spectrum sensing is greatly affected by noise variance uncertainty. Noise uncertainty in spectrum sensing makes the detector unreliable due to "SNR walls". The detection performance of the CSS based on soft combining, where the cooperating CR nodes experience different noise power uncertainties is studied in [52]. A detection scheme is proposed that is more robust to noise uncertainties than the conventional detection schemes. In [25], CSS with adaptive thresholds is proposed to improve the detection performance under noise uncertainty. In this algorithm, each SU uses a two-thresholds detector for local detection and the threshold at each SU is chosen according to the noise uncertainty at that SU. After each detection, the detection results are fused to give the final decision. In [126], the performance under noise uncertainty is analyzed and a new approach to obtain the SNR wall is proposed. In addition, a suboptimal cooperative sensing algorithm with wavelet denoising is proposed to reduce the impact of noise uncertainty. The SNR wall phenomenon under CSS using AND/OR hard decision and EGC soft decision is analyzed.

The cooperative spectrum sensing can also be used for wideband sensing. An overview of the challenges and possible solutions for the design of cooperative wideband spectrum sensing in CR networks is presented in [96]. In [97], the spectrum sensing problem is formulated as a class of optimization problems that maximize the aggregated opportunistic throughput of a cognitive radio system under the constraints as the interference to the primary users. The cooperative sens-

ing problem is also mapped into an optimization problem, for which suboptimal solutions are obtained through mathematical transformation under conditions of practical interest. An expectation maximization (EM) based joint detection and estimation (JDE) scheme for cooperative spectrum sensing in multiuser multi-antenna CR network is proposed in [10], where multiple spatially separated SUs cooperate to detect the state of occupancy of a wideband frequency spectrum. The implementation of a compressive sensing based cooperative wideband sensing is addressed in [71]. In this technique, the implementation of the conventional architecture that relies on fast Fourier transform (FFT) engine has been adopted and modified to include the multi-coset sampling. As a cooperative wideband sensing, the "frugal sensing" has been proposed in [78] to reduce the bandwidth requirements for the control channel. Number of studies on cooperative wideband spectrum sensing can also be found in [33, 75, 105, 111, 120].

CHAPTER 3

Performance of Energy Detection based Spectrum Sensing Over $\eta - \lambda - \mu$ Fading Channel

In the literature, many studies have been dedicated to the analysis of energy detection based spectrum sensing by considering different communication scenarios. In [123], Urkowitz derived the probability of detection (P_D) and probability of false alarm (P_F) under additive white Gaussian noise (AWGN) channel. He found that decision statistic follows central chi-square distribution when the PU is inactive and when it is active it has non-central chi-square behavior. Kostylev in [65], revisited the problem of ED considering the fading conditions. He derived P_D and P_F under Rayleigh, Rice and Nakagami fading channels. The closed form expressions for the average probability of detection $(\bar{P}_D)$ for both single channel and diversity combining scenario under Rayleigh, Rician and Nakagami fading channels are derived in [37]. The performance of ED over wireless channels with composite multipath fading and shadowing is studied in [12]. These effects were modeled by K and K_G channel models. Here, the closed form expressions for $\bar{P}_D$ for no diversity were derived and analysis was then extended to diversity scenario. The performance of energy detector over $\eta - \mu$ fading channel is analyzed in [11]. The authors in [102] discussed the ED performance over $\kappa - \mu$ and $\kappa - \mu$ extreme fading.

The η-λ-μ distribution is a generalized fading model and provides better characterization of the practical channel conditions [91]. In addition to Rayleigh and Nakagami Fading channels, other fading channels occurring in practice can be modeled by adjusting η, λ and μ. Numerical results in [91] show that the η-λ-μ

fading model provides better fit to the experimental data than the other models available in the literature. Also, since the shape of the distribution is set by three parameters, it is more flexible. This distribution includes Rayleigh, Rician, Nakagami-m, Hoyt, $\eta-\mu$, $\lambda-\mu$, etc distributions as special cases. In spite of the usefulness of this model, no work related to the ED considering this fading is reported in the literature. These factors motivate us to study the performance of the energy detection based spectrum sensing by considering the $\eta-\lambda-\mu$ fading. In this chapter, we provide the analysis to ED over η-λ-μ fading channel. We first derive the novel expression for $\bar{P}_D$ for the case of no diversity. The work is then extended to include selection diversity and cooperative spectrum sensing (CSS) scenarios. The $\bar{P}_D$ under composite multipath fading and shadowing is derived. The analysis includes analysis for K and K_G channel model derived in [12] as special cases.

3.1 System and Channel model

3.1.1 Energy Detection (ED)

The received signal at the secondary user can be represented as [37]

$$y(t) = \begin{cases} n(t); & H_0, \\ h \cdot s(t) + n(t); & H_1, \end{cases} \tag{3.1}$$

where, $s(t)$ is an unknown deterministic signal, h denotes the amplitude of the channel coefficient and $n(t)$ is an additive white Gaussian noise (AWGN) process. The hypotheses H_0 and H_1 correspond to absence and presence of the primary signal $s(t)$. The received signal $y(t)$ is filtered by the bandpass filter (BPF) with bandwidth W Hz which removes the out of band noise power. The output of the filter is then squared, integrated and multiplied by $2/N_0$, which is expressed as $T_m = (2/N_0)\int_0^T |y(t)|^2\, dt$ [37], where N_0 (W/Hz) is the one sided power spectral density of the AWGN at the receiver and T is the observation interval. The multiplication factor $2/N_0$ is utilized to normalize the noise variance. Under AWGN

channel, the decision statistic (T_m) follows central chi-square distribution under H_0 and non-central chi-square distribution with $N = 2u$ degrees of freedom under H_1 [37], where $u = TW$ is the time-bandwidth product. Therefore we have

$$T_m \sim \begin{cases} \chi^2_N; & H_0 \\ \chi^2_N(2\gamma); & H_1, \end{cases} \tag{3.2}$$

where, $\gamma = h^2 E_s / N_0$ is the signal to noise ratio (SNR) at the input of secondary user, E_s denotes the signal energy.

At the end of the interval $(0, T)$, the detector decides occupancy status of the primary user by comparing the measured energy with the predefined energy threshold τ. If $T_m \geq \tau$ then the PU is present otherwise it is absent. The P_F and P_D are then obtained as [37]

$$P_F = Pr\{T_m > \tau | H_0\} = \frac{\Gamma\left(\frac{N}{2}, \frac{\tau}{2}\right)}{\Gamma(\frac{N}{2})} \text{ and} \tag{3.3}$$

$$P_D = Pr\{T_m > \tau | H_1\} = Q_{\frac{N}{2}}\left(\sqrt{2\gamma}, \sqrt{\tau}\right), \tag{3.4}$$

where, $\Gamma(x) = \int_0^\infty t^{x-1} e^{-t} dt$ is the gamma function [50], $Q_{\frac{N}{2}}(\cdot, \cdot)$ is the generalized Marcum Q-function [90], $\Gamma(a, x) = \int_x^\infty t^{a-1} e^{-t} dt$ and $\gamma(a, x) = \int_0^x t^{a-1} e^{-t} dt$ represent upper and lower incomplete gamma functions [2], respectively.

3.1.2 η-λ-μ Fading Model

In [91], a new general fading model for mobile communication is proposed. This model combines the properties of the λ-μ and η-μ distribution models. As already discussed, this is a flexible model since it is defined in terms of three parameters η, λ and μ. Here, the parameter η accounts for unequal powers of the in-phase and quadrature components of the fading signal, λ accounts for the correlation between the in-phase and quadrature components while μ represents the number of multipath clusters.

The probability density function (pdf) of instantaneous SNR γ under $\eta - \lambda - \mu$ fading is given by [91]

$$f_\gamma(\gamma) = \frac{\sqrt{\pi}\left(\sqrt{\eta(1-\lambda^2)}\tilde{b}\right)^{2\mu}\gamma^{\mu-\frac{1}{2}}I_{\mu-\frac{1}{2}}\left(\tilde{d}\frac{\gamma}{\bar{\gamma}}\right)}{2^{-\mu-\frac{1}{2}}\Gamma(\mu)\tilde{d}^{\mu-\frac{1}{2}}\bar{\gamma}^{\mu+\frac{1}{2}}e^{\tilde{c}\frac{\gamma}{\bar{\gamma}}}}, \tag{3.5}$$

where, $I_v(\cdot)$ is the modified Bessel function of first kind with order v [2], $\tilde{b} = \frac{\mu(1+\eta)}{2\eta(1-\lambda^2)}$, $\tilde{c} = \frac{\mu(\eta+1)^2}{2\eta(1-\lambda^2)}$, $\tilde{d} = \tilde{b}\sqrt{(\eta-1)^2+4\eta\lambda^2}$, $\bar{\gamma}$ represents the average SNR.

3.2 Average Probability of detection Over η-λ-μ Fading Channel

Here, we consider three cases for detection schemes i.e., no diversity, diversity and cooperative detection. In this work, our aim is to show that the performance can be improved by using diversity as well as by using cooperative detection. Hence, we derive $\bar{P}_D$ considering square law selection (SLS) only. One can also derive $\bar{P}_D$ considering other diversity techniques. Similarly, we derive $\bar{P}_D$ for CSS using OR hard combining only which can be extended to other hard combining techniques.

3.2.1 No Diversity

Eq. (3.3) and Eq. (3.4) give the probability of false alarm (P_F) and probability of detection (P_D) under AWGN channel, respectively. The probability of false alarm remains same under fading conditions since it is independent of SNR and H_0 corresponds to only noise signal. The probability of detection under fading channel is obtained by averaging P_D under AWGN channel in Eq. (3.5) over pdf of SNR over fading channel, i.e.,

$$\bar{P}_D = \int_0^\infty Q_{\frac{N}{2}}(\sqrt{2\gamma}, \sqrt{\tau}) f_\gamma(\gamma) d\gamma. \tag{3.6}$$

Substituting Eq. (3.5) into Eq. (3.6), we get

$$\bar{P}_D = \int_0^\infty \frac{Q_{\frac{N}{2}}(\sqrt{2\gamma}, \sqrt{\tau})\sqrt{\pi}\left(\sqrt{\eta(1-\lambda^2)}\tilde{b}\right)^{2\mu} I_{\mu-\frac{1}{2}}\left(\tilde{d}\frac{\gamma}{\bar{\gamma}}\right)}{2^{-\mu-\frac{1}{2}}\Gamma(\mu)\tilde{d}^{\mu-\frac{1}{2}}\bar{\gamma}^{\mu+\frac{1}{2}}e^{\tilde{c}\frac{\gamma}{\bar{\gamma}}}\gamma^{-\mu+\frac{1}{2}}} d\gamma. \tag{3.7}$$

Using the series representation of generalized Marcum Q function [61, Eq. (29)] and modified Bessel function of first kind [50], i.e.,

$$Q_{\frac{N}{2}}(\sqrt{2\gamma}, \sqrt{\tau}) = e^{-\gamma}\sum_{l=0}^{\infty}\frac{\gamma^l\Gamma(l+u, \frac{\tau}{2})}{\Gamma(l+1)\Gamma(l+u)} \text{ and } I_v(x) = \sum_{j=0}^{\infty}\frac{x^{2j+v}}{j!2^{2j+v}\Gamma j+v+1}, \tag{3.8}$$

we can write $\bar{P}_D$ as

$$\bar{P}_D = \sum_{l=0}^{\infty}\sum_{j=0}^{\infty}\frac{\sqrt{\pi}(\sqrt{\eta(1-\lambda^2)}\tilde{b})^{2\mu}\Gamma(l+u, \frac{\tau}{2})(\tilde{d}^{2j})}{2^{2j-1}\Gamma(\mu)\bar{\gamma}^{2j+2\mu}l!j!\Gamma(l+\frac{N}{2})\Gamma(j+\mu+\frac{1}{2})}\int_0^\infty \gamma^{l+2\mu+2j-1}e^{-\gamma(1+\frac{\tilde{c}}{\bar{\gamma}})}d\gamma. \tag{3.9}$$

Now consider the integral in Eq. (3.9) which is represented by

$$I = \int_0^\infty \gamma^{l+2\mu+2j-1}e^{-\gamma(1+\frac{\tilde{c}}{\bar{\gamma}})}d\gamma. \tag{3.10}$$

Applying the change of variable as $x = \gamma(1+\frac{\tilde{c}}{\bar{\gamma}})$, this integral reduces to

$$I = (1+\frac{\tilde{c}}{\bar{\gamma}})^{-(l+2\mu+2j)}\int_0^\infty x^{l+2\mu+2j-1}e^{-x}dx = (1+\frac{\tilde{c}}{\bar{\gamma}})^{-(l+2\mu+2j)}\Gamma(l+2j+2\mu). \tag{3.11}$$

Substituting back Eq. (3.11) into Eq. (3.10) the series representation for $\bar{P}_D$ can be written as

$$\bar{P}_D = \sum_{l=0}^{\infty}\sum_{j=0}^{\infty}\frac{\bar{\gamma}^l\sqrt{\pi}(\sqrt{\eta(1-\lambda^2)}\tilde{b})^{2\mu}\Gamma(l+u, \frac{\tau}{2})\tilde{d}^{2j}\Gamma(l+2j+2\mu)}{2^{2j-1}\Gamma(\mu)l!j!\Gamma(l+\frac{N}{2})\Gamma(j+\mu+\frac{1}{2})(\bar{\gamma}+\tilde{c})^{l+2\mu+2j}}. \tag{3.12}$$

The series in Eq. (3.12) converges for $l \to \infty$ and $j \to \infty$. However, we observe that the series nearly converges when the sum is considered over a relatively small values of l and j and can be computed easily using a mathematical software (e.g.

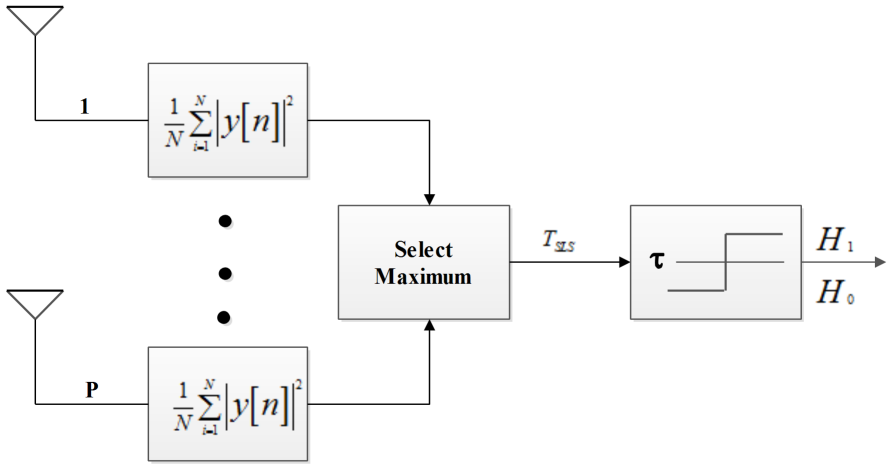

Figure 3.1: Block diagram of SLS diversity technique.

MATHEMATICA [128]). For example, with $\eta = 0.4$, $\lambda = 0.5$, $\mu = 1$, $N = 10$, $\bar{\gamma} = 10$ and $P_F = 0.1$, the series in Eq. (3.12) converges upto four decimal points for $l = 79$ and $j = 11$. Hence, $\bar{P}_D$ for these parameters can be obtained by taking the finite sum as

$$\bar{P}_D = \sum_{l=0}^{79} \sum_{j=0}^{11} \frac{\bar{\gamma}^l \sqrt{\pi} (\sqrt{\eta(1-\lambda^2)}\tilde{b})^{2\mu} \Gamma(l+u, \frac{\tau}{2}) \tilde{d}^{2j} \Gamma(l+2j+2\mu)}{2^{2j-1}\Gamma(\mu) l! j! \Gamma(l+\frac{N}{2}) \Gamma(j+\mu+\frac{1}{2}) (\bar{\gamma}+\tilde{c})^{l+2\mu+2j}}, \tag{3.13}$$

3.2.2 Square Law Selection (SLS) Diversity

As shown in Fig. 3.1, in SLS diversity scheme, the branch with maximum decision statistic is chosen [89], i.e., $T_{SLS} = \max(T_1, T_2, \ldots, T_P)$, where T_{SLS} is the selected diversity branch and P represents the number of diversity branches. The probability of detection (P_D^{SLS}) under AWGN channel with SLS diversity scheme is derived in [37] and is given by

$$P_D^{SLS} = 1 - \prod_{i=1}^{P} \left[1 - Q_{\frac{N}{2}}(\sqrt{2\gamma_i}, \sqrt{\tau}) \right]. \tag{3.14}$$

Based on this, $\bar{P}_D^{SLS}$ in the case of η-λ-μ can be obtained by averaging P_D^{SLS} over P independent branches, i.e.,

$$\bar{P}_D^{SLS} = 1 - \int_0^\infty \cdots \int_0^\infty \prod_{i=0}^{P} \left[1 - Q_{\frac{N}{2}}(\sqrt{2\gamma_i}, \sqrt{\tau})\right] f_{\gamma_i}(\gamma_i) d\gamma_i. \tag{3.15}$$

Since $\int_0^\infty f_{\gamma_i}(\gamma_i) d\gamma_i \triangleq 1$, the average probability of detection with SLS diversity is obtained as

$$\bar{P}_D^{SLS} = 1 - \prod_{i=1}^{P} \left[1 - \int_0^\infty Q_{\frac{N}{2}}(\sqrt{2\gamma_i}, \sqrt{\tau}) f_{\gamma_i}(\gamma_i) d\gamma_i\right]. \tag{3.16}$$

Note that the integral that needs to be evaluated in Eq. (3.16) is same as that of no diversity case. Therefore, following the same steps, $\bar{P}_D^{SLS}$ can obtained as

$$\bar{P}_D^{SLS} = 1 - \prod_{i=1}^{P} \left[1 - \sum_{l=0}^{\infty} \sum_{j=0}^{\infty} \frac{\bar{\gamma}_i{}^l \sqrt{\pi} (\sqrt{\eta(1-\lambda^2)}\tilde{b})^{2\mu} \Gamma(l + \frac{N}{2}, \frac{\tau}{2}) \tilde{d}^{2j} \Gamma(l + 2j + 2\mu)}{2^{2j-1} \Gamma(\mu) l! j! \Gamma(l + \frac{N}{2}) \Gamma(j + \mu + \frac{1}{2}) (\bar{\gamma}_i + \tilde{c})^{l+2\mu+2j}}\right]. \tag{3.17}$$

The probability of false alarm in case of SLS remains same as that of AWGN channel since it is independent of SNR and is given by [37, Eq. (14)]

$$P_F^{SLS} = 1 - \left[1 - \frac{\Gamma(\frac{N}{2}, \frac{\tau}{2})}{\Gamma(\frac{N}{2})}\right]^P. \tag{3.18}$$

3.2.3 Cooperative Spectrum Sensing

Using diversity to improve performance requires multiple diversity branches. The detection performance can also be improved by multiple secondary users sharing their information. The performance of energy detection based spectrum sensing improves when secondary users collaborate by sharing their information. In Fig. 3.2, we show the schematic for centralized cooperative spectrum sensing where all the cooperating secondary users (CSUs) report their sensing information to the fusion center (FC). The FC then takes the final decision on the occupancy of the PU channel. There are two possible way for data fusion at the FC which

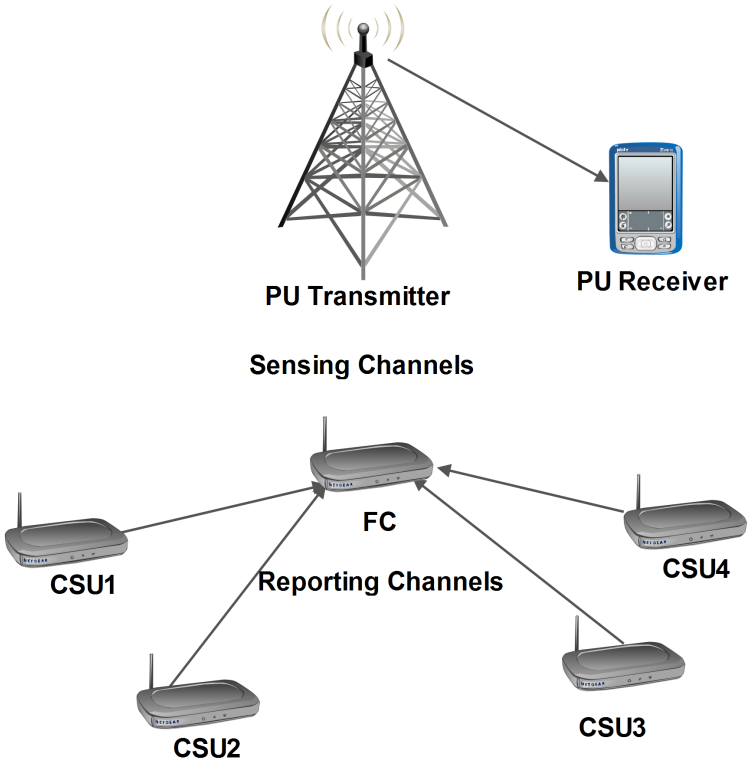

Figure 3.2: Centralized cooperative spectrum sensing.

are hard and soft combining. In this chapter, we focus on one of the hard combining technique, namely, OR combining. In CSS using hard combining, all the CSUs take their own decisions on the occupancy of the PU channel and report their decisions to the FC which then takes decision on the status of PU channel.

In OR combining scheme, if any one CSU reports the PU channel as occupied, the FC declares the PU channel as occupied. The block diagram for CSS using OR combining is shown in Fig. 3.3 with three CSUs where CSU 1 has reported channel as occupied and the other two CSUs have reported channel as free. The FC has declared PU channel as occupied since one of the CSUs has reported the channel as occupied. In this scenario, the average probability of detection and false alarm considering OR hard combining at the FC with M independent CSUs are given by [47]

$$\bar{Q}_D \triangleq 1 - (1 - \bar{P}_D)^M \text{ and } Q_F \triangleq 1 - (1 - P_F)^M. \tag{3.19}$$

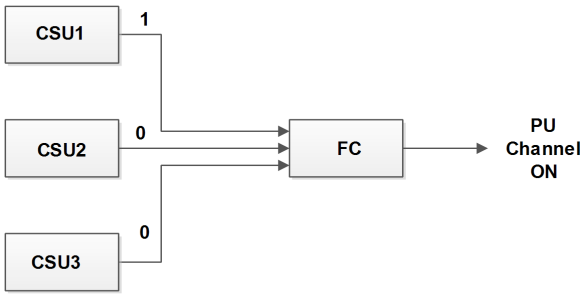

Figure 3.3: Block diagram for CSS using OR combining.

The average probability of detection with M cooperating secondary users is obtained by substituting Eq. (3.12) into $\bar{Q}_D$ in Eq. (3.19) as

$$\bar{Q}_D = 1 - \left[1 - \sum_{l=0}^{\infty}\sum_{j=0}^{\infty} \frac{\bar{\gamma}^l \sqrt{\pi}(\sqrt{\eta(1-\lambda^2)}\tilde{b})^{2\mu}\Gamma(l+u,\frac{\tau}{2})\tilde{d}^{2j}\Gamma(l+2j+2\mu)}{2^{2j-1}\Gamma(\mu)l!j!\Gamma(l+\frac{N}{2})\Gamma(j+\mu+\frac{1}{2})(\bar{\gamma}+\tilde{c})^{l+2\mu+2j}}\right]^M. \tag{3.20}$$

As already stated P_F remains same as under AWGN channel and hence Q_F is given by

$$Q_F = 1 - \left(1 - \frac{\Gamma(\frac{N}{2},\frac{\tau}{2})}{\Gamma(\frac{N}{2})}\right)^M. \tag{3.21}$$

3.3 Average Probability of Detection over channels with $\eta - \lambda - \mu$ Fading and Shadowing

Apart from the multipath fading, the signal received at the SUs also undergo shadowing. The shadowing process is typically modeled by a lognormal distribution [106]. Therefore, some practical communication channels can be modeled as multipath fading superimposed on lognormal shadowing. Due to the difficulty of analyzing spectrum sensing techniques over composite fading models, the shadowing effect is usually neglected in the literature. In this section, we derive the expression for average probability of detection where the signal undergoes shadowing in addition to $\eta - \lambda - \mu$ fading. In [1], Gamma distribution is used to ap-

proximate lognormal distribution to derive K and generalized K (K_G) distribution as a composite multipath fading and shadowing. K channel model corresponds to the mixture of Rayleigh distribution and gamma distribution while K_G represents mixture of Nakagami and Gamma distributions. Average probability of detection under K and K_G channel models have been derived in [12]. Similar procedure is followed here to derive the average probability of detection under $\eta - \lambda - \mu$ fading and shadowing. The average probability of detection under multipath fading and shadowing is given as

$$\bar{P}_D^{Shd} = \int_0^\infty \bar{P}_D^{Fad}(y) f_Y(y) dy, \tag{3.22}$$

where, $\bar{P}_D^{Fad}$ is the average probability of detection under fading only for a specific Y value that represents the SNR with only shadowing effect, which follows a lognormal distribution and can be approximated by gamma distribution [1].

$$f_Y(y) = \frac{y^{k-1} e^{-\frac{y}{\Omega}}}{\Gamma(k)\Omega^k}, \quad y \geq 0, \tag{3.23}$$

where, k is the shaping parameter and Ω represents the scale parameter which is also the mean signal power and $\bar{P}_D^{Fad}(y)$ is obtained by replacing every $\bar{\gamma}$ in Eq. (3.12) with y. Using this $\bar{P}_D^{Fad}(y)$ in Eq. (3.22) and averaging over pdf in Eq. (3.23), we get $\bar{P}_D^{Shd}$ as

$$\begin{aligned}\bar{P}_D^{Shd} = \sum_{l=0}^{\infty}\sum_{j=0}^{\infty} & \frac{\sqrt{\pi}(\sqrt{\eta(1-\lambda^2)}\tilde{b})^{2\mu}\Gamma(l+u,\frac{\tau}{2})\tilde{d}^{2j}}{2^{2j-1}\Gamma(\mu)l!j!\Gamma(l+\frac{N}{2})\Gamma(j+\mu+\frac{1}{2})} \\ & \times \frac{\Gamma(l+2j+2\mu)}{\Gamma(k)\Omega^k}\int_0^\infty y^{l+k-1}(y+\tilde{c})^{-(l+2\mu+2j)} e^{-\frac{y}{\Omega}} dy. \end{aligned} \tag{3.24}$$

The integral in Eq. (3.24) can be written as

$$\begin{aligned} I &= \tilde{c}^{-(l+2\mu+2j)} \int_0^\infty y^{(l+k)-1}(1+\frac{1}{\tilde{c}}y)^{-(l+2\mu+2j)} e^{-\frac{y}{\Omega}} dy \\ &= \Gamma(l+k)\tilde{c}^{k-2\mu-2j} U(l+k; k-2\mu-2j+1; \frac{\tilde{c}}{\Omega}), \end{aligned} \tag{3.25}$$

where, $U(;;)$ is the confluent hypergeometric function of the second kind defined as [50, Eq. (3.383.5)]:

$$\int_0^\infty e^{-px} x^{q-1}(1+ax)^{-v}dx = \frac{\Gamma(q)}{a^q} U(q; q+1-v; \frac{p}{a}) \tag{3.26}$$

with $Re\{q\} > 0$, $Re\{p\} > 0$, $Re\{a\} > 0$ and v is a complex value with $Re(\cdot)$ representing the real operator which gives real part of the complex number.

Substituting Eq. (3.25) into Eq. (3.24), the average detection probability under multipath fading and shadowing can be written as

$$\bar{P_D}^{Shd} = \sum_{l=0}^{\infty}\sum_{j=0}^{\infty} \frac{\sqrt{\pi}(\sqrt{\eta(1-\lambda^2)}\tilde{b})^{2\mu}\Gamma(l+u,\frac{\tau}{2})\tilde{d}^{2j}}{2^{2j-1}\Gamma(\mu)l!j!\Gamma(l+\frac{N}{2})\Gamma(j+\mu+\frac{1}{2})} \times \frac{\Gamma(l+2j+2\mu)\Gamma(l+k)U(l+k;k-2\mu-2j+1;\frac{\tilde{c}}{\Omega})}{\Gamma(k)\Omega^k\tilde{c}^{(2\mu+2j-k)}}. \tag{3.27}$$

It may be of interest to note that the detection performance can be improved by using diversity as well as the cooperative detection. Once $\bar{P}_D^{Shd}$ is obtained, the average probability of detection with fading and shadowing under SLS diversity can be obtained by averaging $\bar{P}_D^{SLS}$ in Eq. (3.17) over gamma distribution in Eq. (3.23) after replacing each $\bar{\gamma}_i$ by y_i in Eq. (3.17) and each y by y_i in Eq. (3.23). The average probability of detection under cooperative detection can be obtained by substituting $\bar{P}_D^{Shd}$ from Eq. (3.27) into Eq. (3.19).

3.4 Results and Discussion

In this section we carry out the analysis for testing the performance of energy detection under η-λ-μ fading channel for several cases of interest. The performance is studied using $\bar{\gamma}$ VS. $\bar{P}_D$ curve, i.e., average SNR VS. average probability of detection and complementary receiver operating characteristic (ROC) curves, i.e., P_F VS. $P_M = 1 - P_D$. In addition, η-λ-μ fading channel provides analysis for other fading channels as special cases.

Fig. 3.4(a) displays $\bar{\gamma}$ VS. $\bar{P}_D$ for no diversity case under η-λ-μ fading channel for $P_F = 0.1$, $N = 4$, $\eta = 0.4$, $\lambda = 0.5$ and $\mu = 1$. As expected, the detection per-

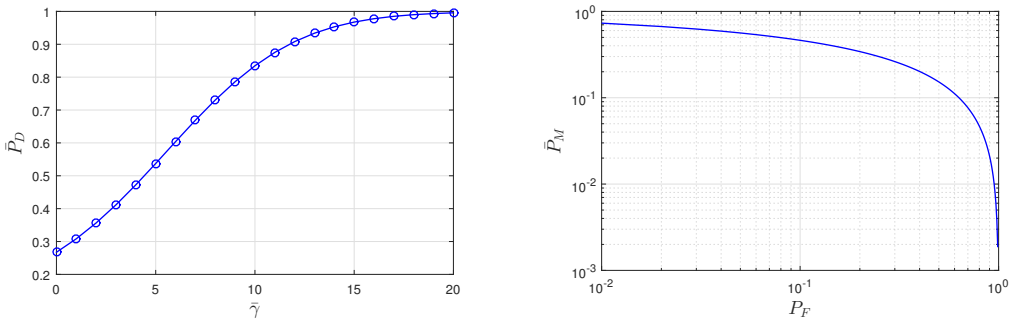

(a) (b)

Figure 3.4: (a) $\bar{\gamma}$ vs $\bar{P}_D$ for no diversity considering for $P_F = 0.1$ and (b) P_F vs $\bar{P}_M$ for $\bar{\gamma} = 5\ dB$ with $N = 4$, $\eta = 0.4$, $\lambda = 0.5$, $\mu = 1$.

formance improves with increase in SNR. Fig. 3.4(b) shows the complementary ROC curve using $\bar{\gamma} = 5\ dB$ and keeping the other parameters same as that of $\bar{\gamma}$ versus $\bar{P}_D$ shown in Fig. 3.4(a).

The analysis for η-λ-μ fading channel is general since the other fading channels are special cases of η-λ-μ fading distribution [91]. The Nakagami-m distribution can be obtained by setting $\eta \to 1$, $\lambda \to 0$ and $\mu = 0.5m$. The Rayleigh, One-Sided Gaussian and Nakagami-q (Hoyt) distribution can be obtained from Nakagami-m distribution by setting $m = 1$, $m = 0.5$ and $m = (1+q^2)^2/2(1+2q^4)$ respectively. The $\eta - \mu$ distribution can be obtained by setting $\lambda \to 0$ and $\mu = \mu'$, where μ' corresponds to the simpler model. Similarly, the $\lambda - \mu$ distribution can be obtained by setting $\eta \to 1$ and $\mu = \mu'$. In Fig. 3.5 we display the complementary ROC curves for different fading channels obtained from η-λ-μ fading channel as special cases discussed above. For this analysis we used $SNR = 10\ dB$ and $N = 10$.

Fig. 3.6(a) shows plots of P_F VS. $\bar{P}_M^{SLS} = 1 - \bar{P}_D^{SLS}$ by varying the number of diversity branches L from 1 to 5 where $P = 1$ corresponds to no diversity. For this analysis, we used $\eta = 0.4$, $\lambda = 0.5$, $\mu = 1$, $N = 4$ and the average SNRs are set to $\bar{\gamma}_1 = 0\ dB$, $\bar{\gamma}_2 = 1\ dB$, $\bar{\gamma}_3 = 2\ dB$, $\bar{\gamma}_4 = 3\ dB$, and $\bar{\gamma}_5 = 4\ dB$. Here, we see that the detection performance improves with the increase in the number diversity branches. For example, for $P_F = 0.1$, the value of $\bar{P}_M$ for $P = 1$ is approximately twice as large as $\bar{P}_M$ for $P = 5$.

Fig. 3.6(b) demonstrates the complementary ROC curve for energy detector under η, λ and μ fading channel considering upto eight cooperating secondary

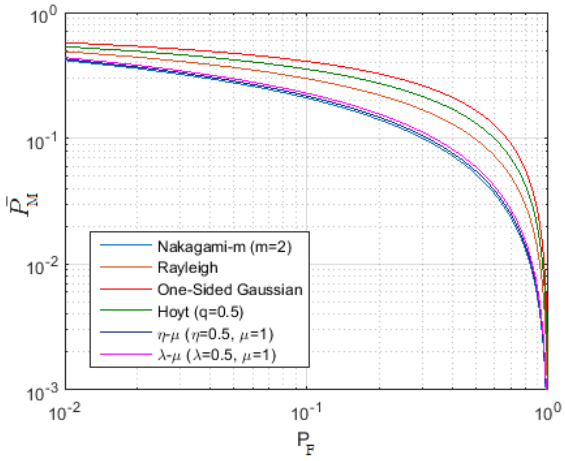

Figure 3.5: P_F vs $\bar{P}_M$ for other fading channels as a special case of η-λ-μ fading distribution with $\bar{\gamma} = 10\ dB$ and $N = 10$.

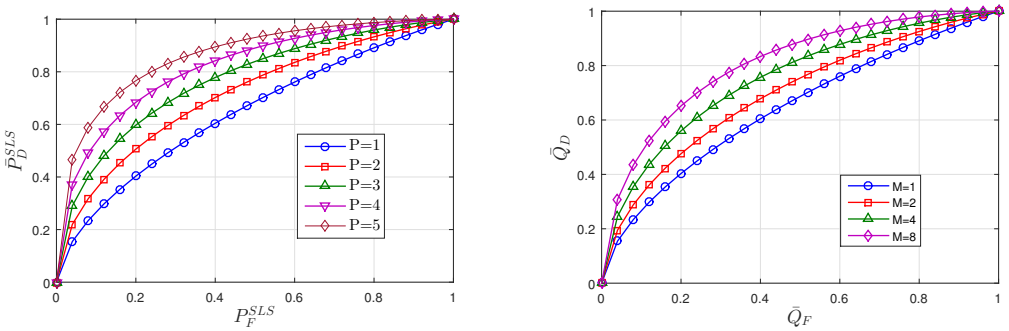

(a) (b)

Figure 3.6: ROC plots under η-λ-μ fading channel using $\eta = 0.4$, $\lambda = 0.5$, $\mu = 1$, $N = 4$ for (a) SLS diversity with $\bar{\gamma}_1 = 0\ dB$, $\bar{\gamma}_2 = 1\ dB$, $\bar{\gamma}_3 = 2\ dB$, $\bar{\gamma}_4 = 3\ dB$, and $\bar{\gamma}_5 = 4\ dB$ for different P values and (b) cooperative spectrum sensing with $\bar{\gamma} = 0$ dB and M cooperative secondary users.

users. The analysis is performed using the same parameters setting as that of SLS diversity scenario, and the $\bar{\gamma}$ is set to $0\ dB$. As expected the detection performance improves with the increase in the number of cooperating secondary users. For example, the value of $\bar{P}_M$ for $M = 1$ is approximately 1.4 times as large as $\bar{P}_M$ for $M = 8$.

Fig. 3.7 shows the plots for $\bar{P}_D^{Shd}$ versus P_F for channel that undergoes shadowing in addition to $\eta - \lambda - \mu$ fading. The plots are obtained by choosing different values for the shadowing parameter k, i.e., by choosing $k = 0.5$ and $k = 1$. The analysis includes the analysis for K and K_G channels as special cases. The analysis for K channel model can be obtained by setting $\eta \to 1$, $\lambda \to 0$, $m = 1$ and

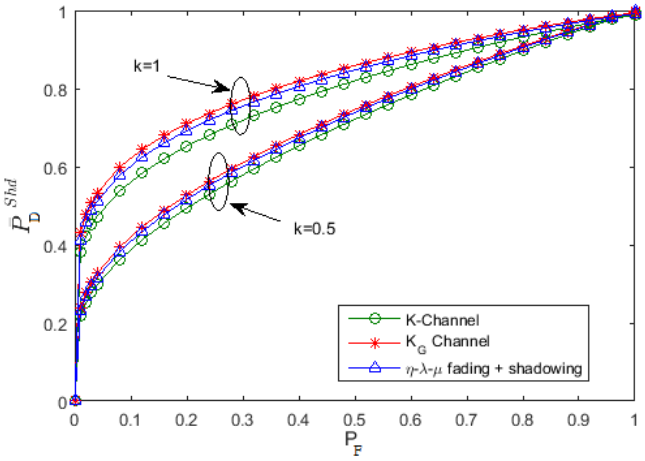

Figure 3.7: P_F vs $\bar{P}_D^{Shd}$ for composite multipath fading and shadowing channel for $k = 0.5$ and $k = 1$ with $\bar{\gamma} = 10\ dB$ and $N = 10$.

$\mu = 0.5m$. Similarly, by setting $\eta \to 1$, $\lambda \to 0$, $m = 2$ and $\mu = 0.5m$, the analysis for K_G channel model can be deduced. The results for K and K_G channel models match the results in [12]. The plot also shows results for shadowing in addition to fading with fading parameters $\eta = 0.4$, $\lambda = 0.5$ and $\mu = 1$ for $\bar{\gamma} = 10\ dB$. As already discussed, the detection performance can be improved by using the diversity schemes and cooperative detection.

3.5 Conclusion

This chapter illustrates the performance of energy detector in η-λ-μ fading channel. It also includes analysis for shadowing in addition to fading. Novel analytical expressions are derived for average probability of detection. The effect of different fading parameters on the detection performance is discussed. The detection performance of other fading channels is also provided since η-λ-μ distribution provides those distributions as special cases. The result for no diversity scenario is then extended to square low selection and cooperative detection. It is found that under selection diversity and cooperative detection, the detection performance improves. The analysis is then extended to the case when there exists shadowing in addition to $\eta - \lambda - \mu$ fading.

CHAPTER 4

SNR Wall for GED in the Presence of Noise Uncertainty and Fading

In Chapter 3, we have discussed conventional energy detector (CED) based spectrum sensing. In this chapter, we discuss generalized energy detector (GED) which is obtained replacing the squaring operation of the received signal amplitude in CED by an arbitrary positive power p. As in CED, here also, the decision on the occupancy of a channel is made based on the predefined threshold. A proper value of threshold can be determined by the noise variance at the input of the SU and hence it plays an important role in determining the performance of the detector. In this chapter, we consider the noise uncertainty (NU) in determining the threshold. One has to know true noise variance to determine the value of this threshold. If known exactly, it is possible to sense the occupancy of PU even at very low SNR if the sensing time is made sufficiently large [62], i.e., a large number of samples (N) are used in sensing. In practice the noise variance at the input of the SU varies with time as well as location and hence it is not possible to find its exact value. Due to this, there exists unpredictability about the true variance of noise which is known as noise uncertainty. The effect of worst case NU is discussed in [104, 116]. In [116], a phenomenon called SNR wall is studied for CED based sensing method, which says that if the noise variance is not known exactly and is confined to an interval, it is not possible to achieve targeted detection performance when the SNR falls below certain value regardless of sensing time. This makes ED an inefficient sensing method.

The effect of uniformly distributed NU on the performance of CED is studied

in [52, 139]. The authors in [139] derive the the expression for SNR wall for CED assuming a uniform distribution for NU. The detection performance of the cooperative spectrum sensing (CSS) is studied in [52]. In [77], an asymptotic analysis of noise power estimation is performed for CED. The condition for existence of SNR wall is obtained and the effect of noise power estimation on the performance of CED is studied. In [59, 60], the performance of GED is studied under NU where in the authors in [59] show that under worst case of NU the SNR wall is independent of value of p. It is also shown that under the assumption of uniform distribution of NU, the CED represents the optimum ED. The expression for SNR wall is obtained in [60] where the NU is once again chosen as uniformly distributed. It is also shown that the SNR wall does not depend on the value of p. The study of the detection performance is then extended to NU having log normal distribution and the SNR wall for the same is calculated numerically.

Authors in [59, 60] derive the SNR wall for GED under NU considering no diversity. The SNR wall for CSS with CED assuming the same SNRs and the noise uncertainties for all the cooperating secondary users (CSUs) is discussed in [126, 133]. However, in practice the SNR varies with the time and the location. Also, the NU depends on calibration error, variations in thermal noise and changes in low nose amplifier gain. Hence, the assumption of the same SNR and NU at all the SUs is not valid in practice. The scenario in which different CSUs have the varying noise uncertainties is studied in [25, 52] but the authors do not discuss the SNR wall. We notice that the existing analysis is only limited to no diversity or CSS case. Also, the available analysis do not consider NU with fading. We know that the diversity is suited to combat the adverse effects of multi-path fading as well as shadowing [11, 12, 37, 38, 89, 102]. Two new diversity schemes namely $p-$law combining (pLC) and $p-$law selection (pLS) are proposed in [16], in which GED is used at each of the diversity branches. Both pLC and pLS diversity schemes are non-coherent combining techniques. Here, they consider diversity and fading without considering NU. This motivates us to analyze the SNR wall for GED under diversity and CSS considering NU and fading. For CSS we consider both hard as well as soft combining. For hard combining we consider all

three possible cases, i.e., OR, AND and k out of M combining rule. We first derive the SNR wall considering AWGN channel and then extend it to the channel with Nakagami fading. It is a generalized fading model and includes Rayleigh, Rice and Hoyt fading models as its special cases and can be used to model propagation in urban and sub-urban areas by setting the Nakagami parameter m. In Chapter 3, we analyzed ED based spectrum sensing under $\eta - \lambda - \mu$ fading channel where we did not consider the NU. Although $\eta - \lambda - \mu$ fading model is more general, theoretical analysis considering this model is mathematically too involved and hence we give theoretical analysis considering Nakagami fading only. To the best of our knowledge, researchers have not worked on GED under diversity and CSS considering NU and fading.

4.1 System Model

In cognitive radio, the signal received at the SU can be written as

$$y(n) = \begin{cases} w(n); & H_0, \\ h(n)s(n) + w(n); & H_1, \end{cases} \tag{4.1}$$

where $h(n), s(n)$ and $w(n)$ correspond to n^{th} sample of the complex fading channel gain, PU signal and the noise, respectively with $n = 1, 2, \cdots, N$. The signal and noise samples are independent and identically distributed (iid) with $s(n) \sim \mathcal{CN}(0, \sigma_s^2)$ and $w(n) \sim \mathcal{CN}(0, \sigma_w^2)$. Here, the notation $\mathcal{CN}(\bar{x}, \sigma_x^2)$ denotes complex Gaussian distribution with mean $\bar{x}$ and variance σ_x^2. The signal and noise are statistically independent of each other. The hypotheses H_0 and H_1 correspond to free and occupied primary channel, respectively.

In CED, the absolute values of received samples are squared and summed over the number of collected samples and then compared with the predetermined threshold to decide on the presence and the absence of the PU. In the generalized energy detector (GED) [28], the squaring operation is replaced by an arbitrary

positive value p. Hence, the received signal decision statistic for GED is given by

$$T = \frac{1}{N} \sum_{n=1}^{N} |y(n)|^p, \tag{4.2}$$

where, $p > 0$ is an arbitrary constant.

4.2 Noise Uncertainty Model

The characterization of AWGN, i.e., $w(n)$, in Eq. (4.1) depends on its variance. In general for many detection methods it is assumed that the true noise variance at the input of SU is known a priori. These methods use this knowledge to choose a threshold in detecting the presence or the absence of PU signal. But in practice, the noise variance may vary over time and location, thus giving rise to a phenomenon called noise uncertainty [116, 139], which makes it difficult to obtain exact noise variance at a particular time and location.

The average value, i.e., the expected value of the noise variance $\hat{\sigma}_w^2$ is known in practice. As already mentioned, let the true noise variance at a particular time and location be σ_w^2 which may vary from the average noise variance giving rise to NU. Using this, the NU factor β is defined as $\beta = \frac{\hat{\sigma}_w^2}{\sigma_w^2}$. Note that β is a random variable since σ_w^2 is random. Let the upper bound on the noise uncertainty be L dB, which is defined as $L = sup\left\{10log_{10}\beta\right\}$.

In this work, we assume that β in dB is uniformly distributed in the range $[-L, L]$ [116], which implies β is restricted in the range $[10^{\frac{-L}{10}}, 10^{\frac{L}{10}}]$. The pdf of β can be obtained by using simple transformation of random variable as

$$f_\beta(x) = \begin{cases} 0, & x < 10^{\frac{-L}{10}} \\ \frac{5}{[ln(10)]Lx}, & 10^{\frac{-L}{10}} < x < 10^{\frac{L}{10}} \\ 0, & x > 10^{\frac{L}{10}} \end{cases} \tag{4.3}$$

where, $\ln(z)$ is the natural logarithm of z.

4.3 SNR Wall for AWGN Channel

For a given SNR > 0, if there exists a threshold for which

$$\lim_{N\to\infty} \bar{P}_F = 0 \text{ and } \lim_{N\to\infty} \bar{P}_D = 1, \tag{4.4}$$

then the sensing scheme is considered as unlimitedly reliable [139]. In other words, if the channel is sensed for sufficiently long time, i.e., $N \to \infty$, one can achieve desired target probability of false alarm and the probability of detection at any SNR level. However, this is possible only when there is no noise uncertainty. When there exists noise uncertainty, it is not possible to achieve this performance even with the use of unlimited sample size (N) below some SNR value [139]. The SNR value below which it is not possible to achieve unlimited reliability is defined as the SNR wall [139]. At least one of the conditions in Eq. (4.4) is not satisfied if the SNR falls below the SNR wall. However, when the SNR is above the SNR wall there exists a threshold for which both the conditions in Eq. (4.4) are satisfied.

In this section, we derive $\bar{P}_F$ and $\bar{P}_D$ in AWGN channel under noise uncertainty for no diversity, diversity and for CSS. Using them, we derive the expressions for SNR wall for each case. For relatively large N, using central limit theorem (CLT), the pdf of the decision statistic given in Eq. (4.2) can be modeled by Gaussian distribution [16, 59, 60, 126, 133] which can be represented by mean and variance only. Using these, the mean and variance of decision statistic are given as

$$\mu_0 = G_p\sigma_w^p,\ \ \sigma_0^2 = \frac{K_p}{N}\sigma_w^{2p}, \text{ and } \mu_1 = G_p(1+\gamma)^{\frac{p}{2}}\sigma_w^p,\ \ \sigma_1^2 = \frac{K_p}{N}(1+\gamma)^p\sigma_w^{2p}, \tag{4.5}$$

where, μ_0, σ_0^2 and μ_1, σ_1^2 correspond to mean and variance of T under H_0 and H_1, respectively. Here, $\gamma = |h|^2\frac{\sigma_s^2}{\sigma_w^2}$ is the instantaneous SNR and since we are considering AWGN channel in this section, $h = 1$. Note that, in the remainder of this chapter, the term "SNR" without instantaneous means the average SNR. The

G_p and K_p are given as

$$G_p = \Gamma\left(\frac{p+2}{2}\right), \text{ and } K_p = \Gamma\left(p+1\right) - \Gamma\left(\frac{p+2}{2}\right)^2. \tag{4.6}$$

4.3.1 No Diversity

Using the means and variances given in Eq. (4.5), one can obtain P_F and P_D as

$$P_F = Q\left(\frac{\tau - \mu_0}{\sigma_0}\right), \text{ and } P_D = Q\left(\frac{\tau - \mu_1}{\sigma_1}\right), \tag{4.7}$$

where $Q(t) = \frac{1}{\sqrt{2\pi}} \int_t^\infty e^{-\left(\frac{x^2}{2}\right)} dx$.

When we consider NU, the mean and the variance of the decision statistic are given by

$$\mu_{0,nu} = G_p \sigma_w^p, \;\; \sigma_{0,nu}^2 = \frac{K_p}{N} \sigma_w^{2p}, \tag{4.8}$$

$$\mu_{1,nu} = G_p (1+\beta\tilde{\gamma})^{\frac{p}{2}} \sigma_w^p, \;\; \sigma_{1,nu}^2 = \frac{K_p}{N} (1+\beta\tilde{\gamma})^p \sigma_w^{2p}, \tag{4.9}$$

where $\mu_{0,nu}$, $\sigma_{0,nu}^2$ and $\mu_{1,nu}$, $\sigma_{1,nu}^2$ correspond to the mean and the variance under H_0 and H_1, respectively and $\tilde{\gamma} = \frac{\sigma_s^2}{\hat{\sigma}_w^2}$ is the average SNR. The subscript nu indicates that the mean and variances are under NU.

Now, P_F and P_D for fixed uncertainty factor β can be obtained by substituting means and variances from Eq. (4.8) and Eq. (4.9) in Eq. (4.7). The threshold τ is chosen as $\lambda \hat{\sigma}_w^p$ for GED, where $\lambda \geq 0$ is a constant. However, when there exists noise uncertainty, β is a random variable. In this case, one can obtain the average P_F and P_D, i.e., $\bar{P}_F$ and $\bar{P}_D$, by averaging the P_F and the P_D obtained for fixed β over the pdf of β given in Eq. (4.3). Since they are functions of random variable β, after carrying out mathematical simplification, $\bar{P}_F$ and $\bar{P}_D$ can be obtained as

$$\bar{P}_F = \int_a^b Q\left(\left(\lambda x^{\frac{p}{2}} - G_p\right)\sqrt{\frac{N}{K_p}}\right) \frac{5}{Lxln(10)} dx, \text{ and} \tag{4.10}$$

$$\bar{P}_D = \int_a^b Q\left(\frac{\lambda x^{\frac{p}{2}} - G_p(1+x\tilde{\gamma})^{\frac{p}{2}}}{(1+x\tilde{\gamma})^{\frac{p}{2}}}\sqrt{\frac{N}{K_p}}\right)\frac{5}{Lxln(10)}dx, \tag{4.11}$$

where, $a = 10^{\frac{-L}{10}}$ and $b = 10^{\frac{L}{10}}$.

To derive the SNR wall, we need to take limits as $N \to \infty$ in the expressions given in Eq. (4.10) and Eq. (4.11). After applying the limit, the reduced expressions for $\bar{P}_F$ and $\bar{P}_D$ are given by Eq. (4.12) and Eq. (4.13), respectively.

$$\bar{P}_F = \begin{cases} 0, & \lambda \geq G_p\,(b)^{\frac{p}{2}} \\ \frac{5}{L\ln(10)}\left[\ln\left(\max\left\{\min\left\{\left(\frac{G_p}{\lambda}\right)^{\frac{2}{p}}, b\right\}, a\right\}\right) - \ln(a)\right], & Gp\,(a)^{\frac{p}{2}} < \lambda < G_p\,(b)^{\frac{p}{2}} \\ 1, & \lambda \leq Gp\,(a)^{\frac{p}{2}} \end{cases} \tag{4.12}$$

$$\bar{P}_D = \begin{cases} 0, & \lambda \geq G_p\,(\tilde{\gamma}+b)^{\frac{p}{2}} \\ \frac{5}{L\ln(10)}\left[\ln\left(\max\left\{\min\left\{\frac{1}{\left(\frac{G_p}{\lambda}\right)^{\frac{2}{p}} - \tilde{\gamma}}, b\right\}, a\right\}\right) - \ln(a)\right], & Gp\,(\tilde{\gamma}+a)^{\frac{p}{2}} < \lambda < G_p\,(\tilde{\gamma}+b)^{\frac{p}{2}} \\ 1, & \lambda \leq Gp\,(\tilde{\gamma}+a)^{\frac{p}{2}} \end{cases} \tag{4.13}$$

Here, we choose not to give the derivation for these expressions since the steps involved in deriving these expressions also appear in Section 4.3.2 for which the steps involved are given in Appendix A.1.

Since the threshold is chosen by setting the value of λ, we need to find λ for which both the conditions given in Eq. (4.4) are satisfied. Using Eq. (4.12) and Eq. (4.13), λ should be chosen as

$$G_p\left(10^{\frac{L}{10}}\right)^{\frac{p}{2}} \geq \lambda \geq G_p\left(\tilde{\gamma} + 10^{\frac{-L}{10}}\right)^{\frac{p}{2}}, \tag{4.14}$$

which gives us the condition on $\tilde{\gamma}$ for unlimited reliability as

$$\tilde{\gamma} \geq 10^{\frac{L}{10}} - 10^{\frac{-L}{10}}. \tag{4.15}$$

The equality sign in Eq. (4.15) gives the lowest SNR for which unlimited reliability can be achieved and hence gives the SNR wall. It can be seen from Eq. (4.15) that when there is no NU, i.e., $L = 0$, it is possible to find the threshold for unlimited reliability for any $\tilde{\gamma} > 0$. Hence, under no noise uncertainty, the GED is unlimitedly reliable. However, when there exists NU, i.e., $L > 0$, GED is not unlimitedly reliable. One can also see from Eq. (4.15) that the SNR wall is independent of the value of p.

4.3.2 pLC Diversity

In pLC diversity scheme, the decision statistic T obtained at all the diversity branches are added and scaled by the total number of diversity branches in order to obtain a new decision statistic. The final decision on primary occupancy is taken after comparing the decision statistic against a threshold. The decision statistic using pLC diversity can be written as

$$T_{plc} = \frac{1}{P} \sum_{i=1}^{P} T_i, \tag{4.16}$$

where, P and T_i represent the total number of diversity branches and the decision statistic obtained at the i^{th} diversity branch, respectively.

In order to make the analysis easy to understand, first we consider a diversity scheme in which we have only two branches, i.e., $P = 2$, which is then extended to any number of diversity branches. Note that in practice the noise uncertainties are different at each diversity branch which makes us to consider varying β's at each branch. Let us also assume that the NU associated with first branch is $\beta_1 = \frac{\hat{\sigma}^2_{w_1}}{\sigma^2_{w_1}}$ and that with branch two is $\beta_2 = \frac{\hat{\sigma}^2_{w_2}}{\sigma^2_{w_2}}$, where $\hat{\sigma}^2_{w_1}$ and $\hat{\sigma}^2_{w_2}$ are the average noise variances at diversity branches 1 and 2, respectively, which are known and $\sigma^2_{w_1}$ and $\sigma^2_{w_2}$ represent the true noise variances. With this setting, we have two noise uncertainties β_1 and β_2 which are uniformly distributed in the range $[-L_1, L_1]$ and $[-L_2, L_2]$, respectively. The NU depends on calibration error, variations in thermal noise and changes in low noise amplifier (LNA) gain and hence different diversity branches can have different noise uncertainties.

Since the decision statistic obtained at two diversity branches, i.e., T_1 and T_2, are Gaussian distributed, the decision statistic T_{plc} also follows Gaussian distribution with means and variances as

$$\mu_{0,nu} = \frac{G_p}{2}\left[\sigma_{w_1}^p + \sigma_{w_2}^p\right], \text{ and } \sigma_{0,nu}^2 = \frac{G_p K_p}{2^2 N}\left[\sigma_{w_1}^{2p} + \sigma_{w_2}^{2p}\right], \tag{4.17}$$

under H_0 and

$$\begin{aligned} \mu_{1,nu} &= \frac{G_p}{2}\left[(1+\beta_1\tilde{\gamma}_1)^{\frac{p}{2}}\sigma_{w_1}^p + (1+\beta_2\tilde{\gamma}_2)^{\frac{p}{2}}\sigma_{w_2}^p\right], \\ \sigma_{1,nu}^2 &= \frac{G_p K_p}{2^2 N}\left[(1+\beta_1\tilde{\gamma}_1)^{p}\sigma_{w_1}^{2p} + (1+\beta_2\tilde{\gamma}_2)^{p}\sigma_{w_2}^{2p}\right], \end{aligned} \tag{4.18}$$

under H_1, respectively. Here, $\tilde{\gamma}_1$ and $\tilde{\gamma}_2$ represent the average SNRs at diversity branches 1 and 2, respectively. We assume that the diversity branches are placed sufficiently far apart so that they are independent and hence can have different SNRs. Note that, though we have obtained mean and variance considering two diversity branches only, this can be extended to any number of diversity branches by following a similar procedure.

Similar to the no diversity case, one can obtain P_F and P_D for fixed β_1 and β_2 by substituting means and variances from Eq. (4.17) and Eq. (4.18) into Eq. (4.7). We know that when there is no diversity, the threshold τ has to be chosen as $\lambda\hat{\sigma}_w^p$ and hence when we consider two diversity branches, the threshold has to be chosen as $\frac{\lambda}{2}\left(\hat{\sigma}_{w_1}^p + \hat{\sigma}_{w_2}^p\right)$. Since $\hat{\sigma}_{w_1}^2$ and $\hat{\sigma}_{w_2}^2$ are known, the threshold in this case can be varied by changing the value of λ. After few mathematical manipulation, P_F and P_D for pLC diversity considering fixed values of β_1 and β_2 can be obtained as

$$P_{F,plc} = Q\left(\frac{2\lambda\beta_1^{\frac{p}{2}}\beta_2^{\frac{p}{2}} - G_p\left(\beta_1^{\frac{p}{2}} + \beta_2^{\frac{p}{2}}\right)}{\sqrt{\beta_1^p + \beta_2^p}}\sqrt{\frac{N}{K_p}}\right) \text{ and,} \tag{4.19}$$

$$P_{D,plc} = Q\left(\frac{2\lambda\beta_1^{\frac{p}{2}}\beta_2^{\frac{p}{2}} - \frac{G_p(1+\beta_1\tilde{\gamma}_1)^{\frac{p}{2}}}{\beta_2^{-\frac{p}{2}}} - \frac{G_p(1+\beta_2\tilde{\gamma}_2)^{\frac{p}{2}}}{\beta_1^{-\frac{p}{2}}}}{\sqrt{\frac{K_p}{N}}\sqrt{(1+\beta_1\tilde{\gamma}_1)^p\beta_2^p + (1+\beta_2\tilde{\gamma}_2)^p\beta_1^p}}\right). \tag{4.20}$$

Now, the NU being a random variable, one can obtain the average probability of false alarm ($\bar{P}_{F,plc}$) and detection ($\bar{P}_{D,plc}$) by averaging $P_{F,plc}$ in Eq. (4.19) and $P_{D,plc}$ in Eq. (4.20) over joint probability density function (jpdf) of random variables β_1 and β_2. Assuming that the two noise uncertainties β_1 and β_2 are independent, the jpdf of β_1 and β_2 can be given by

$$f_{\beta_1,\beta_2}(x,y) = \begin{cases} 0, & x < a_1, y < a_2, \\ \frac{25}{L_1L_2xy[\ln(10)]^2}, & a_1 < x < b_1, a_2 < y < b_2 \\ 0, & x > b_1, y > b_2, \end{cases} \tag{4.21}$$

where, $a_1 = 10^{\frac{-L_1}{10}}$, $b_1 = 10^{\frac{L_1}{10}}$, $a_2 = 10^{\frac{-L_2}{10}}$ and $b_2 = 10^{\frac{L_2}{10}}$. Using Eq. (4.21), $\bar{P}_{F,plc}$ is obtained as

$$\bar{P}_{F,plc} = \int_{a_1}^{b_1}\int_{a_2}^{b_2} Q\left(\frac{2\lambda(xy)^{\frac{p}{2}} - G_p\left(x^{\frac{p}{2}} + y^{\frac{p}{2}}\right)}{\sqrt{x^p + y^p}}\sqrt{\frac{N}{Kp}}\right)\frac{25}{[\ln(10)]^2 L_1L_2xy}dydx. \tag{4.22}$$

Similarly, one can obtain $\bar{P}_{D,plc}$ as

$$\bar{P}_{D,plc} = \int_{a_1}^{b_1}\int_{a_2}^{b_2} Q\left(\frac{2\lambda(xy)^{\frac{p}{2}} - \frac{G_p(1+x\tilde{\gamma}_1)^{\frac{p}{2}}}{y^{-\frac{p}{2}}} - \frac{G_p(1+y\tilde{\gamma}_2)^{\frac{p}{2}}}{x^{-\frac{p}{2}}}}{\sqrt{\frac{K_p}{N}}\sqrt{(1+x\tilde{\gamma}_1)^p y^p + (1+y\tilde{\gamma}_2)^p x^p}}\right)\frac{25}{[\ln(10)]^2 L_1L_2xy}dydx. \tag{4.23}$$

Now, to derive the SNR wall, we need to consider $N \to \infty$ in Eq. (4.22) and Eq. (4.23). After carrying out the mathematical simplifications, the $\bar{P}_{F,plc}$ can be

reduced and the same is given by

$$\bar{P}_{F,plc} = \begin{cases} 0, & \lambda \geq \frac{G_p}{2}\left(e^{\frac{cp}{2}} + e^{\frac{dp}{2}}\right) \\ C_1\left[\frac{dp\,(A_1+A_2)}{2} - \frac{\ln\left(A-e^{-A_2}\right)}{(A_2+\ln(A))^{-1}} + Li_2\left(\frac{A-e^{-A_2}}{A}\right) + \right. & \\ \left. \frac{\ln\left(A-e^{-A_1}\right)}{(A_1+\ln(A))^{-1}} - Li_2\left(\frac{A-e^{-A_1}}{A}\right) + \frac{cdp^2}{2}\right], & \frac{G_p}{2}\left\{e^{\frac{-cp}{2}} + e^{\frac{-dp}{2}}\right\} < \lambda < \frac{G_p}{2}\left(e^{\frac{cp}{2}} + e^{\frac{dp}{2}}\right) \\ 1, & \lambda \leq \frac{G_p}{2}\left(e^{\frac{-cp}{2}} + e^{\frac{-dp}{2}}\right) \end{cases} \tag{4.24}$$

where $Li_n(z)$ represents the polylogarithm [2]. Here also we avoid giving steps involved in the derivation since it involves steps similar to that given in APPENDIX A.1. In the expression given in Eq. (4.24), we have used $c = \ln(b_1)$, $d = \ln(b_2)$, $A = \frac{2\lambda}{G_p}$, $C_1 = \frac{100}{L_1 L_2 [pln(10)]^2}$, $R_1(z) = -\ln\left(A - e^{\frac{zp}{2}}\right)$, $A_1 = \max\left[\frac{-cp}{2}, R_1(-d)\right]$ and $A_2 = \min\left[\frac{cp}{2}, R_1(d)\right]$. Similarly, the expression for $\bar{P}_{D,plc}$ can be derived which can be approximated as given in Eq. (4.25),

$$\bar{P}_{D,plc} \approx \begin{cases} 0, & \lambda \geq \frac{Gp}{2}\left\{\left(\tilde{\gamma}_1 + e^{c}\right)^{\frac{p}{2}} + \left(\tilde{\gamma}_2 + e^{d}\right)^{\frac{p}{2}}\right\} \\ \frac{C_1 p^2}{4}\left(dU_2 + I_1 + 2cd\right), & \frac{Gp}{2}\left\{\left(\tilde{\gamma}_1 + e^{-c}\right)^{\frac{p}{2}} + \left(\tilde{\gamma}_2 + e^{-d}\right)^{\frac{p}{2}}\right\} < \lambda < \frac{Gp}{2}\left\{\left(\tilde{\gamma}_1 + e^{c}\right)^{\frac{p}{2}} + \left(\tilde{\gamma}_2 + e^{d}\right)^{\frac{p}{2}}\right\} \\ 1, & \lambda \leq \frac{Gp}{2}\left\{\left(\tilde{\gamma}_1 + e^{-c}\right)^{\frac{p}{2}} + \left(\tilde{\gamma}_2 + e^{-d}\right)^{\frac{p}{2}}\right\} \end{cases} \tag{4.25}$$

where we use $R_2(z) = -\ln\left(\left(A - \left(e^{z} + \tilde{\gamma}_2\right)^{\frac{p}{2}}\right)^{\frac{2}{p}} - \tilde{\gamma}_1\right)$, $U_2 = \max\left[-c, R_2(-d)\right]$, $U_3 = \min\left[c, R_2(d)\right]$,

$$aa = \left(A - \left(1+\tilde{\gamma}\right)^{\frac{p}{2}}\right)^{\frac{2}{p}}, \;\; \alpha = \frac{-\left[\left(1+\tilde{\gamma}\right)^{\left(\frac{p}{2}-1\right)}\right]}{A - \left(1+\tilde{\gamma}\right)^{\frac{p}{2}}},$$
$$I_1 = \frac{aa}{\alpha}\left(e^{-\alpha U_3} - e^{-\alpha U_2}\right) + \left(1+\tilde{\gamma}_2\right)\left(U_3 - U_2\right) + dU_3.$$

The derivation for $\bar{P}_{D,plc}$ is given in Appendix A.1. Once again, we need to find λ for which both the conditions in Eq. (4.4) are satisfied. Hence, we need to select λ as

$$e^{\frac{cp}{2}} + e^{\frac{dp}{2}} \leq \lambda \geq \left(\tilde{\gamma}_1 + e^{-c}\right)^{\frac{p}{2}} + \left(\tilde{\gamma}_2 + e^{-d}\right)^{\frac{p}{2}}. \tag{4.26}$$

The lowest value of $\tilde{\gamma}_1$ and $\tilde{\gamma}_2$ for which this inequality holds can be found by equating the upper and the lower limits. We can find $\tilde{\gamma}_1$ in terms of $\tilde{\gamma}_2$ for which the upper limit is equal to the lower limit. With this, we get the condition on $\tilde{\gamma}_1$ for unlimited reliability as

$$\tilde{\gamma}_1 \geq \left[e^{\frac{cp}{2}} + e^{\frac{dp}{2}} - \left(\tilde{\gamma}_2 + e^{-d} \right)^{\frac{p}{2}} \right]^{\frac{2}{p}} - e^{-c}. \tag{4.27}$$

Note that, here, we have obtained $\tilde{\gamma}_1$ in terms of $\tilde{\gamma}_2$. However, one can obtain $\tilde{\gamma}_2$ in terms of $\tilde{\gamma}_1$. In Eq. (4.27), one needs to select $\tilde{\gamma}_2$ such that $\tilde{\gamma}_1 \geq 0$ giving us the condition on $\tilde{\gamma}_2$ as

$$0 \leq \tilde{\gamma}_2 \leq \left(e^{\frac{cp}{2}} + e^{\frac{dp}{2}} - e^{\frac{-cp}{2}} \right)^{\frac{2}{p}} - e^{d}. \tag{4.28}$$

The two conditions in Eq. (4.27) and Eq. (4.28) represent the conditions for SNR wall, when we consider the pLC diversity with two diversity branches. Looking at these expressions, one can draw the following conclusions.

- In the absence of NU at the input of both the diversity branches, i.e., $L_1 = L_2 = 0$, from Eq. (4.27) and Eq. (4.28), we get $\tilde{\gamma}_1 > 0$ and $\tilde{\gamma}_2 > 0$. This indicates that, one can find a threshold for which both the conditions in Eq. (4.4) are satisfied at any SNR greater than zero. This means that the sensing scheme is unlimitedly reliable when there is no NU.

- Let us consider that both the branches have same noise uncertainties, i.e., $L_1 = L_2$, and SNR, i.e., $\tilde{\gamma}_1 = \tilde{\gamma}_2$. Substituting $L_1 = L_2 = L$ and $\tilde{\gamma}_1 = \tilde{\gamma}_2 = \tilde{\gamma}$ in Eq. (4.27) we get

  $$\left(\tilde{\gamma} + e^{-c} \right)^{\frac{p}{2}} \geq e^{\frac{cp}{2}} + e^{\frac{dp}{2}} - \left(\tilde{\gamma} + e^{-d} \right)^{\frac{p}{2}}. \tag{4.29}$$

  Since $L_1 = L_2 = L$, we get $c = d$. Substituting for $c = d$ and solving for $\tilde{\gamma}$, we get

  $$\tilde{\gamma} \geq 10^{\frac{L}{10}} - 10^{\frac{-L}{10}}. \tag{4.30}$$

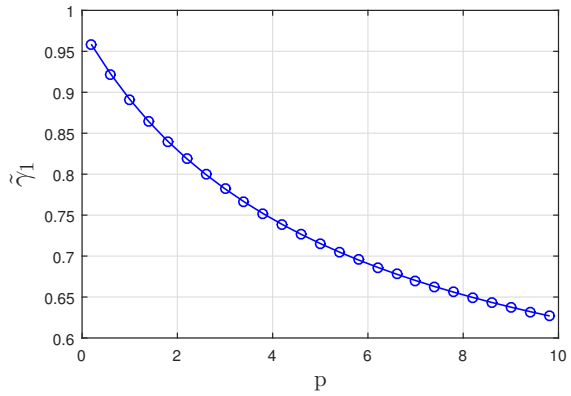

Figure 4.1: p VS. $\tilde{\gamma}_1$ for $\tilde{\gamma}_2 = 0.1$, $L_1 = L_2 = 1\ dB$.

Hence, we get the same SNR wall expression as in Eq. (4.15) that is the SNR wall is the same as in the case of no diversity case. This indicates that, there is no improvement in terms of SNR wall. We also observe that the SNR wall is independent of the value of p.

- In the scenario when both the diversity branches have same SNRs, i.e., $\tilde{\gamma}_1 = \tilde{\gamma}_2 = \tilde{\gamma}$, and different noise uncertainties, i.e., $L_1 \neq L_2$, the SNR walls remain almost the same for all p. For example, with $L_1 = 1\ dB$ and $L_2 = 0.5\ dB$ in Eq. (4.27), we get $\bar{\gamma} = 0.3472$ when $p = 1$ and $\tilde{\gamma} = 0.3677$ as $p \to \infty$ which are approximately the same.

- The advantage of using diversity lies in the fact that the SNR wall is determined by SNRs at different diversity branches, i.e., $\tilde{\gamma}_1$ and $\tilde{\gamma}_2$. Hence, even if the SNR is low at one diversity branch and the other has sufficiently high SNR, we could still satisfy conditions to achieve unlimitedly reliable sensing. For example with $L_1 = L_2 = 1\ dB$ and $p = 2$, the unlimited reliability can be obtained if one of the diversity branches has SNR of 0.3 and the other has SNR of 0.6262.

- The SNR wall depends on the selected value of p, i.e., with increasing value of p, the SNR wall decreases. This is demonstrated with the help of Fig. 4.1, where we plot p VS. $\tilde{\gamma}_1$ for fixed value of $\tilde{\gamma}_2 = 0.1$. We can clearly see that with increasing value of p the value of $\tilde{\gamma}_1$ goes down showing improvement in terms of SNR wall.

- For a fixed value of $\tilde{\gamma}_2$ the smallest value of $\tilde{\gamma}_1$ that can be achieved as we increase p can be found by setting $p \to \infty$ in Eq. (4.27). The value of $\tilde{\gamma}_1$ obtained will now depend on the values of L_1 and L_2. Note that when we consider $L_1 > L_2$, the term $e^{\frac{dp}{2}} - \left(\tilde{\gamma}_2 + e^{-d}\right)^{\frac{p}{2}}$ becomes very small when compared to $e^{\frac{cp}{2}}$ as $p \to \infty$. Under this condition we get

$$\tilde{\gamma}_1 \geq e^{c} - e^{-c} = 10^{\frac{L_1}{10}} - 10^{\frac{-L_1}{10}}. \tag{4.31}$$

Similarly, if $L_2 > L_1$, we get

$$\tilde{\gamma}_1 \geq e^{d} - e^{-c} = 10^{\frac{L_2}{10}} - 10^{\frac{-L_1}{10}}. \tag{4.32}$$

Finally, if $L_1 = L_2 = L$, we get

$$\tilde{\gamma}_1 \geq= 10^{\frac{L}{10}} - 10^{\frac{-L}{10}}. \tag{4.33}$$

For example, with $L_1 = 1\ dB$, $L_2 = 0.5\ dB$ and $\tilde{\gamma}_2 = 0.1$, we require $\tilde{\gamma}_1 \geq 0.4646$ as $p \to \infty$. This shows that with $\tilde{\gamma}_2 = 0.1$, one can have $\tilde{\gamma}_1$ as small as 0.4646 and still get the unlimited performance.

Now the derivation for $P_{F,plc}$ and $P_{D,plc}$ for the two diversity branches given in Eq. (4.19) and Eq. (4.20), respectively, can be extended to P number of branches by selecting the threshold τ as $\tau = \frac{\lambda}{P}(\hat{\sigma}_{w_1}^p + \hat{\sigma}_{w_2}^p + \cdots + \hat{\sigma}_{w_P}^p)$. Following a similar procedure, $P_{F,plc}$ and $P_{D,plc}$ for P number of diversity branches and fixed values of NU factors $\beta_1, \beta_2, \cdots, \beta_P$ are obtained as

$$P_{F,plc} = Q\left(\frac{P\lambda \prod_{i=1}^{P} \beta_i^{\frac{p}{2}} - G_p \sum_{i=1}^{P} \prod_{j=1, j\neq i}^{P} \beta_j^{\frac{p}{2}}}{\sqrt{\sum_{i=1}^{P} \prod_{j=1, j\neq i}^{P} \beta_j^{p}}} \sqrt{\frac{N}{K_p}}\right), \tag{4.34}$$

$$P_{D,plc} = Q\left(\frac{P\lambda\prod_{i=1}^{P}\beta_i^{\frac{p}{2}} - \sum_{i=1}^{P} G_p\left(1+\beta_i\tilde{\gamma}_i\right)^{\frac{p}{2}}\prod_{j=1,j\neq i}^{P}\beta_j^{\frac{p}{2}}}{\sqrt{\frac{K_p}{N}}\sqrt{\sum_{i=1}^{P}\left(1+\beta_i\tilde{\gamma}_i\right)^{p}\prod_{j=1,j\neq i}^{P}\beta_j^{p}}}\right), \tag{4.35}$$

respectively. Averaging the $P_{F,plc}$ and $P_{D,plc}$ in Eq. (4.34) and Eq. (4.35) over jpdf of $\beta_1, \beta_2, \cdots, \beta_P$, we get $\bar{P}_{F,plc}$ and $\bar{P}_{D,plc}$. To derive the SNR wall in this case, one can follow the procedure similar to two diversity branches. To keep it simple, we derive the SNR wall by considering $p = 2$. In this case, to achieve unlimited reliability, we need to select λ as

$$10^{\frac{L_1}{10}} + 10^{\frac{L_2}{10}} + \cdots + 10^{\frac{L_P}{10}} \leq \lambda \leq \tilde{\gamma}_1 + 10^{\frac{-L_1}{10}} + \tilde{\gamma}_2 + 10^{\frac{-L_2}{10}} + \cdots + \tilde{\gamma}_P + 10^{\frac{-L_P}{10}} \tag{4.36}$$

Using this, the SNR wall can be given as

$$\sum_{i=0}^{P}\tilde{\gamma}_i = \sum_{i=0}^{P} 10^{\frac{L_i}{10}} - \sum_{i=0}^{P} 10^{\frac{-L_i}{10}}. \tag{4.37}$$

where, L_i and $\tilde{\gamma}_i$ represent the upper bounds on the NU and the average SNR at the i^{th} diversity branch with $i = 1, 2, \cdots, P$. One can see from Eq. (4.37) that, we need to set the combined SNR, i.e., $\tilde{\gamma}_1 + \tilde{\gamma}_2 + \cdots + \tilde{\gamma}_P$, to achieve unlimited performance. The conclusions that we draw for the case of $P = 2$ can be directly applied to this general case as well.

4.3.3 pLS Diversity

In pLS diversity scheme, the new decision statistic is obtained as the maximum of the decision statistics obtained at the diversity branches which is given as $T_{pls} = max\left\{T_1, T_2, \cdots, T_P\right\}$, where $T_1, T_2, \cdots, T_P$ represent the decision statistics obtained at M diversity branches. The decision on the occupancy of the PU is then taken after comparing T_{pls} against the threshold.

Since we assume that the diversity branches receive independent decision

statistics, the average probability of false alarm can be expressed as

$$\bar{P}_{F,pls} = 1 - \prod_{i=1}^{P} \left(1 - \bar{P}_{F_i}\right), \tag{4.38}$$

where, $\bar{P}_{F_i}$ corresponds to the average probability of false alarm at the i^{th} diversity branch which can be obtained by using Eq. (4.12). Similarly, the average probability of detection in this case can be obtained as

$$\bar{P}_{D,pls} = 1 - \prod_{i=1}^{P} \left(1 - \bar{P}_{D_i}\right), \tag{4.39}$$

where, $\bar{P}_{D_i}$ corresponds to the average probability of detection at the i^{th} diversity branch. The $\bar{P}_{D,pls}$ can be obtained by using Eq. (4.13) in Eq. (4.39).

In this case also, we use $P = 2$ to derive the SNR wall and then extend the analysis to general case. Substituting $P = 2$ in Eq. (4.38), $\bar{P}_{F,pls}$ can be obtained as

$$\bar{P}_{F,pls} = 1 - (1 - \bar{P}_{F_1})(1 - \bar{P}_{F_2}), \tag{4.40}$$

where, $\bar{P}_{F_1}$ and $\bar{P}_{F_2}$ are the average probability of false alarm associated with branches 1 and 2, respectively. It is clear from Eq. (4.40) that to achieve $\lim_{N\to\infty} \bar{P}_{F,pls} = 0$, both $\bar{P}_{F_1}$ and $\bar{P}_{F_2}$ must be 0. Let L_1 and L_2 be upper bound on the uncertainties associated with branches 1 and 2, respectively.

To set $\bar{P}_{F_1} = 0$, using Eq. (4.12) it is clear that λ should be selected as

$$\lambda \geq G_p \left(10^{\frac{L_1}{10}}\right)^{\frac{p}{2}}, \tag{4.41}$$

Similarly, to set $\bar{P}_{F_2} = 0$, λ has to satisfy

$$\lambda \geq G_p \left(10^{\frac{L_2}{10}}\right)^{\frac{p}{2}}, \tag{4.42}$$

Since we need both $\bar{P}_{F_1}$ and $\bar{P}_{F_2}$ as 0, λ has to satisfy

$$\lambda \geq max \left\{ G_p \left(10^{\frac{L_1}{10}} \right)^{\frac{p}{2}}, G_p \left(10^{\frac{L_2}{10}} \right)^{\frac{p}{2}} \right\}, \tag{4.43}$$

After substituting $P = 2$ in Eq. (4.39), we get $\bar{P}_{D,pls}$ as

$$\bar{P}_{D,pls} = 1 - (1 - \bar{P}_{D_1})(1 - \bar{P}_{D_2}), \tag{4.44}$$

where, $\bar{P}_{D_1}$ and $\bar{P}_{D_2}$ are the average probability of detection associated with branch 1 and 2, respectively. We can see from Eq. (4.44) that to achieve $\lim_{N\to\infty} \bar{P}_{D,pls} = 1$, $\bar{P}_{D_1}$ or $\bar{P}_{D_2}$ must be 1. To set $\bar{P}_{D_1} = 1$, λ has to be selected as

$$\lambda \leq G_p \left(10^{\frac{-L_1}{10}} + \tilde{\gamma}_1 \right)^{\frac{p}{2}}. \tag{4.45}$$

Similarly, to set $\bar{P}_{D_2}$ to 1,

$$\lambda \leq G_p \left(10^{\frac{-L_2}{10}} + \tilde{\gamma}_2 \right)^{\frac{p}{2}}. \tag{4.46}$$

Since any one of the conditions given in Eq. (4.45) and Eq. (4.46) must be satisfied to get $\bar{P}_{D,pls} = 1$, they can be written in compact form as

$$\lambda \leq max \left\{ G_p \left(10^{\frac{-L_1}{10}} + \tilde{\gamma}_1 \right)^{\frac{p}{2}}, G_p \left(10^{\frac{-L_2}{10}} + \tilde{\gamma}_2 \right)^{\frac{p}{2}} \right\} \tag{4.47}$$

In order to see the implications of the conditions given in Eq. (4.43) and Eq. (4.47), let us consider $L_1 > L_2$. In this case, the conditions on $\tilde{\gamma}_1$ and $\tilde{\gamma}_2$ can be given by

$$\tilde{\gamma}_1 \geq 10^{\frac{L_1}{10}} - 10^{\frac{-L_1}{10}} \text{ OR } \tilde{\gamma}_2 \geq 10^{\frac{L_1}{10}} - 10^{\frac{-L_2}{10}}. \tag{4.48}$$

From this the SNR wall for pLS diversity is obtained by considering equality sign in Eq. (4.48). Hence, to achieve unlimited reliability, SNR at the input of any one branch has to be $\geq$ its respective SNR wall. To understand this let us take $L_1 = 0.5\ dB$ and $L_2 = 0.3\ dB$. Substituting in Eq. (4.48), we get $\tilde{\gamma}_1 = 0.2308$ and $\tilde{\gamma}_2 =$

0.1888. Therefore, to achieve unlimited reliability we must have either $\tilde{\gamma}_1 \geq 0.2308$ or $\tilde{\gamma}_2 \geq 0.1888$. One can also see from Eq. (4.48) that unlike pLC case the SNR wall in this case is independent of p. Another advantage of pLS diversity is that any one branch should have SNR $\geq$ its SNR wall and hence even if the other branch is experiencing worst channel condition, one can achieve the unlimited reliability with sufficiently high SNR at other branch. Following a similar procedure, the analysis for $P = 2$ can be extended to any P and is given as

$$\tilde{\gamma}_i \geq 10^{\frac{L^+}{10}} - 10^{\frac{-L_i}{10}}, \text{ for } i = 1, 2, \cdots, P, \tag{4.49}$$

where, $L^+ = \max[L_1, L_2, \cdots, L_P]$. In this case, to achieve unlimited reliability, any one among P conditions in Eq. (4.49) must be satisfied.

4.3.4 CSS with Hard Combining

Until now we discussed about deriving the SNR walls when we consider the diversity. We now discuss the same when CSS is used where multiple CSUs collaborate by sharing their information in order to detect the presence or the absence of the PU. Let us consider that there are M number of independent CSUs and each one of them receive N samples during the observation interval. We denote the true and average noise variance at the i^{th} CSU as $\sigma^2_{w_i}$ and $\hat{\sigma}^2_{w_i}$, respectively, where $i = 1, 2, \cdots, M$. Note that, we are not considering diversity reception for CSUs. The decision statistic obtained at the i^{th} CSU is denoted as T_i. Once again we assume that the NU factor β_i at the i^{th} CSU is uniformly distributed in the interval $[-L_i, L_i]$. In the case of hard decision combining, all the CSUs take independent decisions regarding the occupancy of PU and send the results as ON/OFF to the fusion center (FC). The FC then takes the final decision considering all the received decisions. Let $\bar{Q}_F$ and $\bar{Q}_D$ denote the average probability of false alarm and detection at the FC, respectively. When using CSS, one has to modify the definition of SNR wall which is given as follows. Given the different SNRs ($\tilde{\gamma}_i > 0$) at the

SUs, $i = 1, 2, \cdots, M$, if there exists a threshold for which

$$\lim_{N\to\infty} \bar{Q}_F = 0 \text{ and } \lim_{N\to\infty} \bar{Q}_D = 1, \tag{4.50}$$

then the sensing scheme is considered as unlimitedly reliable [139]. We require $\bar{Q}_F$ and $\bar{Q}_D$ as $N \to \infty$ in order to derive the SNR wall and to derive the same, first we need to obtain average probability of false alarm $(\bar{P}_{F_i})$ and detection $(\bar{P}_{D_i})$ for the i^{th} CSU considering $N \to \infty$. Using Eq. (4.10) and Eq. (4.11), $\bar{P}_{F_i}$ and $\bar{P}_{D_i}$ for $N \to \infty$ can be written as

$$\bar{P}_{F_i} = \begin{cases} 0, & \lambda \geq G_p \left(b_i\right)^{\frac{p}{2}} \\ \frac{5}{L_i \ln(10)} \left[\ln\left(\max\left\{\min\left\{\left(\frac{G_p}{\lambda}\right)^{\frac{2}{p}}, b_i\right\}, a_i\right\}\right) - \ln\left(a_i\right)\right], & Gp\left(a_i\right)^{\frac{p}{2}} < \lambda < G_p\left(b_i\right)^{\frac{p}{2}} \\ 1, & \lambda \leq Gp\left(a_i\right)^{\frac{p}{2}} \end{cases} \tag{4.51}$$

$$\bar{P}_{D_i} = \begin{cases} 0, & \lambda \geq G_p \left(\tilde{\gamma}_i + b_i\right)^{\frac{p}{2}} \\ \frac{5}{L_i \ln(10)} \left[\ln\left(\max\left\{\min\left\{\frac{1}{\left(\frac{G_p}{\lambda}\right)^{\frac{2}{p}} - \tilde{\gamma}_i}, b_i\right\}, a_i\right\}\right) - \ln\left(a_i\right)\right], & Gp\left(\tilde{\gamma}_i + a_i\right)^{\frac{p}{2}} < \lambda < G_p\left(\tilde{\gamma}_i + b_i\right)^{\frac{p}{2}} \\ 1, & \lambda \leq Gp\left(\tilde{\gamma}_i + a_i\right)^{\frac{p}{2}} \end{cases} \tag{4.52}$$

where, $a_i = 10^{\frac{-L_i}{10}}$, $b_i = 10^{\frac{L_i}{10}}$ and $\tilde{\gamma}_i$ is the average SNR at the i^{th} CSU. Using these one can obtain $\bar{Q}_F$ and $\bar{Q}_D$ which can then be used to investigate the SNR wall for three combining rules, i.e., OR, AND and k out of M combining rule.

OR Rule

In OR combining rule, the FC declares the PU as active whenever at least one of the CSUs reports the channel as occupied. Considering this, we first derive the SNR wall for $M = 2$ only and then extend the result to any number of CSUs. Let L_1 and L_2 be the upper bounds on the NU factors and $\tilde{\gamma}_1$ and $\tilde{\gamma}_2$ be the SNRs at

the two CSUs. In this case, $\bar{Q}_F$ and $\bar{Q}_D$ at the FC can be written as

$$\bar{Q}_F = \bar{P}_{F_1} + \bar{P}_{F_2} - \bar{P}_{F_1}\bar{P}_{F_2} \text{ and } \bar{Q}_D = \bar{P}_{D_1} + \bar{P}_{D_2} - \bar{P}_{D_1}\bar{P}_{D_2}. \tag{4.53}$$

From Eq. (4.53), it is clear that to satisfy $\lim_{N\to\infty} \bar{Q}_F = 0$, we need both $\bar{P}_{F_1}$ and $\bar{P}_{F_2}$ to be 0. Hence, using Eq. (4.51), one has to set the λ at both the CSUs as

$$\lambda \geq G_p \left(10^{\frac{L_1}{10}}\right)^{\frac{p}{2}} \text{ AND } \lambda \geq G_p \left(10^{\frac{L_2}{10}}\right)^{\frac{p}{2}}. \tag{4.54}$$

The condition in Eq. (4.54) can be written in compact form as

$$\lambda \geq max \left\{ G_p \left(10^{\frac{L_1}{10}}\right)^{\frac{p}{2}}, G_p \left(10^{\frac{L_2}{10}}\right)^{\frac{p}{2}} \right\} \tag{4.55}$$

Similarly, to satisfy the condition $\lim_{N\to\infty} \bar{Q}_D = 1$, we see from Eq. (4.53) that P_{D_1} or P_{D_2} must be 1. Once again, using the Eq. (4.52), we need to set λ as

$$\lambda \leq G_p \left(10^{\frac{-L_1}{10}} + \tilde{\gamma}_1\right)^{\frac{p}{2}} \text{ OR } \lambda \leq G_p \left(10^{\frac{-L_2}{10}} + \tilde{\gamma}_2\right)^{\frac{p}{2}}. \tag{4.56}$$

If we assume $L_1 > L_2$, then using the Eq. (4.55) and Eq. (4.56), λ to be chosen for unlimited reliability should satisfy

$$\begin{aligned} &G_p \left(10^{\frac{L_1}{10}}\right)^{\frac{p}{2}} \leq \lambda \leq G_p \left(10^{\frac{-L_1}{10}} + \tilde{\gamma}_1\right)^{\frac{p}{2}}, \text{ OR} \\ &G_p \left(10^{\frac{L_1}{10}}\right)^{\frac{p}{2}} \leq \lambda \leq G_p \left(10^{\frac{-L_2}{10}} + \tilde{\gamma}_2\right)^{\frac{p}{2}}. \end{aligned} \tag{4.57}$$

Using Eq. (4.57), the condition on $\tilde{\gamma}_1$ and $\tilde{\gamma}_2$ can be given as

$$\tilde{\gamma}_1 \geq 10^{\frac{L_1}{10}} - 10^{\frac{-L_1}{10}} \text{ OR } \tilde{\gamma}_2 \geq 10^{\frac{L_1}{2}} - 10^{\frac{-L_2}{10}}. \tag{4.58}$$

Therefore the SNR wall for the OR case is obtained by considering equality condition in Eq. (4.58). To understand this, let us take $L_1 = 1\ dB$ and $L_2 = 0.5\ dB$. Substituting in Eq. (4.58), we get $\tilde{\gamma}_1 = 0.4646$ and $\tilde{\gamma}_2 = 0.3676$. Therefore one can achieve unlimited reliability if $\tilde{\gamma}_1 \geq 0.4646$ or $\tilde{\gamma}_2 \geq 0.3676$. One can also see from

Eq. (4.58) that the SNR wall in this case is independent of p.

Following a similar procedure, the conditions given for the case of $M = 2$ in Eq. (4.58) can be extended to any M as

$$\tilde{\gamma}_i \geq 10^{\frac{L^+}{10}} - 10^{\frac{-L_i}{10}}, \text{ for } i = 1, 2, \cdots, M, \tag{4.59}$$

where $L^+ = \max\{L_1, L_2, \cdots, L_M\}$. In this case, to achieve unlimited reliability, any one among M conditions in Eq. (4.59) must be satisfied.

AND Rule

Here, the FC declares the channel as occupied only when all the CSUs declare the PU channel as occupied. Similar to OR case, here also we first derive SNR wall by considering $M = 2$ and then extend it to any M. The $\bar{Q}_F$ and $\bar{Q}_D$ can be written as

$$\bar{Q}_F = \bar{P}_{F_1}\bar{P}_{F_2} \text{ and } \bar{Q}_D = \bar{P}_{D_1}\bar{P}_{D_2}. \tag{4.60}$$

It is clear from Eq. (4.60) that in order to satisfy the condition on $\bar{Q}_F$ in Eq. (4.50), either $\bar{P}_{F_1}$ or $\bar{P}_{F_2}$ must be 0. Hence, one has to select λ as

$$\lambda \geq \min\left\{ G_p\left(10^{\frac{L_1}{10}}\right)^{\frac{p}{2}}, G_p\left(10^{\frac{L_2}{10}}\right)^{\frac{p}{2}} \right\}. \tag{4.61}$$

Similarly, to satisfy the condition on $\bar{Q}_D$, both $\bar{P}_{D_1}$ and $P_{\bar{D}_2}$ in Eq. (4.60) must be 1 and hence we need to set λ as

$$\lambda \leq G_p\left(10^{\frac{-L_1}{10}} + \tilde{\gamma}_1\right)^{\frac{p}{2}} \text{ AND } \lambda \leq G_p\left(10^{\frac{-L_2}{10}} + \tilde{\gamma}_2\right)^{\frac{p}{2}}. \tag{4.62}$$

Once again assuming $L_1 > L_2$ and using Eq. (4.61) and Eq. (4.62), λ has to be selected as

$$G_p\left(10^{\frac{L_2}{10}}\right)^{\frac{p}{2}} \leq \lambda \leq G_p\left(10^{\frac{-L_1}{10}} + \tilde{\gamma}_1\right)^{\frac{p}{2}} \text{ AND } G_p\left(10^{\frac{L_2}{10}}\right)^{\frac{p}{2}} \leq \lambda \leq G_p\left(10^{\frac{-L_2}{10}} + \tilde{\gamma}_2\right)^{\frac{p}{2}}. \tag{4.63}$$

Using this, $\tilde{\gamma}_1$ and $\tilde{\gamma}_2$ in this case should satisfy

$$\tilde{\gamma}_1 \geq 10^{\frac{L_2}{10}} - 10^{\frac{-L_1}{10}} \text{ AND } \tilde{\gamma}_2 \geq 10^{\frac{L_2}{10}} - 10^{\frac{-L_2}{10}}. \tag{4.64}$$

From this, the equality condition in the Eq. (4.64) gives us the SNR walls for the two CSUs. Once again considering $L_1 = 1\ dB$ and $L_2 = 0.5\ dB$, the unlimitedly reliable performance can be obtained if $\tilde{\gamma}_1 \geq 0.3277$ and $\tilde{\gamma}_2 \geq 0.2308$. Note that, in this case both the SNRs have to satisfy the inequality conditions. The conditions given in Eq. (4.64) can be extended to any number of M and is given by Eq. (4.59) with $L^+ = \min\{L_1, L_2, \cdots, L_M\}$. Note that all the SNRs must be $\geq$ their respective SNR walls in order to achieve unlimited reliability.

k Out Of M Combining Rule

In this rule, FC declares the channel as occupied when k out of the total of M CSUs report the PU channel as occupied. For this case, we first derive the SNR wall by considering $M = 3$ and $k = 2$, and then extend the result to general case of any M and k. With this setting, $\bar{Q}_F$ and $\bar{Q}_D$ can be written as

$$\bar{Q}_F = \bar{P}_{F_1}\bar{P}_{F_2} + \bar{P}_{F_2}\bar{P}_{F_3} + \bar{P}_{F_1}\bar{P}_{F_3} - 2\bar{P}_{F_1}\bar{P}_{F_2}\bar{P}_{F_3}, \tag{4.65}$$

$$\bar{Q}_D = \bar{P}_{D_1}\bar{P}_{D_2} + \bar{P}_{D_2}\bar{P}_{D_3} + \bar{P}_{D_1}\bar{P}_{D_3} - 2\bar{P}_{D_1}\bar{P}_{D_2}\bar{P}_{D_3}, \tag{4.66}$$

Now for $\lim_{N\to\infty} \bar{Q}_F = 0$, we must have any of the two $\bar{P}_{F_i}$s, $i = 1, 2, 3$ must be 0 in Eq. (4.65). Therefore, λ has to be selected such that

$$\begin{aligned}
&\lambda \geq \max\left\{G_p\left(10^{\frac{L_1}{10}}\right), G_p\left(10^{\frac{L_2}{10}}\right)\right\}, \text{ OR} \\
&\lambda \geq \max\left\{G_p\left(10^{\frac{L_2}{10}}\right), G_p\left(10^{\frac{L_3}{10}}\right)\right\}, \text{ OR} \\
&\lambda \geq \max\left\{G_p\left(10^{\frac{L_1}{10}}\right), G_p\left(10^{\frac{L_3}{10}}\right)\right\}.
\end{aligned} \tag{4.67}$$

To achieve the other condition of $\lim_{N\to\infty} \bar{Q}_D = 1$, using Eq. (4.66), any two $\bar{P}_{D_i}$s, for $i = 1, 2, 3$ must be 1 which is obtained by setting λ as

$$\begin{aligned}
\lambda &\leq \min\left\{ G_p\left(10^{\frac{-L_1}{10}} + \tilde{\gamma}_1\right)^{\frac{p}{2}}, G_p\left(10^{\frac{-L_2}{10}} + \tilde{\gamma}_2\right)^{\frac{p}{2}} \right\} \text{ OR} \\
\lambda &\leq \min\left\{ G_p\left(10^{\frac{-L_1}{10}} + \tilde{\gamma}_1\right)^{\frac{p}{2}}, G_p\left(10^{\frac{-L_3}{10}} + \tilde{\gamma}_3\right)^{\frac{p}{2}} \right\} \text{ OR} \\
\lambda &\leq \min\left\{ G_p\left(10^{\frac{-L_2}{10}} + \tilde{\gamma}_2\right)^{\frac{p}{2}}, G_p\left(10^{\frac{-L_3}{10}} + \tilde{\gamma}_3\right)^{\frac{p}{2}} \right\}
\end{aligned} \tag{4.68}$$

In order to see the implications of these conditions, let us consider $L_1 > L_2 > L_3$. Using Eq. (4.67) and Eq. (4.68), the conditions on $\tilde{\gamma}_1$, $\tilde{\gamma}_2$ and $\tilde{\gamma}_3$ can be given by

$$\tilde{\gamma}_1 \geq 10^{\frac{L_2}{10}} - 10^{\frac{-L_1}{10}}, \tilde{\gamma}_2 \geq 10^{\frac{L_2}{10}} - 10^{\frac{-L_2}{10}}, \tilde{\gamma}_3 \geq 10^{\frac{L_2}{10}} - 10^{\frac{-L_3}{10}}. \tag{4.69}$$

Therefore, for $k = 2$ any two conditions given in Eq. (4.69) must be satisfied, in order to get unlimited reliability. Equality sign in Eq. (4.69) then gives us the SNR wall for 2 out of 3 rule. One can also see from Eq. (4.69) that the SNR wall in this case is independent of the value of p. As an example, let us take $L_1 = 1\ dB$, $L_2 = 0.7\ dB$ and $L_3 = 0.5\ dB$. Substituting in Eq. (4.69), we get the SNR walls for 3 CSUs as $\tilde{\gamma}_1 = 0.3806$, $\tilde{\gamma}_2 = 0.3238$ and $\tilde{\gamma}_3 = 0.2836$. Therefore one can achieve unlimited reliability if any two of the SNRs at the CSUs are $\geq$ to their respective SNR wall values.

Following the similar procedure, the conditions given for the case of $M = 3$ in Eq. (4.69) can be extended to any k out of M CSUs and is given by Eq. (4.59) with $L^+ = \min\{k \text{ largest from } (L_1, L_2, \cdots, L_M)\}$. For example, with $M = 3$, $k = 2$ and $L_1 > L_2 > L_3$ then $L^+ = L_2$ and we arrive at Eq. (4.69). Note that, to achieve unlimited reliability, any k SNRs must be $\geq$ their respective SNR walls. In TABLE 4.1, we list the SNR wall under OR, AND and k out of M combining rule when hard combining is used. We consider $k = 2$ for k out of M combining rule. Note that, the value of k also represents the required number of SNRs are to be $\geq$ their respective SNR walls at the CSUs in order to get the unlimited reliability. Looking at Table 4.1, one may notice that, though the SNR wall values that we get for OR

Table 4.1: Comparison of SNR walls for hard combining. Here, $M = 3$, $L_1 = 1\ dB$, $L_2 = 0.7\ dB$ and $L_3 = 0.5\ dB$.

Decision Rule	$\tilde{\gamma}_1$	$\tilde{\gamma}_2$	$\tilde{\gamma}_3$	k
OR	0.4646	0.4077	0.3677	1
AND	0.3277	0.2708	0.2307	3
2 out of 3	0.3806	0.3238	0.2836	2

combining rule are higher when compared to other two rules, it requires only a one SNR to be $\geq$ the respective SNR wall value to achieve unlimited reliability. When AND combining rule is used, the SNR wall values are smallest but we require all three SNRs $\geq$ their SNR wall values for achieving unlimited reliability. With k out of M combining rule, the SNR wall values lie between those of OR and AND combining rules, and any k SNR values at the CSUs have to be $\geq$ their respective SNR wall values. The use of combining rule depends on the channel conditions of the secondary users (SUs). If one of the SUs is experiencing good channel conditions so that the received SNR is high, then it is better to use OR combining rule. On the other hand, if all the SUs are experiencing low SNRs due to faded channel conditions, then one can employ AND combining rule. The K out N rule is useful when few secondary users are having good channel conditions.

4.3.5 CSS with Soft Combining

We investigate the SNR wall for soft decision combining when equal gain combining (EGC) is used at the FC. Here, the decision on PU being ON/OFF is not taken by the CSUs. Instead, the decision statistics from all the CSUs are sent to the FC where they are added to obtain a new decision statistic and the decision is taken by FC based this. Let T_i be the decision statistic at the i^{th} CSU. Then, the new decision statistic at the FC is obtained as

$$T = \frac{1}{M} \sum_{i=1}^{M} T_i. \tag{4.70}$$

We see that, the derivation for $\bar{Q}_F$ and $\bar{Q}_D$ in this case is same as that of $\bar{P}_{F,plc}$ and $\bar{P}_{D,plc}$ for pLC diversity given in Section 4.3.2, only the interpretation of the variables change. Specifically, L_i and $\tilde{\gamma}_i$ used in Section 4.3.2 are now interpreted as the upper bound on the NU and the average SNR at the i^{th} CSU.

4.4 SNR Wall for Fading Channel

In this section we first derive $\bar{P}_D$ under Nakagami fading and NU for both no diversity and diversity cases. Since we know that $\bar{P}_F$ is independent of SNR, here we give the derivation for $\bar{P}_D$ only. We then discuss the SNR wall for each case.

4.4.1 No Diversity

The instantaneous SNR when we consider fading and no NU is given by $\gamma = |h|^2 \frac{\sigma_s^2}{\sigma_w^2} = |h|^2 \frac{\sigma_s^2}{\hat{\sigma}_w^2}$ since $\sigma_w^2 = \hat{\sigma}_w^2$ in this case. This SNR at the input of the SU with Nakagami fading depends upon the random fading channel gain ζ as given in [15] as

$$f_\zeta(z) = \frac{m^m}{\Gamma(m)} z^{m-1} e^{-mz},\ z \geq 0, \tag{4.71}$$

where, m represents the Nakagami parameter. To obtain average probability of detection under Nakagami fading, i.e., $\bar{P}_D^{Nak}$, we need to replace $\tilde{\gamma}$ with $\bar{\gamma}\zeta$ in Eq. (4.11) and average over the pdf of ζ given in Eq. (4.71) where $\bar{\gamma}$ is the average SNR when fading is considered. Note that $\tilde{\gamma}$ defined earlier in Section 4.3 is different from $\bar{\gamma}$. With this, $\bar{P}_D^{Nak}$ under Nakagami fading can be written as

$$\bar{P}_D^{Nak} = \int_0^\infty \int_a^b Q\left(\frac{\lambda x^{\frac{p}{2}} - G_p(1+\bar{\gamma}xz)^{\frac{p}{2}}}{(1+\bar{\gamma}xz)^{\frac{p}{2}}} \sqrt{\frac{N}{K_p}} \right) \frac{5}{Lx\ln(10)} \frac{m^m}{\Gamma(m)} z^{m-1} e^{-mz} dx dz. \tag{4.72}$$

Now, to obtain the SNR wall, we need to apply limit $N \to \infty$ to Eq. (4.72). In order to derive the expression, we define $R_3(z) = \left(\frac{1}{\bar{\gamma}} \left(\frac{\lambda}{G_p} \right)^{\frac{2}{p}} - \frac{1}{z\bar{\gamma}} \right)$, $U_5 = \max[0, R_3(a)]$ and $U_6 = \max[0, R_3(b)]$. After carrying out the mathematical sim-

plifications, the $\bar{P}_D^{Nak}$ can be expressed as

$$\bar{P}_D^{Nak} = \frac{5}{L\ln(10)}\Bigg[\left(1-\left(\frac{\lambda}{G_p}\right)^{\frac{2}{p}}\right)\left[P\left(m,mU_6\right)-P\left(m,mU_5\right)\right]-\ln\left(a\right)Q(m,mU_5) + \bar{\gamma}\left[P\left(m+1,mU_6\right)-P\left(m+1,mU_5\right)\right]+\ln\left(b\right)Q\left(m,mU_6\right)\Bigg] \quad (4.73)$$

given in Eq. (4.73) which is given on the top of next page, where $P\left(a,z\right)$ and $Q\left(a,z\right)$ represent the regularized lower and lower incomplete Gamma functions [2]. The derivation for the same is given in Appendix A.2.

Once the $\bar{P}_D^{Nak}$ is obtained, we need to obtain the condition on λ such that both the conditions in Eq. (4.4) are satisfied. To get $\lim\limits_{N-\rightarrow\infty}\bar{P}_D^{Nak}=1$, using Eq. (4.72) we get the condition on λ as

$$\lambda \leq Gp\left(10^{\frac{-L}{10}}\right)^{\frac{p}{2}}, \quad (4.74)$$

Using Eq. (4.12), to set $\bar{P}_F=0$, we need to select λ as

$$\lambda \geq Gp\left(10^{\frac{L}{10}}\right)^{\frac{p}{2}}, \quad (4.75)$$

One can notice that, these two conditions can not be satisfied simultaneously. For example, with $L=1\ dB$, we need $\lambda \geq 1.2589$ to make $\bar{P}_F^{Nak}=0$ and $\lambda \leq 0.7943$ to achieve $\bar{P}_D^{Nak}=1$. Such contradictory conditions arise because of the approximation of decision statistic as Gaussian. Hence, the expression given in Eq. (4.73) can never reach 1 for $\lambda \geq Gp\left(10^{\frac{L}{10}}\right)^{\frac{p}{2}}$. In such a situation, one can find the SNR wall numerically which can be done as follows. The condition given in Eq. (4.75) implies that to obtain $\lim_{N\rightarrow\infty}\bar{P}_F=0$, we need to choose $\lambda \geq G_p\left(10^{\frac{L}{10}}\right)^{\frac{p}{2}}$. Now to maximize the probability of detection, we have to select the threshold as small as possible and hence λ can be chosen as $G_p\left(10^{\frac{L}{10}}\right)^{\frac{p}{2}}$. With this, the SNR wall can be obtained by using this chosen threshold in Eq. (4.73) and finding the lowest value of SNR, i.e., $\bar{\gamma}$, for which $\bar{P}_D^{Nak}$ approximates 1. With $\lambda \geq G_p\left(10^{\frac{L}{10}}\right)^{\frac{p}{2}}$, the $\bar{P}_D^{Nak}$ never reaches 1 and hence we consider the SNR wall as that value of $\bar{\gamma}$ for which Eq. (4.73) approximates to 1, for example say 0.99. With $p=2$, $L=0.5\ dB$

and $m = 2$, we get the SNR wall as $\bar{\gamma} = 1.841$. For the same parameter settings, when we do not consider fading $\tilde{\gamma} = 0.2308$.

4.4.2 pLC Diversity

The $\bar{P}_{D,plc}^{Nak}$ considering two diversity branches can be obtained by averaging $\bar{P}_{D,plc}$ in Eq. (4.23) over the pdfs of ζ_1 and ζ_2 which is given by

$$\bar{P}_{D,plc}^{Nak} = C_2 \int_0^{\infty}\int_0^{\infty}\int_{a_1}^{b_1}\int_{a_2}^{b_2} Q\left(\frac{2\lambda(xy)^{\frac{p}{2}} - \frac{G_p(1+\bar{\gamma}_1 xz)^{\frac{p}{2}}}{y^{-\frac{p}{2}}} - \frac{G_p(1+\bar{\gamma}_2 yw)^{\frac{p}{2}}}{x^{-\frac{p}{2}}}}{\sqrt{\frac{K_p}{N}}\sqrt{(1+\bar{\gamma}_1 xz)^p y^p + (1+\bar{\gamma}_2 yw)^p x^p}}\right) \frac{1}{xy}(zw)^{m-1} e^{-m(z+w)} dydxdzdw. \tag{4.76}$$

where $C_2 = \frac{25m^{2m}[\Gamma(m)]^{-2}}{L_1 L_2 \ln(10)^2}$. Here, $\bar{\gamma}_1$ and $\bar{\gamma}_2$ represent average SNRs under fading at diversity branches 1 and 2, respectively. Note that, we can reduce this expressions following the procedure given in Appendix A.2 for no diversity case but the final expression becomes too lengthy and complicated. Hence, in Appendix A.3, we give few initial steps of reduction to arrive at Eq. (4.77) which has three integrals to be reduced.

$$\bar{P}_{D,plc}^{Nak} = C_2 \int_0^{\infty}\int_0^{\infty}\int_{\ln(a_1)}^{\ln(b_1)} \left[\max\left[\min\left[\ln(b_2), -\ln\left(\left(A - \left(\gamma_1 z + e^{-t}\right)^{\frac{p}{2}}\right)^{\frac{2}{p}} - \gamma_2 w\right)\right], \ln(a_2)\right] - \ln(a_2)\right] z^{m-1} e^{-mz} w^{m-1} e^{-mw} dtdzdw \tag{4.77}$$

Here, we assume that both the diversity branches are experiencing independent fading. The analysis for $\bar{P}_{D,plc}^{Nak}$ can be extended to P diversity branches by following the similar procedure and in that case the expression has $2P$ integrals where P integrals are for averaging over NU and another P for averaging over the fading.

In this case also, the SNR wall has to be obtained numerically for the same reason explained in Section 4.4.1. Using Eq. (4.24), to achieve $\lim_{N\to\infty} \bar{P}_{F,plc} = 0$, we get the condition on λ as

$$\lambda \geq \frac{G_p}{2}\left(\left(10^{\frac{L_1}{10}}\right)^{\frac{p}{2}} + \left(10^{\frac{L_2}{10}}\right)^{\frac{p}{2}}\right). \tag{4.78}$$

In this case, the SNR wall when both the diversity branches have the same SNR can be obtained by using $\bar{\gamma}_1 = \bar{\gamma}_2 = \bar{\gamma}$ in Eq. (4.77) and finding $\bar{\gamma}$ by considering $\lambda = (G_p/2)\left(\left(10^{\frac{L_1}{10}}\right)^{\frac{p}{2}} + \left(10^{\frac{L_2}{10}}\right)^{\frac{p}{2}}\right)$ for which $\bar{P}_{D,plc}^{Nak}$ attains 0.99. For example, with $L_1 = L_2 = 0.5\ dB$, $p = 2$ and $m = 2$, we get the SNR wall at the two diversity branches as $\bar{\gamma}_1 = \bar{\gamma}_2 = 0.67$. For no diversity case with $L = 0.5$, we get SNR wall as $\bar{\gamma} = 1.82$. We can observe that with the use of pLC diversity, we get improvement in terms of SNR wall. Finding SNR wall when we consider $\bar{\gamma}_1 \neq \bar{\gamma}_2$ is not possible unless we have additional constraints, since substituting λ in Eq. (4.77) results in one equation with two unknowns which has infinite solutions. In this case, one can find the SNR wall by fixing the value of SNR at one of the diversity branches and then finding the other value numerically. For example, with the same parameter settings as given above and with $\bar{\gamma}_1 \neq \bar{\gamma}_2$, one combination of SNR for which unlimitedly reliable performance can be obtained is $\bar{\gamma}_1 = 0.5$ and $\bar{\gamma}_2 = 0.84$. One can follow the similar procedure to obtain the SNR wall when we consider more number of diversity branches.

4.4.3 pLS Diversity

The average probability of detection under Nakagami fading, i.e., $\bar{P}_{D,pls}^{Nak}$, can be obtained by using Eq. (4.39) and Eq. (4.73). The average probability of false alarm remains the same as in AWGN case given in Eq. (4.38).

In this case, one can select λ as given in Eq. (4.43) and substitute the same in Eq. (4.73) to obtain the SNR walls for two diversity branches numerically. For example, with $L_1 = 0.5\ dB$, $L_2 = 0.3\ dB$, $m = 2$, and $p = 2$, we get the SNR walls at the two branches as $\bar{\gamma}_1 = 1.82$ and $\bar{\gamma}_2 = 1.71$. Once again, we see that any one of the two branches should have SNR above their respective SNR wall values to achieve the unlimited reliability. Similar procedure can be followed to obtain SNR wall for the general case of P diversity branches. In this case also, the SNR walls are independent of the value of p.

4.4.4 CSS with Hard Combining

We now consider the cooperative spectrum sensing scenario. In this case, to derive $\bar{Q}_F$ and $\bar{Q}_D$, we need to obtain the average probability of false alarm ($\bar{P}_{F_i}^{Nak}$) and detection ($\bar{P}_{D_i}^{Nak}$) at the i^{th} CSU under Nakagami fading. Since $\bar{P}_{F_i}^{Nak}$ is independent of SNR, it remains the same as that of AWGN case given in Eq. (4.51). The derivation of $\bar{P}_{D_i}^{Nak}$ is the same as that of Eq. (4.73) which can be obtained by replacing L and $\tilde{\gamma}$ with L_i and $\tilde{\gamma}_i$, respectively, in Eq. (4.73) and is given as

$$\bar{P}_{D_i}^{Nak} = \frac{5}{L_i \ln(10)} \Bigg[\left(1 - \left(\frac{\lambda}{G_p}\right)^{\frac{2}{p}}\right) \left[P\left(m, mU_6\right) - P\left(m, mU_5\right)\right] - \ln\left(a_i\right) Q(m, mU_5) + \bar{\gamma}_i \left[P\left(m+1, mU_6\right) - P\left(m+1, mU_5\right)\right] + \ln\left(b_i\right) Q\left(m, mU_6\right) \Bigg] \quad (4.79)$$

where, $R_3(z) = \left(\frac{1}{\bar{\gamma}_i}\left(\frac{\lambda}{G_p}\right)^{\frac{2}{p}} - \frac{1}{z\bar{\gamma}_i}\right)$, $U_5 = \max\left[0, R_3(a_i)\right]$ and $U_6 = \max\left[0, R_3(b_i)\right]$.

Here, we derive the SNR walls considering k out of M rule and the other two are discussed as the special cases. We first derive them by considering $M = 3$ and $k = 2$ and then extend it to general case. Using Eq. (4.51) and Eq. (4.79), to achieve $\bar{P}_{F_i} = 0$ and $\bar{P}_{D_i} = 1$, we need to select λ as

$$\lambda \geq G_p \ \left(b_i\right)^{\frac{p}{2}} \text{ and } \lambda \leq G_p \ \left(a_i\right)^{\frac{p}{2}} \text{ for } i = 1, 2, 3, \quad (4.80)$$

respectively. Suppose we consider $L_1 > L_2 > L_3$. In that case, using Eq. (4.80), we need to set $\lambda \geq G_p (b_2)^{\frac{p}{2}}$ and $\lambda \leq G_p \left(a_2\right)^{\frac{p}{2}}$, respectively. However, these two conditions are contradictory and cannot be satisfied simultaneously. For example, with $p = 2$, $L_1 = 1\ dB$, $L_2 = 0.7\ dB$ and $L_3 = 0.5\ dB$, we need to select $\lambda \geq 1.1749$ and $\lambda \leq 0.8511$. In such a situation, the expression given in Eq. (4.79) can never reach 1 for $\lambda \geq G_p \left(b_2\right)^{\frac{p}{2}}$ and we need to obtain the SNR walls numerically which can be done as follows. Note that, we always try to set λ as small as possible since it maximizes the probability of detection. Hence, choosing $\lambda = G_p \left(b_2\right)^{\frac{p}{2}}$, the SNR wall for i^{th} CSU can be found by using this threshold in Eq. (4.79) and by finding the lowest values of SNR, i.e., $\bar{\gamma}_i$ $i = 1, 2, 3$, for which $\bar{P}_{D_i}^{Nak} \approx 1$. To do this, one may consider the SNR for which $\bar{P}_{D_i}^{Nak}$ reaches 0.99 (close to 1) as the SNR wall.

Table 4.2: Comparison of SNR walls for hard combining under Nakagami fading. Here, $M = 3$, $L_1 = 1\ dB$, $L_2 = 0.7\ dB$ and $L_3 = 0.5\ dB$.

Decision Rule	$\bar{\gamma}_1$	$\bar{\gamma}_2$	$\bar{\gamma}_3$	k
2 out of 3	2.88	2.62	2.49	2
OR	3.85	3.67	3.58	1
AND	2.32	2.02	1.84	3

For example, for the chosen uncertainties, we get the SNR walls as $\bar{\gamma}_1 = 2.88$, $\bar{\gamma}_2 = 2.62$ and $\bar{\gamma}_3 = 2.49$. Since $k = 2$, the SNRs at any two CSUs must be $\geq$ their respective SNR walls in order to achieve unlimited reliability. The case of $M = 3$ can be extended to any M by choosing the threshold as $\lambda = G_p\left(10^{\frac{L^+}{10}}\right)^{\frac{p}{2}}$, where $L^+ = \min\{k \text{ largest from } (L_1, L_2, \cdots, L_M)\}$, and finding $\bar{\gamma}_i$ for which $\bar{P}_{D_i}^{Nak}$ approximates 1. In this case, any k SNRs must be $\geq$ their respective SNR walls in order to achieve unlimited reliability. We next discuss OR and AND combining as the special cases of k out of M combining rule where the procedure to obtain SNR wall remains the same but the value of L^+ changes.

OR Combining

In OR combining, FC declares PU channel as occupied when at least one CSU declares channel as occupied. The SNR wall in this can be obtained by choosing $k = 1$ in k out of M rule. Hence, we get $L^+ = \max\{L_1, L_2, \cdots, L_M\}$. Similar to k out of M rule, by choosing the threshold as $\lambda = G_p\left(10^{\frac{L^+}{10}}\right)^{\frac{p}{2}}$ in Eq. (4.79) and finding the smallest $\bar{\gamma}_i$ for which we get $\bar{P}_{D_i}^{Nak} \approx 1$ gives us the SNR walls. Here, SNR at any one CSU needs to be $\geq$ its respective SNR wall in order to get unlimited reliability.

AND Combining

When AND combining is used, PU is considered as occupied when all the CSUs report it as occupied and using $k = M$ one can get the SNR walls. with $k = M$ we get $L^+ = \min\{L_1, L_2, \cdots, L_M\}$. Following the procedure similar to OR case one can easily obtain the SNR walls numerically. Note that, since $k = M$, all CSUs must have SNRs $\geq$ their SNR walls in this case.

In TABLE 4.2, we list the SNR walls for different combining rules where the value of k represents the required number of SNRs that are to be $\geq$ their respective SNR walls at the CSUs in order to get the unlimited reliability. One can see that the values of SNR walls obtained for the AND case are the lowest but we need to have SNRs of all CSU above these values to achieve unlimited reliability. Although, the SNR walls for OR combining are high, only one CSU needs to have SNR $\geq$ its SNR wall. For k out of M rule, the SNR wall values lie between OR and AND combining rule. Another important point worth mentioning is that, the SNR walls for hard combining are independent of p, i.e., we get the same SNR wall values as given in TABLE 4.2 for any value of p.

4.4.5 CSS with Soft Combining

We need to obtain the SNR in this case numerically for the same reasons explained in Section 4.4.4. Once again, the process to obtain the SNR wall remains same as that for pLC diversity under Nakagami fading given in Section 4.4.2. The conclusions drawn in Section 4.4.2 are also valid in this case with L_i and $\bar{\gamma}_i$ representing upper bound on the NU and the average SNR under Nakagami fading at the i^{th} CSU, respectively.

4.5 Results and Discussion

In this section, we validate the theoretical analysis that is carried out using Monte Carlo simulations. For simulation, we generate both the PU signal and the noise as complex Gaussian and the results are averaged over 10^5 iterations. We first validate the expressions for SNR walls derived in Section 4.3 for the case of AWGN channel. Then the validation of the same for fading case given in Section 4.4 is discussed.

4.5.1 SNR wall for AWGN Case

In this section, we consider experiments to verify the validity of SNR wall expressions derived in Section 4.3 and 4.4. Since our major contribution lies in deriving

the SNR wall by considering diversity and CSS, we show the plots for validating the expressions for diversity and CSS cases only. We have already shown that the SNR wall is independent of p for pLS diversity and CSS with hard combining. Therefore, we illustrate the validity of SNR wall by considering any p for pLC diversity and by considering $p = 2$ for pLS diversity and CSS (hard combining). Note that, one can easily obtain the plots to validate SNR walls for no diversity, pLS diversity and CSS with hard combining with any p but to avoid repetition of similar plots we have omitted those plots.

In Section 4.3.2 (Fig. 4.1), we conclude that with increase in the value of p, the SNR wall decreases. We first validate this conclusion using Monte Carlo simulation. Here, we plot threshold τ VS. detection probabilities $\bar{P}_{F,plc}$, $\bar{P}_{D,plc}$, by selecting a large N as required in establishing the SNR wall condition and by choosing $L_1 = L_2 = 1\ dB$ and $\tilde{\gamma}_2 = 0.1$. The infinite sample size is approximated by a very large N, i.e., $N = 10^7$. Fig. 4.2(a) and Fig. 4.2(b) are plotted for $p = 1$ and $p = 5$, respectively. The vertical line in Fig. 4.2 gives us the threshold τ for which both the conditions in Eq. (4.4) are satisfied. This means that if we set $\tau \approx 0.9944$ for $p = 1$ and choose a very large value of N, we can achieve $\bar{P}_{F,plc} = 0$ and $\bar{P}_{D,plc} = 1$. In both these figures we can see that unlimited performance is indeed achieved but the required value of $\tilde{\gamma}_1$ (see Fig. 4.1) to achieve unlimited reliability for $p = 1$ is 0.8914 where as for $p = 5$ it is 0.7153. We see that the value of SNR wall required at the branch 1 for $p = 5$ is 0.9958 dB lower than that for $p = 1$. One can also obtain plots by choosing the values of $\tilde{\gamma}_1$ and $\tilde{\gamma}_2$ not satisfying the SNR wall conditions. In that case, it is not possible to find τ for which the conditions in Eq. (4.4) are satisfied. The plots in Fig. 4.2 are shown for the scenario where both the diversity branches have different SNRs. One can also validate the other conclusions drawn in Section 4.3.2.

In Fig. 4.3, we show the plots of τ VS. detection probabilities for pLS diversity with two branches. The simulation is carried out using $L_1 = 0.5\ dB$ and $L_2 = 0.3\ dB$. On substituting L_1 and L_2 in Eq. (4.48), we obtain the SNR walls as $\tilde{\gamma}_1 = 0.2308$ and $\tilde{\gamma}_2 = 0.1888$. As discussed in Section 4.3.3, any one of the SNRs at the two branches must be $\geq$ their respective SNR wall values in order to achieve

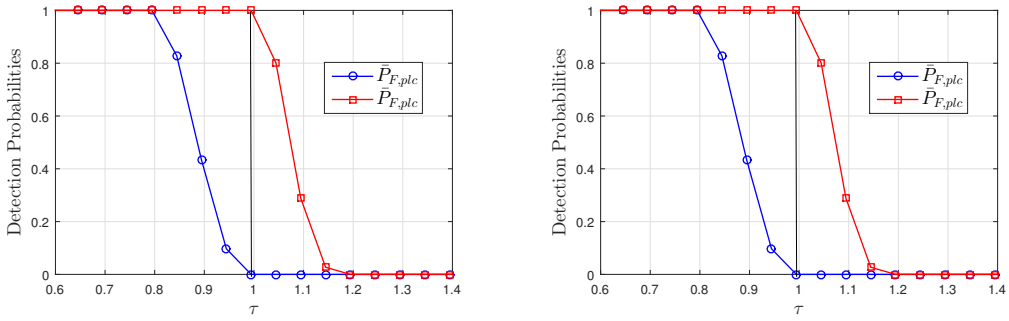

Figure 4.2: Threshold (τ) VS. detection probabilities for pLC diversity with two branches under AWGN channel using $L_1 = 1\ dB$, $L_2 = 1\ dB$, $\tilde{\gamma}_2 = 0.1$, $N = 10^7$ (a) for $p = 1$ and $\tilde{\gamma}_1 = 0.8914$ (b) for $p = 5$ and $\tilde{\gamma}_1 = 0.7153$.

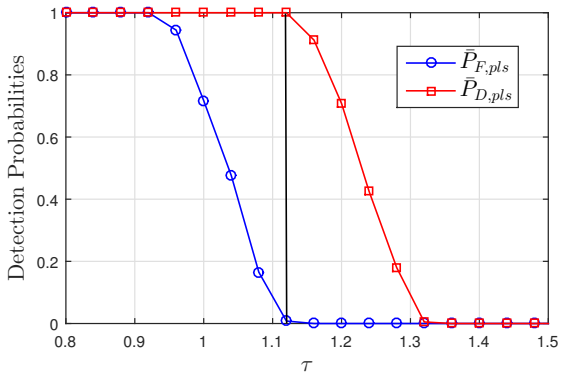

Figure 4.3: Threshold (τ) VS. detection probabilities for pLS diversity with two branches under AWGN channel using $L_1 = 0.5\ dB$, $L_2 = 0.3\ dB$, $\tilde{\gamma}_1 = 0.2$, $\tilde{\gamma}_2 = 0.1888$, $p = 2$, $N = 10^7$.

unlimited reliability. Hence, we choose $\tilde{\gamma}_1 = 0.2$ which is below the SNR wall at first diversity branch and $\tilde{\gamma}_2 = 0.1888$ which is equal to the SNR wall value at the second branch. It can be seen from Fig. 4.3 that by setting $\tau \approx 1.12$ and using high N, one can achieve unlimitedly reliable performance. This is shown by the vertical line in Fig. 4.3.

We next show the plots for CSS with one of the hard decision combining, i.e., k out of M combining rule. In Fig. 4.4, we demonstrate the SNR wall for k out of M combining rule and consider three CSUs, i.e., $M = 3$, having $L_1 = 1\ dB$, $L_2 = 0.7\ dB$ and $L_3 = 0.5\ dB$ with $k = 2$. Using these parameters in Eq. (4.69), we compute the SNR walls as $\tilde{\gamma}_1 = 0.3806$, $\tilde{\gamma}_2 = 0.3238$ and $\tilde{\gamma}_3 = 0.2836$. In Fig. 3, we show the plots by choosing $\tilde{\gamma}_1 = 0.2$ which is below the required value of

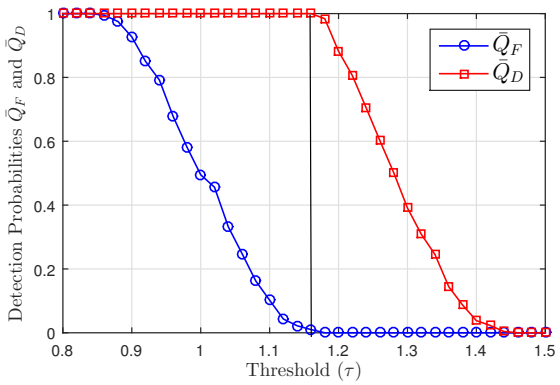

Figure 4.4: Plots of τ VS. $\bar{Q}_F$ and $\bar{Q}_D$ for k out of M combining rule. Here, $N = 10^6$, $M = 3$, $L_1 = 1\ dB$, $L_2 = 0.7\ dB$, $L_3 = 0.5\ dB$, $p = 2$, $\tilde{\gamma}_1 = 0.2$, $\tilde{\gamma}_2 = 0.3238$ and $\tilde{\gamma}_3 = 0.2836$.

SNR wall and $\tilde{\gamma}_2 = 0.3238$ and $\tilde{\gamma}_3 = 0.2836$ which are equal to their SNR walls. Since we have $k = 2$, and 2 out of 3 CSUs have the inputs with SNR $\geq$ their SNR walls, an unlimited operation is obtained. We can see from Fig. 4.4 that choosing a value of $\tau = 1.16$ (threshold corresponding to the vertical line) gives the unlimited reliability, i.e., choosing this threshold value with two of the three SNRs $\geq$ their SNR walls gives us $\bar{Q}_F = 0$ and $\bar{Q}_D = 1$. In order to reduce the repetition of the similar plots, here we give plots for k out of M combining rule only. One can show similar plots for OR as well as AND combining rules.

The SNR wall for CSS with soft combining is similar to the pLC diversity. Hence, one can consider plots given in Fig. 4.2 to understand the SNR walls for soft combining. For CSS with soft combining $\tilde{\gamma}_1$ and $\tilde{\gamma}_2$ represent the average SNRs at CSU 1 and 2, respectively, and L_1 and L_2 represent the NU levels at CSU 1 and 2, respectively. We can see that for fixed value of SNR at CSU 2, i.e., $\tilde{\gamma}_2 = 0.1$, the required value of SNR at CSU 1, i.e., $\tilde{\gamma}_1$, in order to achieve unlimited reliability is 0.8914 for $p = 1$ and 0.7153 for $p = 5$ showing the improvement in SNR wall with increasing value of p.

4.5.2 SNR Wall for Fading Case

In this section we consider fading in addition to noise uncertainty and use Monte Carlo simulations to validate the SNR wall. We first consider the case of no diversity and then extend it diversity and CSS. As already discussed, the SNR walls

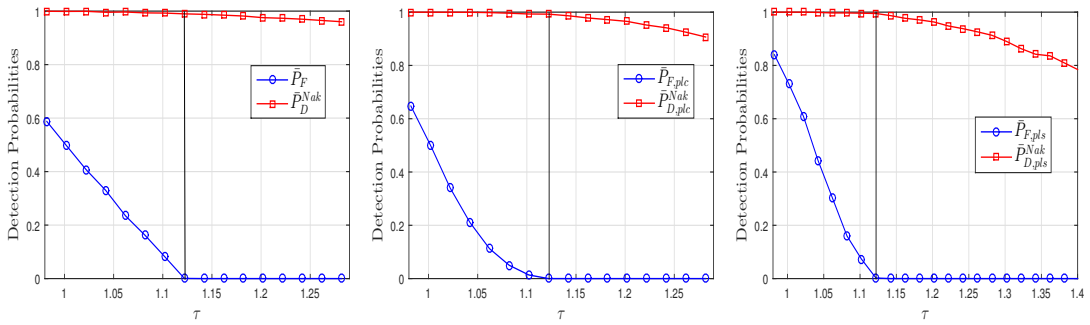

(a) (b) (c)

Figure 4.5: Threshold (τ) VS. detection probabilities for no diversity under Nakagami fading channel using $p = 2$, $N = 10^7$ for (a) no diversity with $L = 0.5\ dB$, $\bar{\gamma} = 1.82$, (b) pLC diversity using $L_1 = L_2 = 0.5\ dB$, $\bar{\gamma}_1 = \bar{\gamma}_2 = 0.67$ and (c) pLS diversity using $L_1 = 0.5\ dB$, $L_2 = 0.3$, $\bar{\gamma}_1 = 0.1$, $\bar{\gamma}_2 = 1.71$.

in this case have been obtained numerically and one can find a threshold theoretically for which the probability of false alarm is 0 with infinite sample size. We then need to find the SNR for which the probability of detection becomes 1 with this threshold to get the SNR wall.

In Fig. 4.5(a), we show the plots for no diversity case. As discussed in Section 4.4.1, to achieve $\bar{P}_F^{Nak} = 0$, λ should satisfy the condition given in Eq. (4.75). For $L = 0.5\,dB$ and $p = 2$, using Eq. (4.75), we get $\lambda \geq 1.122$. As already discussed, we always try to set the threshold as small as possible and hence we choose $\lambda = 1.122$. Since we assume $\hat{\sigma}_w^2 = 1$, λ gives us the threshold. Using this λ in Eq. (4.73) and finding $\bar{\gamma}$ for which $\bar{P}_D^{Nak} = 1$ gives us the SNR wall as $\bar{\gamma} = 1.82$. In Fig. 4.5(a), the vertical line shows that we can achieve unlimited reliability by setting $\tau = 1.122$. Note that, here we have shown plot for $p = 2$ only. In this case, it turns out that the SNR wall is independent of value of p. Hence, for any value of p, SNR wall values will remain the same.

We next consider the case of pLC diversity. Here, we assume that both the diversity branches have the same SNRs, i.e., $\bar{\gamma}_1 = \bar{\gamma}_2 = \bar{\gamma}$ and we choose $L_1 = L_2 = 0.5\ dB$. Using Eq. (4.78), we obtain the threshold as $\tau = \lambda = 1.122$. Using this threshold in Eq. (4.77) to find the values of $\bar{\gamma}_1$ and $\bar{\gamma}_2$ for which $\bar{P}_{D,plc}^{Nak} = 1$ give us the SNR walls as $\bar{\gamma}_1 = 0.67$ and $\bar{\gamma}_2 = 0.67$. The vertical line at $\tau = 1.122$ in Fig. 4.5(b) shows that by choosing $\tau = 1.122$ with large sample size, one can

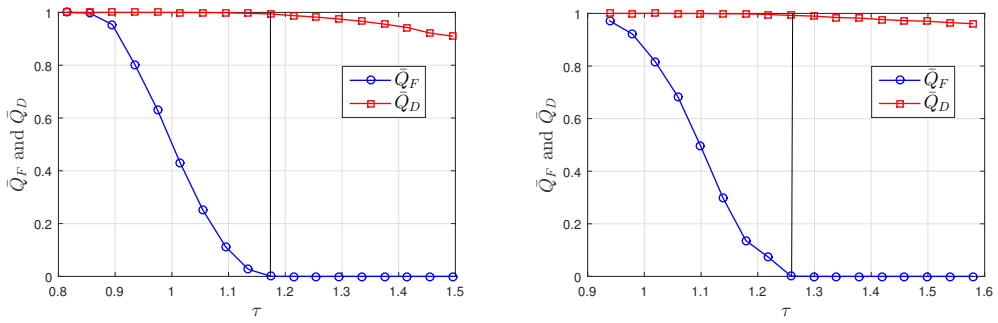

(a) (b)

Figure 4.6: Threshold (τ) VS. $\bar{Q}_F$ and $\bar{Q}_D$, for hard combining under fading channel using $N = 10^7$, $M = 3$, $p = 2$, (a) k out of M combining, (b) OR combining.

obtain $\bar{P}_{F,plc} = 0$ and $\bar{P}_{D,plc}^{Nak} = 1$. Note that, although we have shown the plots by considering only one case of $\bar{\gamma}_1 = \bar{\gamma}_2$ and $L_1 = L_2$, one can obtain SNR wall for different scenarios where $\bar{\gamma}_1 \neq \bar{\gamma}_2$ and $L_1 \neq L_2$. For example, with $L_1 = L_2 = 0.5\ dB$, we get one combination of SNR walls as $\bar{\gamma}_1 = 0.5$ and $\bar{\gamma}_2 = 0.84$ which also gives the sum as 1.34. Similarly, with $\bar{\gamma}_1 = \bar{\gamma}_2$ with $L_1 = 0.5\ dB$ and $L_2 = 0.3\ dB$, we get the SNR walls as $\bar{\gamma}_1 = \bar{\gamma}_2 = 0.64$.

In Fig. 4.5(c), we demonstrate the SNR wall for pLS diversity under fading. We choose $L_1 = 0.5\ dB$ and $L_2 = 0.3\ dB$, and hence using Eq. (4.43), we get the threshold as $\lambda = 1.122$. Using Eq. (4.39) and Eq. (4.72), we get the SNR walls as $\bar{\gamma}_1 = 1.82$ and $\bar{\gamma}_2 = 1.71$. As discussed in Section 4.4.3, any one diversity branch should have SNR $\geq$ its respective SNR wall value to achieve unlimited reliability. In Fig. 4.5(c), we choose $\bar{\gamma}_1 = 0.1$ which is below to its SNR wall value and $\bar{\gamma}_2 = 1.71$ which is equal the SNR wall. The vertical line in Fig. 4.5(c) shows that unlimited performance can be obtained by using the given setting. As done in case of pLC, one can consider different scenarios to obtain SNR wall in this case as well.

We next validate the SNR wall for hard combining obtained in Section 4.4.4 and listed in TABLE 4.2. In Fig. 4.6(a), we show the plot of τ VS. $\bar{Q}_F$ and $\bar{Q}_D$, for k out of M rule considering $L_1 = 1\ dB$, $L_2 = 0.7\ dB$, $L_3 = 0.5\ dB$, $k = 2$ and $M = 3$. For these parameters, we obtained the SNR walls as listed in TABLE 4.2. In Fig. 4.6(a), we show the plots by choosing $\bar{\gamma}_1 = 0.3$ which is below the required value of SNR wall and $\bar{\gamma}_2 = 2.62$ and $\bar{\gamma}_1 = 2.49$ which are equal to their respective SNR

walls. Since we have $k = 2$, and 2 out of 3 CSUs have the inputs with SNR $\geq$ their SNR walls, we should get the unlimited reliability. We can see from Fig. 4.6(a) that choosing a value of $\tau = 1.1749$ gives us the unlimited reliability which is marked as the vertical line. We next validate the OR combining with the same parameter settings. We get the SNR walls as $\bar{\gamma}_1 = 3.85$, $\bar{\gamma}_2 = 3.67$ and $\bar{\gamma}_1 = 3.58$. In this case, it is required that at least one CSU has the SNR $\geq$ its SNR wall in order to achieve the unlimited reliability. With $\bar{\gamma}_1 = 0.1$, $\bar{\gamma}_2 = 0.1$ and $\bar{\gamma}_1 = 3.58$, the plot in Fig. 4.6(b) shows the vertical line at $\tau = 1.2589$ to get the unlimited reliability. One can also show similar plot for AND combining. Here, we need to choose SNRs at all the CSUs $\geq$ their SNR walls which are listed in TABLE 4.2. Finally, the SNR wall for soft combining under Nakagami fading is similar to that of pLC where $\bar{\gamma}_1$ and $\bar{\gamma}_2$ interpreted as SNRs at CSUs 1 and 2, respectively. We can consider plot in Fig. 4.5(b) as the plot for soft combining under Nakagami fading.

4.6 Conclusion

In this work, we study the SNR wall for generalized energy detector under no diversity, diversity and CSS in the presence of both the NU and the fading. We consider hard as well as soft combining for CSS. We derive closed form expressions for $\bar{P}_F$ and $\bar{P}_D$ for no diversity, diversity and CSS considering very large sample size. Using those expressions, we first derive the SNR wall for AWGN channel case under NU. This analysis is then extended to the case when there exist Nakagami fading in addition to NU in which the SNR wall is obtained numerically. All the derived expressions are validated using Monte Carlo simulations. Our future research work involves analysis of SNR wall for GED by considering noise uncertainty and more general fading models.

CHAPTER 5

Wideband Spectrum Sensing Under Fading: Use of Diversity

In all our previous works, we looked at the problem of narrowband spectrum sensing. In this work, we consider wideband spectrum sensing (WSS) where multiple frequency bands are sensed for finding spectrum opportunities. If the SUs can sense multiple frequency bands at a time, they provide multiple spectrum opportunities. Authors in [96, 97], propose the optimal multiband joint detection for WSS in CR. The bank of multiple narrowband detectors are jointly optimized to improve the aggregate opportunistic throughput of a CR system while limiting the interference to the PU system. The Nyquist sampling rate required to sample the wideband is very high and can be practically challenging. In order to overcome this problem, many researchers have attempted the use of compressed sensing to acquire the signal at sub-Nyquist rates [8, 30, 79, 107, 118, 130]. However, these sampling schemes are complex and their implementation is expensive. In general, a SU may not be interested in finding all the spectrum opportunities, instead the interest lies in finding sufficient numbers of spectrum opportunity. For example, a SU may be interested in finding a single spectrum opportunity for its transmission. This can be achieved if we consider only a part of the wideband spectrum for sensing. Keeping this into consideration, authors in [112] propose partial band Nyquist sampling (PBNS) which samples part of the wideband instead of entire wideband thus reducing the sampling rate.

Different detection techniques have been proposed by the researchers for finding the presence or the absence of signal while using WSS. Authors in [112], have

proposed two detection algorithms, namely, channel by channel detection (CCD) and ranked channel detection (RCD) by considering the primary signal and the noise as additive white Gaussian noise (AWGN). However, in practice, the received signal often undergoes fading. Limited work is done on WSS considering the fading [34, 110]. In [20], the performance of these detection algorithms is analyzed for two different fading channels, namely, Rayleigh and Nakagami fading. None of these approaches consider diversity reception. It may be of interest to note that the performance can be improved by using diversity reception. Limited work is done on the use of diversity to improve the performance of WSS [6, 99]. Here in this work, we propose two new detection algorithms, namely, ranked square law combining (R-SLC) and ranked square law selection (R-SLS), where SLC and SLS diversities are used to improve the performance of WSS under fading. In our work we use PBNS as the wideband sampling scheme. We provide complete theoretical analysis of the proposed detection algorithms under Nakagami fading channel. To quantify the performance we use recently proposed performance metrics, namely, the probability of excessive interference opportunity (P_{EIO}) and the probability of insufficient spectrum opportunity (P_{ISO}) [112]. Mathematical analysis is verified by Monte Carlo simulation. We also study the effect of different parameters on the performance of the proposed algorithms. We observe that proposed algorithms outperform RCD without diversity. Also, the R-SLC algorithm performs better than R-SLS. Note that throughout this chapter, when detection algorithm is used without the diversity it is referred to as RCD and when used with the diversity they are referred to as R-SLC and R-SLS.

5.1 System Model and Performance Metrics

The wideband signal is modeled as the collection of U subbands, i.e., narrowband channels, each of bandwidth B_0 making the total bandwidth as $B = UB_0$. In [8, 9, 55, 94, 112, 113], similar channel model is used. The primary transmission within each subband is subject to flat fading. Let H_m denotes the primary occupancy of the m^{th} subband, with $H_m = 0$ and $H_m = 1$ corresponding to PU being OFF

and ON, respectively. We assume that the occupancy status of the PU remains unchanged during the observation interval. It is also assumed that all the PUs have equal priorities. In this work, the discussion is restricted to one sensing window with a fixed duration of $T_w = UNT_N$, where $F_N = 1/T_N = 2B$ is the Nyquist sampling frequency and N represents number of Nyquist samples per subband. We would like to mention here that the terms subband and channel are used interchangeably.

We assume that the occupancy status of subbands as well as their transmissions are independent of each other. Assuming the occupancy probability (OP) of subbands as p, the state of each subband is modeled by a Bernoulli random variable and the probability mass function (PMF) of the same given as

$$f(H_m, p) = \begin{cases} p, & \text{if } H_m = 1 \\ 1-p, & \text{if } H_m = 0. \end{cases} \tag{5.1}$$

With the number of ON channels as K, PMF of primary occupancy is given by Binomial distribution as

$$f(K, U, p) = \binom{U}{K} p^K (1-p)^{U-K}. \tag{5.2}$$

Note that in order to detect the free primary channels the detector has to decide on their presence or absence. The received signal at the SU due to m^{th} primary subband can now be modeled as

$$y_m(t) = h_m \cdot s_m(t) + n_m(t), \tag{5.3}$$

where, $s_m(t)$ represents the transmitted signal in the m^{th} primary subband, $n_m(t)$ represents AWGN and h_m represents the channel coefficient for the m^{th} primary subband. Note that, in this chapter we do not consider noise uncertainty.

Authors in [51, 55, 79, 118, 127] use mean-square estimation error (MSE) as the criteria for measuring performance. In [8, 53, 94, 107], the probability of miss detection (P_M) and false alarm (P_F) or their average over the channels are used

as performance measures. These measures are more suitable for single channel detection. However, the goal of WSS can be different from that of single channel sensing. The SUs in CR may not be interested in finding all the spectrum opportunities. A fraction of spectrum opportunities may be sufficient for the SUs and hence WSS can tolerate much higher P_F. Keeping this in perspective, new performance metrics are proposed in [112] that are more suitable for WSS. We use these two new performance metrics, i.e., P_{EIO} and P_{ISO}, in order to characterize the performance of the detection algorithms. Let S be the number of spectrum opportunity, i.e., the number of successfully identified OFF channels and let S_d be the desired number of spectrum opportunity. Then P_{ISO} is defined as

$$P_{ISO} = Pr\{S < S_d\} \tag{5.4}$$

where, Pr represents probability. Similarly, P_{ISO} is defined as

$$P_{EIO} = Pr\{I > I_d\}. \tag{5.5}$$

where, I represents the number of missed ON channels and I_d corresponds to the maximum number of allowed interference to the primary channels.

5.2 Detection Algorithms

Various diversity schemes have been studied in the literature [12, 37, 38, 58, 102], to name a few, maximum ratio combining (MRC), equal gain combining (EGC), square law selection (SLS), switched combining, square law combining (SLC), etc. MRC represents the optimal combining technique and it gives the best possible performance that can be achieved by using diversity. However, the disadvantage here is that it requires complete channel state information (CSI) at the SU and hence the complexity is very high. EGC is a suboptimal diversity technique and has reduced complexity compared to the MRC technique. Though it does not require channel fading amplitudes, we still need to use channel carrier phase estimation. The SLS combining technique selects the strongest signal branch for

detection and is simple to implement when compared to MRC and EGC. In SLC diversity scheme, the decision statistic obtained at all the diversity branches are added in order to obtain new decision statistic and the decision is taken based on that. Both SLS and SLC are non-coherent combining schemes and are easy to implement. Taking into consideration all the above points, we propose two new detection algorithms, namely, R-SLC and R-SLS, which use SLC and SLS diversities, respectively.

5.2.1 Ranked Square law Combining (R-SLC) Detection

Consider P diversity branches that receive wideband signal consisting of U channels. The PBNS is used at the input of all the diversity branches. As already discussed earlier, a SU may not be interested in finding all the spectrum opportunity, instead the interest lies in finding sufficient numbers of SO. This motivates the idea of PBNS, which samples only the fraction of the entire wideband at the corresponding Nyquist rate. PBNS is characterized by the number of channels in the partial band (L) and filters out L channels from the wideband having M channels. The received signal after filtering is sampled at the Nyquist rate of $2LB_0$ on which the fast Fourier transform (FFT) is performed. We take N samples for each channel. Hence, the number of samples in the sensing window is NL. Let $V[k]$ denote the frequency samples in PBNS. Then, $V[k] = Y[k],\ \text{for } 0 \leq k \leq NL-1$, where $Y[k]$ denotes the normalized discrete Fourier transform (DFT) of the received wideband signal consisting of U channels. The energy within m^{th} narrowband channel is then calculated as

$$T_m = \sum_{k \in I_m} |V[k]|^2, \tag{5.6}$$

where $1 \leq m \leq L$ and I_m is the set of frequency indices that fall into channel m.

Fig. 5.1, represents the block schematic of R-SLC detection schemes and the steps involved in implementing it are given in Algorithm 1. As shown in Fig. 5.1, energies are computed for each of the L channels from all P diversity branches. The energies within each of the L channels from all the diversity branches are

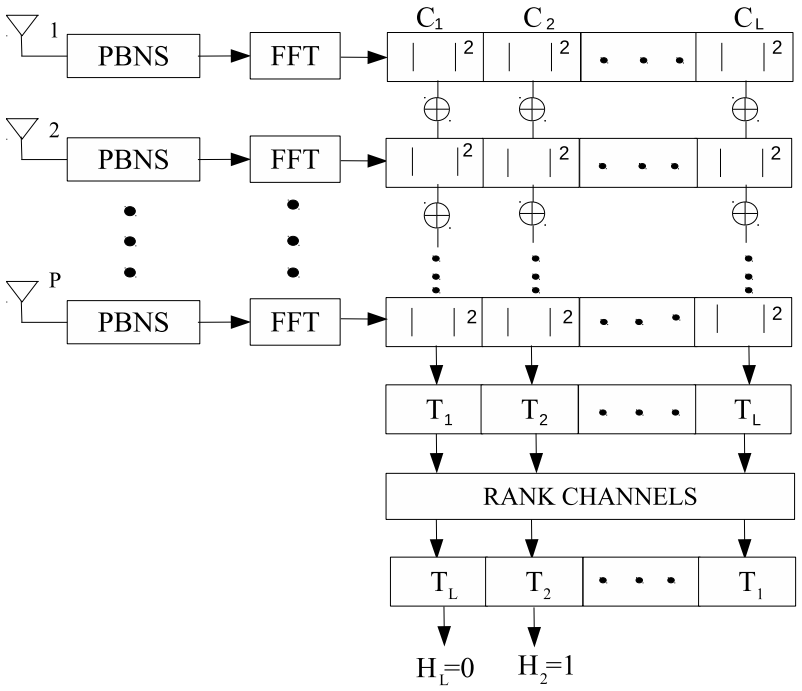

Figure 5.1: Block diagram of ranked square law combining (R-SLC) detection.

added to obtain $T_1, T_2, \cdots, T_L$. Once this is done, the channels are ranked, i.e., arranged in ascending order with regard to T_m, $m = 1, 2, \cdots, L$. Then the decision is taken on first L_d channels, where $L_d \leq S_d \leq L$. Remaining $U - L_d$ channels are ignored. Referring to Fig. 5.1, let $L_d = 2$ and let channels L and 2 have the least received energy. Based on the decision made, channels L and 2 are declared as free and occupied, respectively. Note that, considering $P = 1$ in R-SLC results in RCD proposed in [112].

Algorithm 1 Ranked Square Law Combining

1: Compute energy for each of the L channels from all P diversity branches.
2: Add the energy within each of the L channels from all the diversity branches. The resulting new energies are denoted by $T_m,\ m = 1, 2, \cdots, L$.
3: Sort the selected channels in ascending order with regard to T_m.
4: Make decisions for first L_d channels, where $S_d \leq L_d \leq L$, using energy detection with the given threshold τ. Ignore the remaining $U - L_d$ channels.

5.2.2 Ranked Square Law Selection (R-SLS) Detection

Fig. 5.2 represents the block diagram of R-SLS detection scheme. As shown in Fig. 5.2, energy computed within each of the L channels from all the diversity branches are given as input to a selector. The selector selects highest energy for each of the L channels. Once, this is done, the selected channels are ranked, i.e., arranged in ascending order with regard to T_m, $m = 1, 2, \cdots, L$. Then the decision is taken on first L_d channels, where $L_d \leq S_d \leq L$. Remaining $U - L_d$ channels are ignored. Fig. 5.2 represents the case with $L_d = 2$. Here, $C_1, C_2, \cdots, C_L$ represent L narrowband channels. Here, diversity branches P and 1 are shown to be selected for channel 1 and 2, i.e., $T^P_{max_1}$ and $T^1_{max_2}$, respectively. As shown in Fig.5.2, diversity branches P and 1 have maximum energies $T^P_{max_1}$ and $T^1_{max_2}$ for channels C_1 and C_2, respectively. Note that, in $T^j_{max_i}$, max_i and j represent the selected maximum energy in channel i and the corresponding diversity branch j, respectively, where $i = 1, 2, \cdots, L$ and $j = 1, 2, \cdots, P$. After ranking C_L is shown to have the lowest energy and C_2 has next lowest energy from the selected maximum energies. The detection is made on these channels L and 2. Based on threshold τ, C_L and C_2 are shown as free and occupied, respectively. Note that reducing the number of diversity branches to one results in RCD proposed in [112]. The steps involved in detection using a fixed threshold τ are listed in Algorithm 2.

Algorithm 2 Ranked square law selection (R-SLS) with fixed threshold τ

1: Select maximum energy for each of the L channels from all P diversity branches.
2: Sort the selected channels in ascending order with regard to T_m.
3: Make decisions for first L_d channels, where $S_d \leq L_d \leq L$, using energy detection with the given threshold τ. Ignore the remaining $U - L_d$ channels.

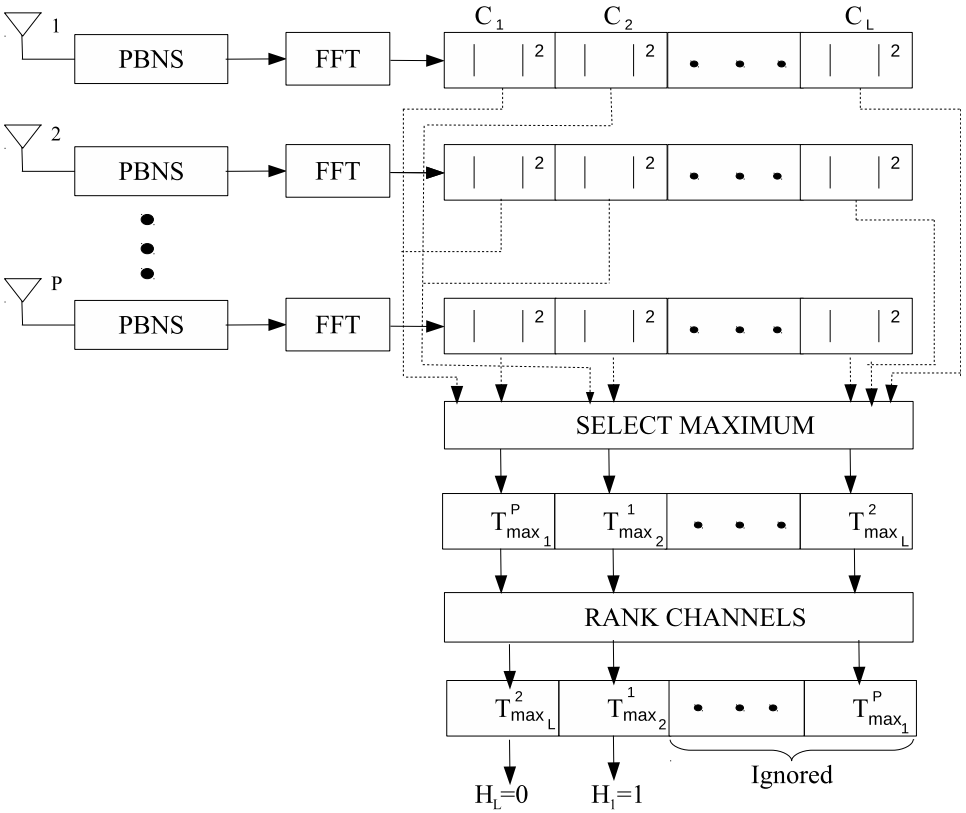

Figure 5.2: Block diagram of ranked square law selection (R-SLS) detection.

5.3 Approximation of Decision Statistic

The probability density function (pdf) of received energy under Nakagami fading is given as [65],

$$f_{T_m}(t) = \begin{cases} \frac{1(t)t^{G-1}e^{-\frac{t}{2}}}{(G-1)!2^G D}{}_1F_1\left(m_1; G; tE\right), & H_m = 1 \\ \chi^2_N, & H_m = 0 \end{cases} \tag{5.7}$$

where χ^2_N is the chi-square pdf with N degrees of freedom, $D = (1+\bar{\gamma}/m_1)^{m_1}$, $E = 0.5 - 0.5m_1/(m_1+\bar{\gamma})$, $\bar{\gamma}$ is the average SNR, $G = N/2$, $M = G-1$, m_1 is the Nakagami parameter, ${}_1F_1(\cdot;\cdot;\cdot)$ is the confluent hypergeometric function [50] and $1(t)$ is the unit step function.

If the pdf under $H_m = 1$ is directly used to obtain the expressions for performance metrics, they lead to infinite series representation and one may find it difficult to draw insight of different parameters from these expressions. In order

to resolve this problem, we first approximate the pdf of T_m under $H_m = 1$ using a simple expression by performing the asymptotic analysis. Using the Taylor series expansion of a function $f(t)$, we can write [36]

$$f(t) = at^q + a_1 t^{q+1} + O(t^{q+2}) \text{ as } t \to 0^+. \tag{5.8}$$

Here, a, a_1 and q represent real constants and $O(t^{q+2})$ is the error term as $t \to 0^+$. Using Eq. (5.8), the authors in [36] propose the approximation as

$$f(t) \approx at^q e^{-\alpha t}, \text{ as } t \to 0^+, \tag{5.9}$$

where $\alpha = -\frac{a_1}{a}$. The Taylor series expansion of Eq. (5.7) under $H_m = 1$ can be obtained as

$$f_{T_m}(t) = \frac{1}{2^G D\Gamma(G)} t^{G-1} + \frac{2m_1 E - G}{2^{G+1} D\Gamma(G+1)} t^G + O(t^{G+1}), \tag{5.10}$$

as $t \to 0^+$. On comparing Eq. (5.10) with Eq. (5.8) we get $a = \frac{1}{2^G D\Gamma(G)}$, $a_1 = \frac{(2m_1 E - G)}{2^{G+1} D\Gamma(G+1)}$, $\alpha = -\frac{a1}{a}$ and $q = G - 1$. With this, the approximated pdf of T_m is given by,

$$f_{T_m}(t) = \begin{cases} 1(t) a e^{-\alpha t} t^q, & H_m = 1 \\ \chi^2_N, & H_m = 0 \end{cases} \tag{5.11}$$

This approximation may not result in proper pdf, i.e., the area under $f_{T_m}(t)$ is not necessarily 1. However, it better approximates expression given in Eq. (5.7) under low $\bar{\gamma}$. In Fig. 5.3, we show the plots for actual and approximated pdf for different values of $\bar{\gamma}$. One can see that for $\bar{\gamma} = 0\ dB$, the approximation slightly deviates from the actual pdf, where as for $\bar{\gamma} = -5\ dB$ and $\bar{\gamma} = -10\ dB$ the approximated pdf almost overlaps with the actual pdf. For $\bar{\gamma} > 0\ dB$, we observe that the approximation deviates from the actual pdf. Hence, we conclude that the approximated pdf can be used to analyze the performance of the algorithms for $\bar{\gamma} \leq 0\ dB$. This is acceptable since in order to implement the CR without interfer-

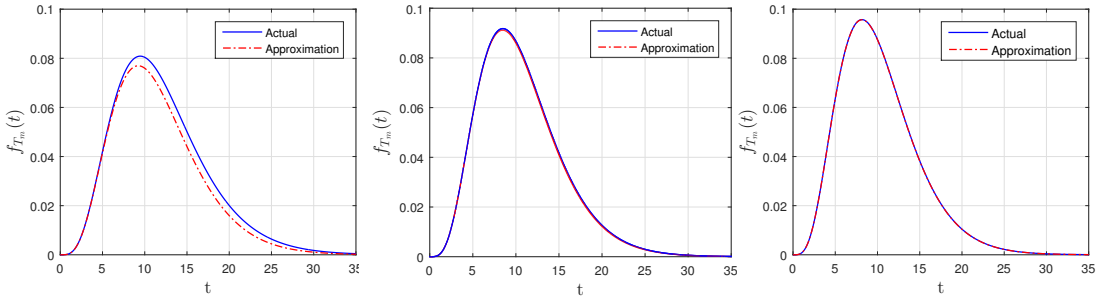

(a) (b) (c)

Figure 5.3: Plots showing the actual and approximated pdf considering $N = 10$, $m_1 = 2$ for (a) $\bar{\gamma} = 0\ dB$, (b) $\bar{\gamma} = -5\ dB$ and (c) $\bar{\gamma} = -10\ dB$.

ence to the PU, it is important to be able to detect the existence of the PU under very low SNR environment. Also, if the detection algorithms perform better under low SNR, they also perform well under high SNR since the density functions under H_0 and H_1 are well separated.

5.3.1 PDF for SLC Diversity

As already discussed, under the SLC diversity scheme, the measured energy from different diversity branches are added to obtain the new decision statistic [37, 38]. Assuming same average SNR ($\bar{\gamma}$) for all the diversity branches, pdf of sums of independent random variables can be obtained by convolving their marginal pdfs. Considering received energy as independent and identically distributed (iid) random variable, the pdf of decision statistic for SLC can be obtained by convolving branch pdfs of T_m, $m = 1, 2, \cdots, L$. Under $H_m = 0$, adding P iid central chi-square random variables, each with N degrees of freedom results in another chi-square random variable with PN degrees of freedom [37]. The pdf of T_m under $H_m = 1$ with P diversity branches can be obtained by successive convolution of Eq. (5.11) with itself. With this, the pdf of decision statistic can be summarized as

$$f_{T_m}(t) \approx \begin{cases} \frac{1(t)a^P\Gamma(1+q)^P t^{Pq+P-1}e^{-\alpha t}}{\Gamma(pq+P)}, & H_m = 1 \\ \chi^2_{PN}, & H_m = 0 \end{cases} \tag{5.12}$$

The derivation for the pdf in Eq. (5.12) is given in Appendix B.1. Note that substituting $P = 1$ results in no diversity case and $f_{T_m}(t)$ corresponds to that given in Eq. (5.11).

5.3.2 PDF for SLS Diversity

In SLS diversity, we select maximum energy for each of the L channels from all P diversity branches, i.e., $T_{max_m} = \max\left\{T_m^1, T_m^2, \cdots, T_m^P\right\}$, where the subscript $m = 1, 2, \cdots, L$ represents the index of the channel and the superscript represents the index of the diversity branch. The pdf of T_{max_m} can be obtained as [92]

$$f_{T_{max_m}}(t) = P\left(F_{T_m}(t)\right)^{P-1} f_{T_m}(t) \tag{5.13}$$

where, $f_{T_m}(t)$ and $F_{T_m}(t)$ represent the pdf and cdf of decision statistic for m^{th} channel. Using $f_{T_m}(t)$ given in Eq. (5.11), one can derive $F_{T_m}(t)$. Using these, we obtain the pdf of T_{max_m} as

$$f_{T_{max_m}}(t) \approx \begin{cases} P\left[\frac{a\gamma(q+1,\alpha t)}{\alpha^{q+1}}\right]^{P-1} a e^{-\alpha t} t^q, & H_m = 1 \\ P\left[\frac{\gamma\left(G,\frac{t}{2}\right)}{\Gamma(G)}\right]^{P-1} \frac{t^{G-1} e^{-\frac{t}{2}}}{2^G \Gamma(G)}. & H_m = 0 \end{cases} \tag{5.14}$$

5.4 Theoretical Analysis of Detection Algorithms

In this section, first we derive the expressions for P_{ISO} and P_{EIO} for R-SLC and then the same are derived for R-SLS. Note that, in the subsequent explanation the superscript Nak represents the Nakagami fading.

5.4.1 Theoretical Analysis for R-SLC

To make the analysis easy to understand, we first considering only two channels in the partial band, i.e., $L = 2$ and then extend the analysis to general case. We assume the desired number of spectrum opportunity as one, i.e., $S_d = 1$ and $I_d = 0$, i.e., no primary channel interference. We take a decision on one channel only, i.e., $L_d = 1$. With these parameter settings, the energies for the two channels are com-

puted which are represented as T_1 and T_2 for channel 1 and 2, respectively. These energies are ranked, i.e., they are arranged in ascending order by computing the minimum of the two energies, i.e., $T_{min} = min\{T_1, T_2\}$. Since $L_d = 1$, decision is made on T_{min} and the other channels are declared ON. Now if $T_{min} < \tau$, channel is declared as OFF otherwise it is declared as ON. For example, suppose $T_2 < T_1$, then channel 1 is declared ON and decision is made on channel 2.

In order to obtain P_{ISO} and P_{EIO}, we need to derive the probability of spectrum opportunity (PS) and the probability of interference opportunity (PI). Since we use $L = 2$, depending on the number of ON channels, there are three possible cases for primary occupancy of two channels, i.e., both channels are OFF, only one channel is ON and both channels are ON.

If both the channels are OFF, the probability of spectrum opportunity, i.e., $PS_{00}^{Nak}(\tau)$ can be obtained by calculating probability of $T_{min} < \tau$ under $H_1 = H_2 = 0$. i.e.,

$$PS(\tau|H_1, H_2 = 0) = PS_{00}^{Nak}(\tau) = Pr\left\{T_{min} < \tau\right\}, \tag{5.15}$$

Here, $T_{min} = min(T_1, T_2)$. If we consider L iid random variables, the pdf of minimum, i.e., $T_{min} = min\left(T_1, T_2, \cdots, T_L\right)$ is obtained as [92],

$$f_{T_{min}}(t) = L f_T(t)\left(1 - F_T(t)\right)^{L-1} = L f_T(t) \bar{F}_T(t)^{L-1}, \tag{5.16}$$

where, $F_T(t)$ and $\bar{F}_T(t) = 1 - F_T(t)$ are the cumulative distribution functions (cdf) and the complementary cdf (ccdf) of $f_T(t)$, respectively.

Using Eq. (5.12) in Eq. (5.16) and substituting L=2, one can obtain the pdf of T_m when both the channels are off as

$$f_{T_{min}}(t) = \frac{t^{PG-1} e^{-\frac{t}{2}} \Gamma(P \cdot G, \frac{t}{2})}{2^{P \cdot G - 1} \Gamma(P \cdot G)^2}. \tag{5.17}$$

Now, PS can be obtained by using series representation of $\Gamma(n, x)$ for integer n from [7, 8.69] in Eq. (5.17) and integrating the same from 0 to τ. After performing

mathematical simplifications we obtain the expression for PS as

$$PS_{00}^{Nak}(\tau) = \sum_{k=0}^{P\cdot G-1} \frac{\gamma(P\cdot G+k,\tau)}{2^{PG+k-1}\, k!\, \Gamma(P\cdot G)}. \tag{5.18}$$

Since both the channels are OFF, there is no chance of interference and hence $PI(\tau|H_1, H_2 = 0) = PI_{00}^{Nak}(\tau) = 0$.

We now consider the case when both the channels are ON. In this case, spectrum opportunity does not exist and hence $PS(\tau|H_1, H_2 = 1) = PS_{11}^{Nak}(\tau) = 0$. The probability of interference opportunity, i.e., $PI_{11}^{Nak}(\tau)$ in this scenario can be obtained by calculating the probability of $T_{min} < \tau$ under $H_1 = H_2 = 1$.

$$PI(\tau|H_1, H_2 = 1) = PI_{11}^{Nak}(\tau) = Pr\left\{T_{min} < \tau\right\}. \tag{5.19}$$

Once again using Eq. (5.12) but under $H_m = 1$ in Eq (5.16) and substituting $L = 2$, we obtain the pdf of T_m as

$$f_{T_{min}}(t) = \frac{2a^P\Gamma(1+q)^P t^{Pq+P-1}e^{-\alpha t}}{\Gamma(Pq+P)} - \frac{2a^{2P}\Gamma(1+q)^{2P}t^{Pq+P-1}e^{-\alpha t}\gamma\left(Pq+P,\alpha t\right)}{\Gamma(Pq+P)^2\alpha^{Pq+P}}. \tag{5.20}$$

From this, $PI_{11}^{Nak}(\tau)$ is obtained by integrating Eq. (5.20) from 0 to τ, which can be shown to be

$$\begin{aligned} PI_{11}^{Nak}(\tau) = \sum_{k=0}^{Pq+P-1} & \frac{a^{2P}\Gamma(1+q)^{2P}\gamma(Pq+P+k,2\alpha\tau)}{\Gamma(Pq+P)\alpha^{2Pq+2P}k!2^{Pq+P+k-1}} \\ & + \frac{2a^P(q!)^P\gamma(Pq+P,\alpha\tau)\left(\alpha^{Pq+P} - a^P\Gamma(1+q)^P\right)}{\Gamma(Pq+P)\alpha^{2Pq+2P}}. \end{aligned} \tag{5.21}$$

Finally, if only one channel is ON (assuming channel 1 is OFF and channel 2 is ON), $PS_{01}^{Nak}(\tau)$ can be obtained by calculating the probability of event $\{T_1 < T_2, T_1 < \tau\}$, i.e.,

$$\begin{aligned} PS(\tau|H_1 = 0, H_2 = 1) = PS_{01}^{Nak}(\tau) &= Pr\left\{T_1 < T_2, T_1 < \tau\right\} \\ &= \int_0^\tau \left(f_{T_1}(t_1)\int_{t_1}^\infty f_{T_2}(t_2)dt_2\right)dt_1 = \int_0^\tau f_{T_1}(t_1)\bar{F}_{T_2}(t_1)dt_1, \end{aligned} \tag{5.22}$$

where, $f_{T_1}(t)$ and $f_{T_2}(t)$ are the pdfs of energy received in channel 1 and 2, respectively, and $\bar{F}_{T_2}(t)$ is the ccdf of $f_{T_2}(t)$. Substituting pdfs from Eq. (5.12) into Eq. (5.22) and integrating using variable transformation, $PS_{01}^{Nak}(\tau)$ is given by

$$PS_{01}^{Nak}(\tau) = \sum_{k=0}^{Pq+P-1} \frac{a^P \Gamma(q+1)^P \gamma(P \cdot G + k, (\alpha + \frac{1}{2})\tau)}{2^{P \cdot G} \Gamma(P \cdot G) \alpha^{Pq+P-k} k! (\alpha + \frac{1}{2})^{P \cdot G + k}}. \tag{5.23}$$

The PI in this case can be obtained using

$$\begin{aligned} PI(\tau | H_1 = 0, H_2 = 1) = PI_{01}^{Nak}(\tau) &= Pr\{T_2 < T_1, T_2 < \tau\} \\ &= \int_0^\tau \left(f_{T_2}(t_2) \int_{t_1}^\infty f_{T_1}(t_1) dt_1 \right) dt_2 = \int_0^\tau f_{T_2}(t_2) \bar{F}_{T_1}(t_2) dt_2. \end{aligned} \tag{5.24}$$

The $PI_{01}^{Nak}(\tau)$ is derived by substituting pdfs from Eq. (5.12) into Eq. (5.24) and performing the integration. After simplification, it is given by

$$PI_{01}^{Nak}(\tau) = \sum_{k=0}^{P \cdot G - 1} \frac{a^P \Gamma(1+q)^P \gamma(Pq + P + k, \left(\alpha + \frac{1}{2}\right) \tau)}{\Gamma(Pq + P) 2^k \, k! \, \left(\alpha + \frac{1}{2}\right)^{Pq+P+k}}. \tag{5.25}$$

Note that, if we consider channel 1 as ON and channel 2 as OFF, we obtain the same results as in Eq. (5.23) and Eq. (5.25), respectively, i.e., $PS_{01}^{Nak}(\tau) = PS_{10}^{Nak}(\tau)$ and $PI_{01}^{Nak}(\tau) = PI_{10}^{Nak}(\tau)$. Once, PS and PI are available for all three cases, P_{ISO} and P_{EIO} can be obtained as

$$P_{ISO}^{Nak}(\tau) = 1 - \sum_{i=0}^{1} \sum_{j=0}^{1} (1-p)^{L-i-j} p^{i+j} PS_{ij}^{Nak}(\tau), \tag{5.26}$$

$$P_{EIO}^{Nak}(\tau) = \sum_{i=0}^{1} \sum_{j=0}^{1} (1-p)^{L-i-j} p^{i+j} PI_{ij}^{Nak}(\tau), \tag{5.27}$$

respectively.

The analysis considering 3 channels in the partial band is given in Appendix B.2. Looking at the analysis for $L = 2$ and $L = 3$, we observe that there exists a pattern and hence the analysis for the general case of any number of channels in

the partial band (L) can be easily arrived at. To do this, let us use Eq. (5.11) to write the pdfs and ccdfs of the received decision statistic as follows

$$f_{H0}(t) = \frac{t^{P\cdot G-1}e^{-\frac{t}{2}}}{2^{P\cdot G}\Gamma(P\cdot G)}, \text{ pdf under } H_m = 0, \tag{5.28}$$

$$f_{H1}(t) = \frac{a^P\Gamma(1+q)^P t^{Pq+P-1}}{e^{\alpha t}\Gamma(Pq+P)}, \text{ pdf under } H_m = 1, \tag{5.29}$$

$$\bar{F}_{H0}(t) = \frac{\Gamma(P\cdot G, \frac{t}{2})}{\Gamma(P\cdot G)}, \text{ ccdf of } f_{H0}(t), \tag{5.30}$$

$$\bar{F}_{H1}(t) = \frac{\Gamma(1+q)^P\Gamma(Pq+p, \alpha t)}{a^{-P}\Gamma(Pq+P)\alpha^{Pq+P}}, \text{ ccdf of } f_{H1}(t). \tag{5.31}$$

Using these equations, $P_{ISO}^{Nak}(\tau)$ and $P_{EIO}^{Nak}(\tau)$ for any L can be given by

$$P_{ISO}^{Nak}(\tau) = 1 - \sum_{i=0}^{L}\binom{L}{i}(1-p)^{L-i}p^i(L-i)\int_0^\tau f_{H0}(t)\left(\bar{F}_{H0}(t)\right)^{L-i-1}\left(\bar{F}_{H1}(t)\right)^i dt \tag{5.32}$$

$$P_{EIO}^{Nak}(\tau) = \sum_{i=0}^{L}\binom{L}{i}(1-p)^{L-i}p^i\, i\int_0^\tau f_{H1}(t)\left(\bar{F}_{H1}(t)\right)^{i-1}\left(\bar{F}_{H0}(t)\right)^{(L-i)} dt \tag{5.33}$$

Note that, if we use $P = 1$ in the analysis, it results in no diversity case, i.e., RCD. Also, Eq. (5.32) and Eq. (5.33) are general and can be used with any fading model once the pdf of decision statistic under that fading is available.

5.4.2 Theoretical Analysis of R-SLS

In this section we provide theoretical analysis of R-SLS detection algorithm. The analysis here is similar to that carried out for R-SLC in Section 5.4.1. We first consider a case with $L = P = 2$, $L_d = 1 = S_d = 1$, $I_d = 0$ and same SNRs at the

input of all diversity branches and then extend it to general case.

Since we have $L = P = 2$, we first select maximum energy T_{max_m} i.e., $T_{max_m} = max\{T_m^1, T_m^2\}$, $m = 1, 2$ represents the index of the channel and the superscripts 1 and 2 represent indices of the diversity branches. The pdf of T_{max_m} is obtained by using $P = 2$ in Eq. (5.14). Now, there are three possible cases for occupancy of the two channels C_1 and C_2. These correspond to: 1. Both the channels are OFF, 2. Only one channel is ON and 3. Both the channels are ON. If both the channels are OFF, one can write the probability of spectrum opportunity (PS) as

$$PS(\tau|H_1 = 0, H_2 = 0) = PS_{00}(\tau) = 2\int_0^{\tau} \left(f_{T_{max_1}}(t_1) \int_{t_1}^{\infty} f_{T_{max_2}}(t_2) dt_2 \right) dt_1, \tag{5.34}$$

where, $T_{min} = min\{T_{max_1}, T_{max_2}\}$. Here, $T_{max_1} = max\left\{T_1^1, T_1^2\right\}$ and $T_{max_2} = max\left\{T_2^1, T_2^2\right\}$. Since both the channels are OFF, we have $f_{T_{max_1}}(t_1) = f_{T_{max}}(t) = f_{T_{max}}(t)$ which is given in Eq. (5.14) under $H_m = 0$. It is mathematically too involved to arrive at the close form expression for Eq. (5.34) and hence we keep it in integral form only. Since both the channels are OFF, there is no chance of interference and hence, $PI(\tau|H_1 = 0, H_2 = 0) = PI_{00}(\tau) = 0$.

Next, we consider the case when only one channel is ON. Assuming channel 1 is OFF and channel 2 is ON, PS can be written as

$$PS(\tau|H_1 = 0, H_2 = 1) = PS_{01}(\tau) = Pr\{T_{max_1} < T_{max_2}, T_{max_1} < \tau\}. \tag{5.35}$$

Now, PS in this scenario can be obtained as

$$PS_{01}(\tau) = \int_0^{\tau} \left(f_{T_{max_1}}(t_1) \int_{t_1}^{\infty} f_{T_{max_2}}(t_2) dt_2 \right) dt_1, \tag{5.36}$$

where, $f_{T_{max_1}}(t_1)$ and $f_{T_{max_2}}(t_2)$ are the pdfs given in Eq. (5.14) under $H_m = 0$ and $H_m = 1$, respectively. Similarly, the probability of interference opportunity (PI) can be written as

$$PI(\tau|H_1 = 0, H_2 = 1) = PI_{01}(\tau) = Pr\{T_{max_2} < T_{max_1}, T_{max_2} < \tau\}. \tag{5.37}$$

This can be obtained as

$$PI_{01}(\tau) = \int_0^{\tau} \left(f_{T_{max_2}}(t_2) \int_{t_2}^{\infty} f_{T_{max_1}}(t_1) dt_1 \right) dt_2 \tag{5.38}$$

Note that, one can obtain the same expressions for PS and PI assuming channel 1 as ON and channel 2 as OFF, i.e., $PS_{01}(\tau) = PS_{10}(\tau)$ and $PI_{01}(\tau) = PI_{10}(\tau)$.

Now, if both channels are ON, we have $PS(\tau|H_1 = 1, H_2 = 1) = PS_{11}(\tau) = 0$, as this results in zero spectrum opportunities. The PI in this case can be written as

$$PI(\tau|H_1 = 1, H_2 = 1) = PI_{11}(\tau) = 2 \int_0^{\tau} \left(f_{T_{max_1}}(t_1) \int_{t_1}^{\infty} f_{T_{max_2}}(t_2) dt_2 \right) dt_1. \tag{5.39}$$

Here, we consider both the channels as ON and hence $f_{T_{max_1}}(t_1) = f_{T_{max_2}}(t_2) = f_{T_{max}}(t)$ which is given by Eq. (5.14) under $H_m = 1$.

Using $PS_{ij}(\tau)$ and $PI_{ij}(\tau)$, for $i, j = 0, 1$, probability of a spectrum opportunity $(PS(\tau))$ and the probability of interference opportunity $(PI(\tau))$ for the selected threshold τ can be computed using

$$PS(\tau) = (1-p)^2 PS_{00}(\tau) + 2p(1-p) PS_{01}(\tau) + p^2 PS_{11}(\tau) \text{ and} \tag{5.40}$$

$$PI(\tau) = (1-p)^2 PI_{00}(\tau) + 2p(1-p) PI_{01}(\tau) + p^2 PI_{11}(\tau). \tag{5.41}$$

Finally, using Eq. (5.40) and Eq. (5.41), P_{ISO} and P_{EIO} can be obtained as

$$P_{ISO}(\tau) = Pr\{S < S_d\} = 1 - PS(\tau) \text{ and } P_{EIO}(\tau) = Pr\{I > I_d\} = PI(\tau), \tag{5.42}$$

respectively. The expressions for P_{ISO} and P_{EIO} given in Eq. (5.32) and Eq. (5.33), respectively, can be used for general analysis of R-SLS detection algorithm.

5.5 Results and Discussion

In this section, we carry out the experiments using theoretical analysis given in Section 5.4. The performance is illustrated using the plots of P_{EIO} VS P_{ISO} under

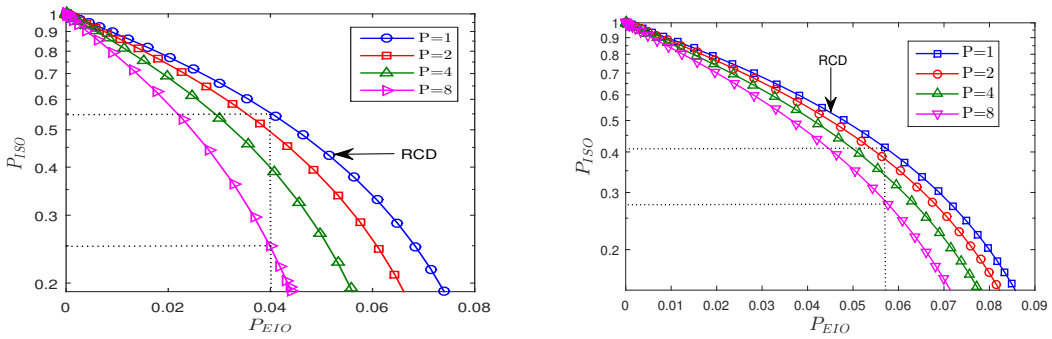

Figure 5.4: P_{EIO} VS P_{ISO} for different P considering $m_1 = 2$, $p = 0.1$, $S_d = 1$, $I_d = 0$, $L_d = 1$, $N = 10$, $\bar{\gamma} = -5\ dB$ for (a) R-SLC with $L = 16$ and (b) R-SLS with $L = 2$.

Nakagami fading channels. The Monte-Carlo simulations are also carried out in order to discuss the effect of different parameters on the performance of the proposed detection schemes. For Monte-Carlo simulations, the results are averaged over 10^5 realizations. Here, the plots shown in Fig. 5.4 to 5.7 are obtained using the mathematical expressions derived in Section V and those in Fig. 5.9 are obtained using Monte-Carlo simulations. Fig. 5.8 has the plots obtained using both the approaches.

In Fig. 5.4(a), we display P_{EIO} VS P_{ISO} for the proposed R-SLC considering different number of diversity branches P. The plots are shown for P ranging from 1 to 8. Note that $P = 1$ in R-SLC corresponds to no diversity case, i.e., RCD. Looking at the plot, we see that for a $P_{EIO} \approx 0.040$, the $P_{ISO} \approx 0.544$ for RCD and it is 0.250 for R-SLC with $P = 8$ indicating that P_{ISO} is much smaller for given P_{EIO} when we use diversity. This is illustrated in Fig. 5.4(a) using the dotted lines.

Fig. 5.4(b) demonstrates the effect of increasing P on the performance of R-SLS. Once again P is varied from 1 to 8. We see that for a value of $P_{EIO} \approx 0.057$, the values of P_{ISO} for RCD and R-SLC with $P = 8$ are 0.412 and 0.275, respectively, indicating the improvement in the performance when diversity is used. The dotted lines in the figure indicate this.

In Fig. 5.5 we show the comparison of the two proposed algorithms. We observe that among the two algorithms, R-SLC performs better than R-SLS. For example, for P_{EIO} of approximately 0.063 we observe $P_{ISO} \approx 0.260$ for R-SLC and

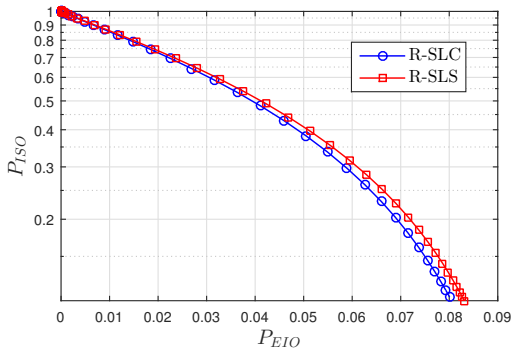

Figure 5.5: P_{EIO} VS P_{ISO} showing the comparison of R-SLC with R-SLS considering $m_1 = 2$, $p = 0.1$, $L = 2$, $P = 4$, $S_d = 1$, $I_d = 0$, $L_d = 1$, $N = 10$, $\bar{\gamma} = -5\,dB$.

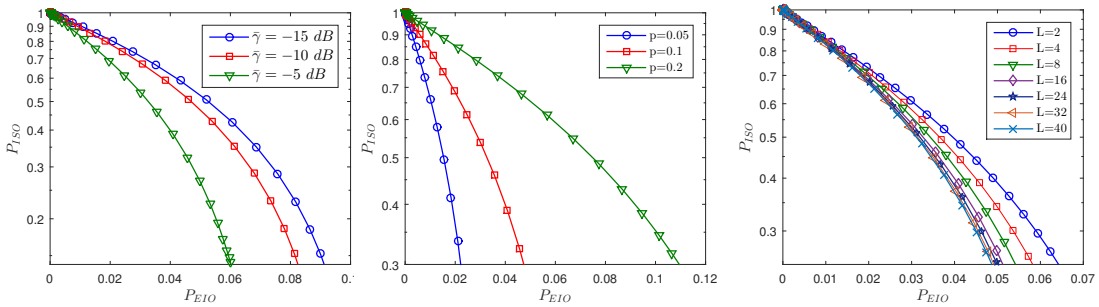

(a) (b) (c)

Figure 5.6: P_{EIO} VS P_{ISO} for varying $\bar{\gamma}$, p and L using $m_1 = 2$, $N = 10$, $S_d = 1$, $I_d = 0$, $L_d = 1$, $P = 4$, (a) with $p = 0.1$, $L = 16$, for different $\bar{\gamma}$, (b) with $\bar{\gamma} = -5\,dB$, $L = 16$ for different p, (c) with $\bar{\gamma} = -5\,dB$, $p = 0.1$ for different L.

0.282 for R-SLS.

We next show the effect of different parameters on the performance of the R-SLC detection algorithm. In Fig. 5.6 we display the effect of average SNR ($\bar{\gamma}$), occupancy probability p and the number of channels in the partial band L. Fig 5.6(a) shows the effect of increasing $\bar{\gamma}$ for $p = 0.1$ and $L = 16$ where $\bar{\gamma}$ is increased from $-15\,dB$ to $-5\,dB$. It is observed that with the increase in $\bar{\gamma}$, the performance improves. In Fig. 5.6(b), the effect of increase in p of PUs is shown using $\bar{\gamma} = -5\,dB$ and $L = 16$. As p increases the number of occupied channels in the partial band increases resulting in higher interference and lower spectrum opportunity and hence the performance degrades which is clearly seen in the plots. The effect of increasing L is illustrated in Fig. 5.6(c). Here, the simulation is done by varying L from 2 to 40 keeping $\bar{\gamma} = -5\,dB$ and $p = 0.1$. We see that increase in L results

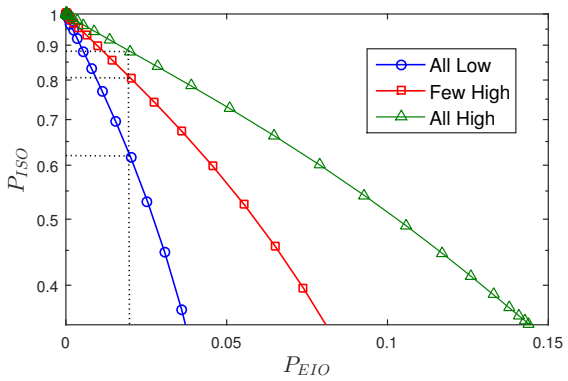

Figure 5.7: P_{EIO} VS P_{ISO} plots considering different p for channels in the partial band for $m_1 = 2$, $L = P = 8$, $S_d = 1$, $I_d = 0$, $L_d = 1$, $N = 10$, $\bar{\gamma} = -5\,dB$.

Table 5.1: Occupancy Probabilities for $L = 8$ subbands

Occupancy Probability	p_1	p_2	p_3	p_4	p_5	p_6	p_7	p_8
All Low	0.09	0.07	0.11	0.12	0.08	0.12	0.13	0.1
Few High	0.1	0.2	0.09	0.3	0.4	0.12	0.25	0.08
All High	0.2	0.25	0.3	0.15	0.4	0.35	0.2	0.45

in improved performance. This is because increasing L results in more number of free channels in the partial band. It can also be observed that when L exceeds a certain value, the improvement is not significant thus validating the use of PBNS. Since the SUs do not require all the channels for use, it is not required to sense the entire wideband. For example, in Fig. 5.6(c), there is not much improvement in the performance for $L > 16$ and hence there is no advantage in sensing more than 16 channels.

In Fig. 5.7, we show the P_{EIO} VS. P_{ISO} plots considering different p for primary channels. These plots are obtained for three scenarios namely: 1. all the channels have low occupancy probability, 2. only few channels have high occupancy probability and 3. all channels have high occupancy probability. Different p's considered for $L = 8$ are given in TABLE 5.1. We observe that the performance is better when all the channels have lower p and the performance degrades when all of them have high p. For example, for P_{EIO} of approximately 0.020 we observe P_{ISO} as approximately 0.616, 0.804, and 0.881 for three cases of all low, few high and all high, respectively. From this one can deduce that those groups of chan-

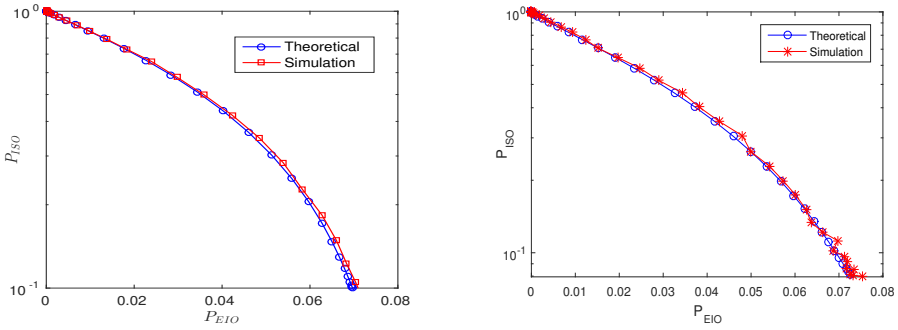

(a) (b)

Figure 5.8: P_{EIO} VS P_{ISO} for R-SLC and R-SLS using theoretical analysis and Monte-Carlo simulation considering $m_1 = 2$, $p = 0.1$, $S_d = 1$, $I_d = 0$, $L_d = 1$, $N = 10$ for (a) R-SLC with $L = P = 4$, and $\bar{\gamma} = -5\ dB$ and (b) R-SLS with $P = L = 2$ with $\bar{\gamma} = 0\ dB$.

nels where occupancy probabilities are not significantly high have to be selected to yield better sensing performance.

In Fig. 5.8, we show the plots obtained using theoretical expressions derived in Section 5.4 and using the Monte-Carlo simulations. We see that the plots almost overlap validating the theoretical analysis carried out for both R-SLC and R-SLS.

Finally, in Fig. 5.9 we show the effect of L_d, S_d and I_d on the performance of R-SLC using Monte-Carlo simulations. Fig. 5.9(a) shows the effect of increasing L_d by considering $L = 8$ and keeping the other parameters fixed. We see that increasing L_d degrades the performance. This is because although increasing L_d enhances the chance of getting free channels it also increases interference to the PUs. With $I_d = 0$, increasing L_d, degrades the performance. From this result, we can say that it is advantageous to choose $L_d = S_d$. Next, we illustrate the effect of increase in S_d in Fig. 5.9(b). As seen from the plots, it is clear that as S_d increases, the performance degrades. This happens because, if we increase S_d, it requires L_d to be increased since $S_d \leq L_d$. But increasing L_d results in higher interference to the PUs causing degradation in the performance. Finally, in Fig. 5.9(c), we demonstrate the effect of varying I_d on the performance. Increasing I_d (i.e., $I_d > 0$) implies SUs are allowed to interfere with the PUs. For example, with $I_d = 1$, interference to any one of the PU channels is allowed. From the simulation, we observe that performance improves as I_d increases. Note that, we

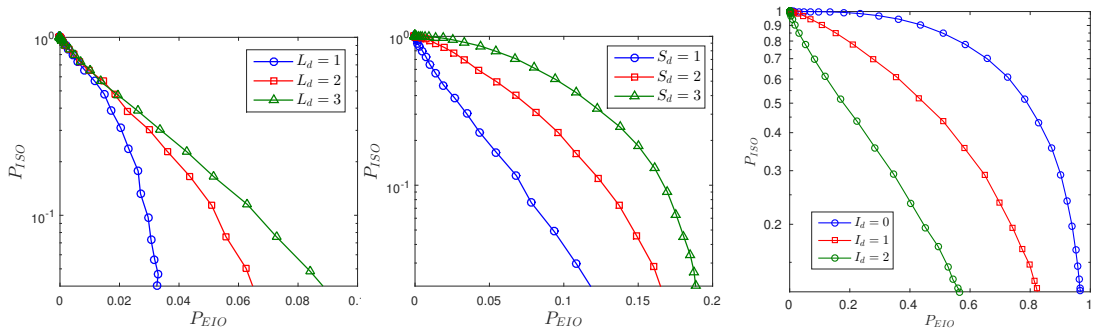

(a) (b) (c)

Figure 5.9: P_{EIO} VS P_{ISO} for varying L_d, S_d and I_d using $m_1 = 2$, $N = 10$, $P = 4$, $\bar{\gamma} = 0\ dB$. (a) with $S_d = 1$, $I_d = 0$, $p = 0.1$, $L = 8$, for different values of L_d, (b) with $L_d = 4$, $p = 0.1$, $L = 8$, $I_d = 0$ for different values of S_d, (c) with $S_d = 4$, $p = 0.5$, $L = 16$, $L_d = 8$ for different values of I_d.

have given plots showing the effect of different parameters on the performance of R-SLC, only. One can also show similar plots for R-SLS. All the conclusions drawn for R-SLC are also valid for R-SLS.

5.6 Conclusion

In this work, we have proposed two new detection algorithms for WSS that use diversity to improve the detection performance. We have given complete mathematical analysis to find the performance of WSS with and without diversity by considering Nakagami fading. Our analysis is general and can be used with any fading model and any diversity technique. From the analysis, it is clear that the use of diversity improves the detection performance. We have also demonstrated the effect of different parameters on the performance. We observe that R-SLC technique outperforms R-SLS. Our future work involves the use of other diversity schemes and more general fading models including frequency selective fading for finding the performance of WSS. Next, an optimization technique can be used for finding the optimal thresholds when different priorities, and different occupancy probabilities are considered for PU channels. Furthermore, the approach in this chapter can be extended to cooperative WSS where multiple SUs cooperate in detecting the presence of PUs.

CHAPTER 6

Detection Algorithm for Cooperative Wideband Spectrum Sensing

In our previous work, we used antenna diversity for wideband spectrum sensing (WSS) to improve the detection performance. For antenna diversity, the spacing between antennas has to be sufficiently high in order to receive independent observations which incurs limit on the number of antennas that can be used at the secondary users. The cooperative spectrum sensing (CSS) has been shown as an effective method that improves the detection performance by exploiting the spatial diversity. An expectation maximization based joint detection and estimation (JDE) scheme for cooperative spectrum sensing in multiuser multiantenna CR network is proposed in [10], where multiple spatially separated SUs cooperate to detect the state of occupancy of a wideband frequency spectrum. In [97], the spectrum sensing problem is formulated as a class of optimization problems that maximize the aggregated opportunistic throughput of a CR system under the constraints as the interference to the primary users. All these techniques use traditional sampling technique for wideband sensing and hence require higher sampling rates. In this work, we propose a novel algorithm based on CSS with hard combining for wideband spectrum sensing. We make use of PBNS at all the CSUs to reduce the higher sampling rate requirements. We use hard combining for data fusion which requires reduced control channel bandwidth when compared to soft combining. The experiments are carried out using theoretical analysis and also verified using Monte Carlo (MC) simulations. Our analysis shows that the proposed approach outperforms the ranked channel detection used un-

der no cooperation. We show that by choosing appropriate number of CSUs, the algorithm performs better than both R-SLC and R-SLS algorithms.

6.1 System Model

The wideband signal received at the CSUs can be modeled as the collection of U subbands, i.e., narrowband channels, each of bandwidth B_0 making the total bandwidth as $B = UB_0$. A similar channel model is used in [8, 94, 112]. Let H_m denotes the occupancy status of m^{th} subband of primary user with $H_m = 0$ and $H_m = 1$ corresponding to PU being OFF and ON, respectively. Since the observation interval is small, the occupancy status of the PU remains unchanged during this time which is a reasonable assumption. We assume that the occupancy status of subbands is independent of each other and all the PUs have equal priorities. In this work, the discussion is restricted to one sensing window with a fixed duration of $T_w = UNT_N$, where $F_N = 1/T_N = 2B$ is the Nyquist sampling frequency and N is the number of samples per subband. We would like to mention here that we use the two terms subband and channel interchangeably. Once again, the state of each channel is modeled as a Bernoulli random variable whose PMF is given in Eq. (5.1). The PMF of number of ON channels (K) in the wideband is given by Binomial distribution given in Eq. (5.2).

Note that in order to find the availability of the free primary channels, the detector has to decide on their presence or absence. Here, we consider the case of cooperative spectrum sensing where M number of SUs cooperate to find the occupancy of the wide frequency band. Let $y_i(t)$, $s_i(t)$ and $z_i(t)$ be the received signal, the wideband PU signal after propagation, and the additive white Gaussian noise (AWGN) at time t at the i$^{\text{th}}$ SU, respectively, where $i = 1, 2, \cdots, M$. The CSUs receive $y_i(t) = s_i(t) + z_i(t)$ when there is transmission from PU and $y_i(t) = z_i(t)$ when there is no transmission. Let $y_i[n]$, $s_i[n]$, and $z_i[n]$ denote their corresponding wideband Nyquist samples. Using an AWGN model for the primary signal within each channel, one can model both the signal and the noise as $s_i[n] \sim \mathcal{CN}(0, \sigma_{s_i}^2)$ and $z_i[n] \sim \mathcal{CN}(0, \sigma_{z_i}^2)$, where, $\sigma_{s_i}^2$ and $\sigma_{z_i}^2$ represent the average

power of $s_i[n]$ and $z_i[n]$, respectively, at the i^{th} CSU. It is reasonable to assume that the signal and noise are statistically independent. Also, in this work we assume that all the CSUs experience the same SNR at their inputs. This makes $\sigma_{s_i}^2 = \sigma_s^2$ and $\sigma_{z_i}^2 = \sigma_z^2$. Note that we have not considered fading in this case.

6.2 Proposed Detection Algorithm

Consider M number of CSUs receiving the wideband signal consisting of U channels. Since the SU may not be interested in finding all the spectrum opportunities, instead the interest lies in finding sufficient numbers of spectrum opportunity, we use the idea of PBNS, which samples only a fraction of the entire wideband. PBNS filters out L channels from the wideband having U channels. The signal after filtering is sampled at the Nyquist rate of $2LB_0$ on which the FFT is performed. Taking N samples per channel, the number of samples in the sensing window becomes NL. Considering $V[k]$ as the frequency samples in PBNS, we can write $V[k] = Y[k]$, for $0 \leq k \leq NL-1$, where $Y[k]$ denotes the normalized DFT of the received wideband signal having U channels. The energy, i.e., decision statistic, within m^{th} narrowband channel is then calculated as

$$T_m = \frac{1}{N} \sum_{k \in I_m} |V[k]|^2, \tag{6.1}$$

where $1 \leq m \leq L$ and I_m is the set of frequency indices that fall into channel m.

In CSS, number of SUs cooperate in order to detect spectrum holes. In the proposed algorithm, we make use of CSS with hard combining where all the CSUs take their own decision on the occupancy of the channels and send the final results to the FC which takes the final decision. Fig. 6.1 shows the block schematic of the proposed detection algorithm and the steps involved in implementing it are given in Algorithm 3. In Fig. 6.1, we consider $L = 2$ and $M = 3$. We number the two channels in the partial band as channel 1 and 2, respectively. Let L_d and X_d represent the number of channels on which the FC and CSUs take the decision, respectively. Let F_d represents the total number of times a channel must be reported as OFF by the CSUs in order for it to be declared free. We consider

$S_d = L_d = X_d = 1$, $I_d = 0$. The proposed detection scheme works as follows. After receiving the wideband signal, all three CSUs perform PBNS. Each CSU performs ranked channel detection (RCD), i.e., computes the decision statistic for both the channels, arranges them in ascending order and then take decision on the first channel only. If this channel is declared as free, the CSUs send the channel number to the FC which in turn computes how many times a particular channel is reported as free. The FC then arranges them in descending order with regard to the number of times a particular channel is reported as free. In Fig. 6.1, channel 1 is reported free once where as the channel 2 is reported as free twice. If we consider $S_d = L_d = 1$, the FC takes decision on the channel which is appearing on the top of the order. As shown in Fig. 6.1, the channel 2 is reported as free twice which is greater than $F_d = 1$ and hence the FC declares channel 2 as free. Now if two channels are reported free for equal number of times and are reported more than F_d times, the FC choses any one channel from them with equal probability. For example, with $M = 4$, if both channels are reported free twice, the FC declares any one of them as free with probability of 0.5.

Algorithm 3

1: At each CSU: Compute decision statistic (Eq. 6.1) for each of the L channels in the partial band and arrange them in ascending order. Take decision on first X_d channels.

2: Each CSU reports the free channel numbers to the fusion center (FC).

3: FC counts the number of times a particular channel is reported free and then arranges them in descending order with regard to it.

4: At FC: Take decision on first L_d channels, where $S_d \leq L_d \leq X_d \leq L$, and report the channels as free if they are reported free $> F_d$ times. If channels are reported free for equal number of times and are reported free $> F_d$ times, the FC declares them as free with equal probability.

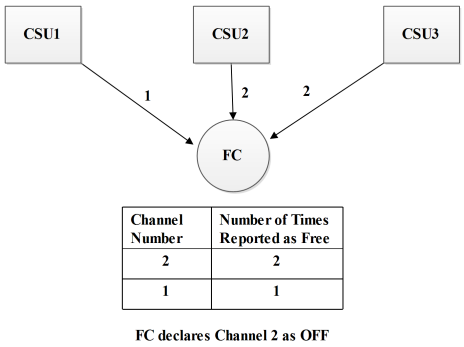

Figure 6.1: Block diagram of proposed detection algorithm with $L = 2$, $M = 3$, $S_d = L_d = X_d = 1$, $I_d = 0$, $F_d = 1$.

6.3 Theoretical Analysis of The Detection Algorithm

Nyquist sampling ensures independent observations across channels for the system model described in Section 6.1. Hence, the decision statistic in Eq. (6.1) for the m^{th} channel follows Gamma distribution with pdf given as

$$f_{T_m}(x) = \begin{cases} \frac{1}{\Gamma(k_0)\theta_0^{k_0}} x^{k_0-1} e^{-\frac{x}{\theta_0}}, & \text{if } H_m = 0 \\ \frac{1}{\Gamma(k_1)\theta_1^{k_1}} x^{k_1-1} e^{-\frac{x}{\theta_1}}, & \text{if } H_m = 1. \end{cases} \tag{6.2}$$

where, $k_0 = k_1 = N$, $\theta_0 = \frac{1}{N}$, $\theta_1 = \frac{1}{N}(1+\gamma)$ and $\gamma = \frac{\sigma_s^2}{\sigma_z^2}$ is the average SNR.

The theoretical analysis for the proposed detection scheme when we consider any value of M and L is mathematically involved and hence we derive the general expressions by considering any M and any L separately. To make the analysis easy to understand, we first derive the expressions for P_{EIO} and P_{ISO} for $L = 2$, $M = 3$, $S_d = L_d = X_d = F_d = 1$ and $I_d = 0$. With $X_d = 1$, each CSU performs RCD and takes decision on the channel which is appearing first after arranging them in ascending order. If this channel is found free, it sends the channel number to the FC which then counts the number of times a particular channel is reported free and arranges them in descending order. Since $L_d = 1$, the FC takes decision on one channel only. With $F_d = 1$, if a channel is reported free more than once, the FC declares that channel as free. Since $L = 2$, there are three possible cases for the occupancy of the channels, i.e., both the channels are OFF, any one channel is OFF

and both the channels are ON.

We start with the case when both the channels are OFF. Since each CSU performs RCD, with $L = 2$ and $X_d = 1$, the probability that CSUs report channel number 1 as free, i.e., $P_{00}^{1}(\tau)$, is

$$P_{00}^{1}(\tau) = \int_{0}^{\tau} \left[f_{T_1}(t_1) \int_{t_1}^{\infty} f_{T_2}(t_2) dt_2 \right] dt_1, \tag{6.3}$$

where, $f_{T_1}(t_1)$ and $f_{T_2}(t_2)$ are the pdfs of decision statistic for the channel 1 and 2, respectively which are given in Eq. (6.2). Since $H_1 = H_2 = 0$ in this case, $f_{T_1}(t_1) = f_{T_2}(t_2)$. Here, $Pr\{\cdot\}$ represents the probability. Note that, the subscript 00 and the superscript 1 in $P_{00}^{1}(\tau)$ represent the case of both the channels being OFF and the channel number 1, respectively. Due to page limitations, we keep Eq. (6.3) in integral form itself. These integrals can be reduced in closed form by using the series representations of incomplete gamma functions. Since both the channels are OFF, the probability that a CSU sends channel number 1 and 2 as free is equal, i.e., $P_{00}^{1}(\tau) = P_{00}^{2}(\tau)$. To compute the probability of spectrum opportunity (PS), we need to consider all the possible combinations of received channel numbers from the CSUs for which the FC declares any one channel as free. For example, one possible combination of received free channel numbers could be CSU1 and CSU2 sending channel number 1, and CSU3 sending channel number 2. In this case the FC declares channel 1 as free. Note that with $F_d = 1$, only two CSUs reporting same channel number as free is sufficient to declare that channel as free. Considering this, PS in this case, i.e., PS_{00}, can be obtained as

$$PS_{00}(\tau) = 8 \left[P_{00}^{1}(\tau) \right]^3 + 6 \left[P_{00}^{1}(\tau) \right]^2 \left[1 - 2P_{00}^{1}(\tau) \right]. \tag{6.4}$$

In this case, there is no chance of interference and hence the probability of interference (PI) is zero, i.e., $PI_{00}(\tau) = 0$.

We now consider the case when only one channel is ON. Let us assume that channel 1 is OFF and channel 2 is ON. In this case, the probability that a CSU

reports channel 1 as free, i.e., $P_{01}^{1}(\tau)$, can be obtained as

$$P_{01}^{1}(\tau) = \int_{0}^{\tau} \left[f_{T_1}(t_1) \int_{t_1}^{\infty} f_{T_2}(t_2) dt_2 \right] dt_1. \tag{6.5}$$

Similarly, the probability that a CSU reports channel 2 as free, i.e., $P_{01}^{2}(\tau)$, can be obtained as

$$P_{01}^{2}(\tau) = \int_{0}^{\tau} \left[f_{T_2}(t_2) \int_{t_2}^{\infty} f_{T_1}(t_1) dt_1 \right] dt_2. \tag{6.6}$$

Since $H_1 = 0$ and $H_2 = 1$, $f_{T_1}(t)$ and $f_{T_2}(t)$ are to be used from Eq. (6.2) under $H_m = 0$ and $H_m = 1$, respectively.

In this case, we get the SO if the channel 1 is reported as free at least two times. For example, we get spectrum opportunity when CSUs 1 and 2 report channel number 1 as free and CSU 3 reports channel 2 as free. Considering all such possible combinations, the PS, i.e., $PS_{01}(\tau)$, can be obtained as

$$PS_{01}(\tau) = \left[P_{01}^{1}(\tau) \right]^3 + 3 \left[P_{01}^{1}(\tau) \right]^2 P_{01}^{2}(\tau) + 3 \left[P_{01}^{1}(\tau) \right]^2 \left[1 - P_{01}^{1}(\tau) - P_{01}^{2}(\tau) \right]. \tag{6.7}$$

Similarly, it results in interference if the channel 2 is reported as free at least two times. In this case, the probability of interference, i.e., PI_{01}, can be obtained as

$$PI_{01}(\tau) = \left[P_{01}^{2}(\tau) \right]^3 + 3 \left[P_{01}^{2}(\tau) \right]^2 P_{01}^{1}(\tau) + 3 \left[P_{01}^{2}(\tau) \right]^2 \left[1 - P_{01}^{2}(\tau) - P_{01}^{1}(\tau) \right]. \tag{6.8}$$

Note that, if we consider channel 1 as ON and channel 2 as OFF, we get the same results, i.e., $PS_{01}(\tau) = PS_{10}(\tau)$ and $PI_{01}(\tau) = PI_{10}(\tau)$.

Finally, we consider the case when both the channels are ON. In this case there is no chance of spectrum opportunity and hence $PS_{11}(\tau) = 0$. The probability of reporting channel 1 as free, i.e., $P_{11}^{1}(\tau)$, by the CSU can be obtained as

$$P_{11}^{1}(\tau) = \int_{0}^{\tau} \left[f_{T_1}(t_1) \int_{t_1}^{\infty} f_{T_2}(t_2) dt_2 \right] dt_1. \tag{6.9}$$

Since both the channels are ON, the probability that CSU sends channel number 1 and 2 is equal, i.e., $P_{11}^1(\tau) = P_{11}^2(\tau)$. The probability of interference in this case, i.e., $PI_{11}(\tau)$, can be obtained as

$$PI_{11}(\tau) = 8\left[P_{11}^1(\tau)\right]^3 + 6\left[P_{11}^1(\tau)\right]^2\left[1 - 2P_{11}^1(\tau)\right]. \tag{6.10}$$

Once the PS and the PI for all three cases are obtained, $P_{ISO}(\tau)$ and $P_{EIO}(\tau)$ can be obtained as

$$P_{ISO}(\tau) = 1 - (1-p)^2 PS_{00}(\tau) - 2p(1-p)PS_{01}(\tau) \text{ and} \tag{6.11}$$

$$P_{EIO}(\tau) = 2p(1-p)PI_{01}(\tau) + p^2 PI_{11}(\tau), \tag{6.12}$$

respectively.

6.3.1 Performance Using any Value of M with Fixed L

In this section we extend the performance analysis to any value of M while keeping $L = 2$, $S_d = L_d = X_d = F_d = 1$ and $I_d = 0$. Once again with $L = 2$, there are three possible cases. When both the channels are OFF, $PS_{00}(\tau)$ can be obtained as

$$PS_{00}(\tau) = \sum_{i=0}^{M-3} 2^{(M-i)}\binom{M}{i}\left[P_{00}^1(\tau)\right]^{(M-i)}\left[1 - 2P_{00}^1(\tau)\right]^i + 2\binom{M}{M-2}\left[P_{00}^1(\tau)\right]^2\left[1 - 2P_{00}^1(\tau)\right]^{(M-2)} \tag{6.13}$$

When channel 1 is OFF and 2 is ON, $PS_{01}(\tau)$ and $PI_{01}(\tau)$ can be given by

$$PS_{01}(\tau) = \sum_{i=0}^{M-3}\binom{M}{i}\sum_{j=0}^{\lfloor\frac{M-i}{2}\rfloor - 1}\left[\binom{M-i}{j}\left[P_{01}^1(\tau)\right]^{M-i-j}\left[P_{01}^2(\tau)\right]^j\left[1 - P_{01}^1(\tau) - P_{01}^2(\tau)\right]^i\right] + \frac{\binom{M-i}{\lfloor\frac{M-i}{2}\rfloor}\left[P_{01}^1(\tau)\right]^{M-i-\lfloor\frac{M-i}{2}\rfloor}\left[P_{01}^1(\tau)\right]^{\lfloor\frac{M-i}{2}\rfloor}\left[1 - P_{01}^1(\tau) - P_{01}^2(\tau)\right]^i}{gcd\,(i-1,2)\,mod(M,2) + gcd(i,2)mod(M-1,2)} + \binom{M}{M-2}\left[P_{01}^1(\tau)\right]^2\left[1 - P_{01}^1(\tau) - P_{01}^2(\tau)\right]^{M-2}. \tag{6.14}$$

$$PI_{01}(\tau) = \sum_{i=0}^{M-3} \binom{M}{i} \sum_{j=0}^{\lfloor \frac{M-i}{2} \rfloor - 1} \left[\binom{M-i}{j} \left[P_{01}^2(\tau)\right]^{M-i-j} \left[P_{01}^1(\tau)\right]^j \left[1 - P_{01}^2(\tau) - P_{01}^1(\tau)\right]^i \right] + \frac{\binom{M-i}{\lfloor \frac{M-i}{2} \rfloor} \left[P_{01}^2(\tau)\right]^{M-i-\lfloor \frac{M-i}{2} \rfloor} \left[P_{01}^2(\tau)\right]^{\lfloor \frac{M-i}{2} \rfloor} \left[1 - P_{01}^2(\tau) - P_{01}^1(\tau)\right]^i}{gcd\,(i-1,2)\,mod(M,2) + gcd(i,2) mod(M-1,2)} + \binom{M}{M-2} \left[P_{01}^2(\tau)\right]^2 \left[1 - P_{01}^2(\tau) - P_{01}^1(\tau)\right]^{M-2}. \quad (6.15)$$

where, $gcd(a,b)$ represents the greatest common divisor of a and b and $mod(a,b)$ represents the modulo operation. Finally, when we consider both the channels as ON, the $PI_{11}(\tau)$ can be obtained as

$$PI_{11}(\tau) = \sum_{i=0}^{M-3} 2^{(M-i)} \binom{M}{i} \left[P_{11}^1(\tau)\right]^{(M-i)} \left[1 - 2P_{11}^1(\tau)\right]^i + 2\binom{M}{M-2} \left[P_{11}^1(\tau)\right]^2 \left[1 - 2P_{11}^1(\tau)\right]^{(M-2)}. \quad (6.16)$$

Substituting Eq. (6.13) to Eq. (6.16) in Eq. (6.11) and Eq. (6.12) give us $P_{ISO}(\tau)$ and $P_{EIO}(\tau)$.

6.3.2 Performance using any Value of L with Fixed M

We now derive the expressions for P_{ISO} and P_{EIO} for any value of L by considering $M = 3$, $S_d = L_d = X_d = F_d = 1$ and $I_d = 0$. To do this, let us denote pdfs in Eq. (6.2) as

$$f_{H0}(x) = \frac{N^N x^{N-1}}{\Gamma(N) e^{xN}}, \text{ and } f_{H1}(x) = \frac{N^N x^{N-1} e^{\frac{-xN}{(1+\gamma)}}}{\Gamma(N)\,(1+\gamma)^N},, \quad (6.17)$$

under $H_m = 0$ and $H_m = 1$, respectively. The respective complementary cumulative distribution functions (ccdfs) are

$$\bar{F}_{H0}(x) = \frac{\Gamma\,(N, Nx)}{\Gamma(N)}, \text{ and } \bar{F}_{H1}(x) = \frac{\Gamma\left(N, \frac{Nx}{(1+\gamma)}\right)}{\Gamma(N)}. \quad (6.18)$$

Using these, one can obtain $P_{ISO}(\tau)$ and $P_{EIO}(\tau)$ as

$$P_{ISO}(\tau) = 1 - \sum_{i=0}^{L-1} \frac{L!(1-p)^{L-i}p^i}{i!(L-i-1)!} \Big[(1 + 3\,(L-i-1))\, I_1^3 + 3iI_1^2 I_2 + 3I_1^2\,(1 - (L-i)\,I_1 - iI_2) \Big], \quad (6.19)$$

$$P_{EIO}(\tau) = \sum_{i=1}^{L} \binom{L}{i} (1-p)^{L-i} p^i \Big[(i + 3i(i-1))\, I_2^3 + 3i(L-i) I_2^2 I_1 + 3iI_2^2\,(1 - (L-i) I_1 - iI_2) \Big], \quad (6.20)$$

where I_1 and I_2 are given by the following integrals

$$I_1 = \int_0^\tau f_{H0}(x)\,[\bar{F}_{H0}(x)]^{L-i-1}\,[\bar{F}_{H_1}(x)]^i\,dx \quad (6.21)$$

$$I_2 = \int_0^\tau f_{H1}(x)\,[\bar{F}_{H1}(x)]^{i-1}\,[\bar{F}_{H_0}(x)]^{L-i}\,dx \quad (6.22)$$

6.4 Results and Discussion

In this section we carry out the experiments using the theoretical analysis given in Section 6.3. The performance is illustrated using the plots of P_{EIO} VS. P_{ISO}. Monte Carlo simulations are also carried out to validate the theoretical analysis and to study the effect of different parameters on the performance of the proposed algorithm. For MC simulation we consider both the PU signal and the noise as complex Gaussian and the results are averaged over 10^5 realizations. In Fig. 6.2, we show the plots obtained using both Monte Carlo simulations and theoretical analysis to validate expressions derived in Section 6.3. The plots shown in Fig. 6.3 and Fig. 6.4 are obtained using theoretical analysis given in Section 6.3 and those in Fig. 6.5 are obtained using MC simulation.

Fig. 6.2(a) validates the general theoretical analysis for any value of M with fixed L given in Section 6.3.1 where as Fig. 6.2(b) validates the expressions given

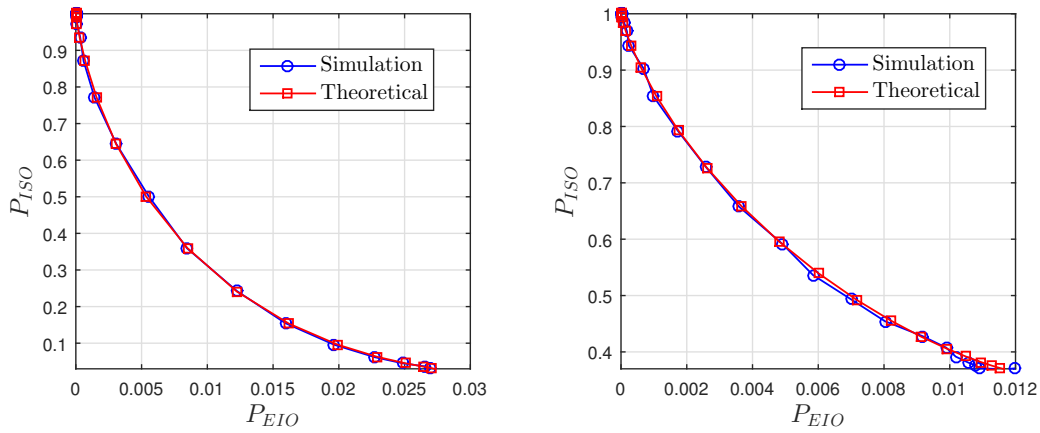

Figure 6.2: P_{EIO} VS. P_{ISO} for the proposed algorithm using theoretical analysis and Monte Carlo simulation considering $S_d = L_d = X_d = F_d = 1$, $I_d = 0$, $N = 10$, $\gamma = -5\ dB$ (a) theoretical analysis in Section 6.3.1 with $M = 8$ and $L = 2$, (b) theoretical analysis in Section 6.3.2 with $L = 4$ and $M = 3$.

in Section 6.3.2 for any value of L with fixed M. Overlapping of the plots conforms the correctness of our analysis.

In Fig. 6.3, we compare the performance of the proposed algorithm against RCD [112], R-SLC [23] and R-SLS [22]. The plot for proposed algorithm is obtained using $M = 5$. It can be clearly observed that the proposed algorithm out performs the RCD. For example, for $P_{EIO} \approx 0.02$, the P_{ISO} for the proposed algorithm is 57.515% smaller than that of RCD. Also, the proposed algorithm performs better than both R-SLC and R-SLS having two diversity branches, i.e., $P = 2$. For example, for $P_{EIO} \approx 0.02$, the P_{ISO} for the proposed algorithm is 20.905% and 35.167% smaller than R-SLC and R-SLS, respectively. We can see that by choosing the appropriate number of CSUs, the proposed algorithm performs better than both R-SLC and R-SLS. This happens despite the fact that R-SLS uses detection scheme similar to the soft combining used in CSS. Also, note that for antenna diversity the spacing between antennas has to be sufficiently high in order to receive independent observations. This makes the implementation of both R-SLC and R-SLS difficult when the number of diversity branches increases.

In Fig. 6.4(a), we demonstrate the effect of increasing the number of CSUs, i.e., M, on the performance where we vary M between 4 and 16. We see that for a

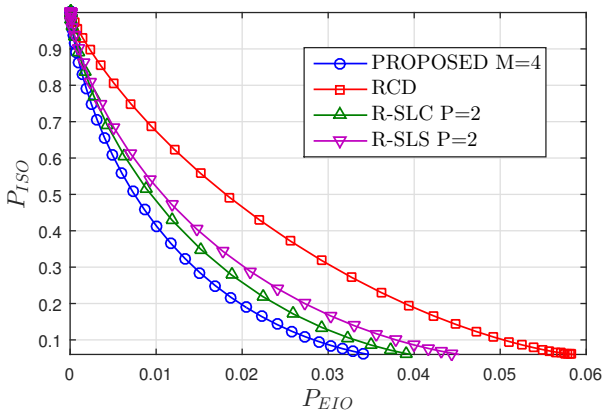

Figure 6.3: P_{EIO} VS. P_{ISO} showing comparison of the proposed, RCD, R-SLC ($P = 2$) and R-SLS ($P = 2$) considering $L = 2$, $M = 5$, $S_d = L_d = X_d = F_d = 1$, $I_d = 0$, $N = 10$ and $\gamma = -5\ dB$.

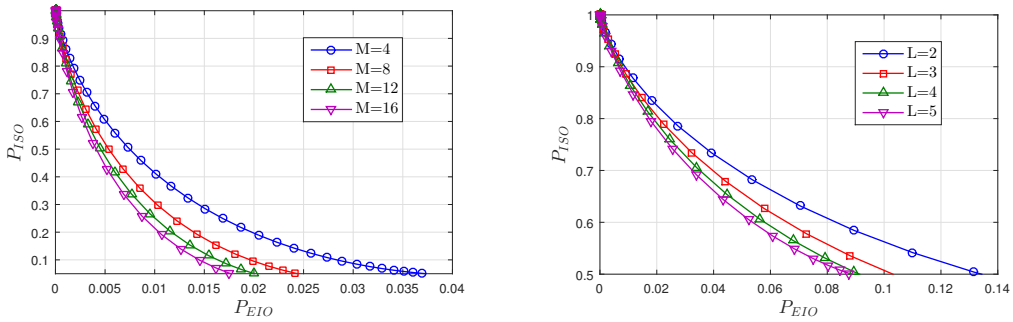

(a) (b)

Figure 6.4: P_{EIO} VS P_{ISO} for varying M and L using $N = 10$, $S_d = L_d = X_d = F_d = 1$, $I_d = 0$, $p = 0.1$, $\gamma = -5\ dB$, (a) with $L = 2$ for different M, (b) with $M = 3$ for different L.

value of $P_{EIO} \approx 0.016$, the values of P_{ISO} with $M = 4$ and $M = 16$ are 0.249 and 0.071, respectively, indicating that the P_{ISO} with $M = 16$ is 71.188% smaller than with $M = 4$. This shows that the performance can be significantly improved by increasing the number of CSUs. The effect of increasing number of channels in the partial band, i.e., L, is illustrated in Fig. 6.4(b). We observe that with increase in L, the performance improves. This is because, increasing L results in more number of free channels in the partial band. One can see that the performance improvement is not significant when L is increased from 4 to 5. From this we may conclude that after certain value of L, the improvement tends to saturate and one does not get an advantage by simply increasing L.

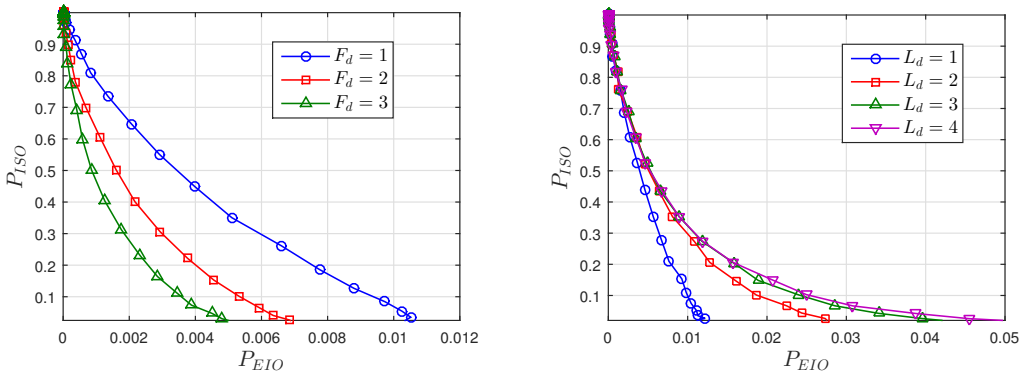

(a) (b)

Figure 6.5: P_{EIO} VS P_{ISO} for varying F_d and L_d using $N = 10$, $S_d = 1$, $I_d = 0$, $p = 0.1$, $\gamma = -5\ dB$, (a) with $X_d = 2$, $L = 4$, $M = 8$, $L_d = 2$ for different F_d, (b) $X_d = 4$, $L = 8$, $M = 4$, $F_d = 1$ for different L_d.

Finally, in Fig. 6.5, we demonstrate the effect of increasing F_d and L_d on the performance. In Fig. 6.5(a), we show the effect of varying the F_d. We know that in order to declare a channel as free, it must be reported as free at least $F_d + 1$ times. This indicates that with the increase in F_d, we are providing more security against the interference to the PU. In Fig. 6.5(a), we can see the clear improvement in the performance with the increase in F_d. One has to choose the value of F_d appropriately because it also decides the maximum possible probability of spectrum opportunity. If the number of CSUs are more, higher value of F_d can be selected. In Fig. 6.5(b), we demonstrate the effect of increasing L_d on the performance. One can observe that increasing L_d degrades the performance. The reason for performance degradation when L_d is increased is as follows. Although increasing the L_d results in higher probability of obtaining the free channels, it also increases the interference to the PU that degrades the performance. The FC arranges the reported free channels in descending order with regard to number of times channels are reported as free and hence the probability of channels which are at the top after ordering being free is high. Hence one should choose $S_d = L_d$.

6.5 Conclusion

In this work, we propose a novel algorithm based on cooperative spectrum sensing with hard combining for wideband spectrum sensing. We provide the complete theoretical analysis of the proposed algorithm. From the analysis, it is clear that with the use of cooperation from the SUs, the detection performance can be improved. We validate the theoretical analysis using the Monte Carlo simulations. We show that the proposed algorithm out performs ranked channel detection algorithm. We show that by choosing appropriate number of CSUs, the proposed algorithm performs better than ranked square law combining and ranked square law selection. It is shown that the proposed algorithm performs comparable to both R-SLC and R-SLS at very low SNR. We also demonstrate the effect of different parameters on the detection performance using theoretical analysis and the simulations. Our future work involves the use of soft combining for cooperative spectrum sensing and to include fading channels for analysis.

CHAPTER 7

Conclusions and Future Research Directions

In this chapter, we provide the conclusions by summarizing our main contributions and also indicate future research directions.

7.1 Conclusions

In this thesis we have addressed the problem of spectrum sensing for cognitive radio by providing theoretical analysis of energy detection based approach considering practical scenarios and by proposing novel detection algorithms. We began with the discussion of energy detection based spectrum sensing over $\eta - \lambda - \mu$ fading channel. The $\eta - \lambda - \mu$ fading model represents a general model which includes other existing models as special cases. The performance improvement was shown using diversity and cooperative spectrum sensing. The analysis was then extended to the case of shadowing in addition to fading.

In our next work, we have analyzed the performance of generalized energy detector in the presence of noise uncertainty and fading. First, the expressions for detection probabilities considering AWGN channel were derived for three cases namely, no diversity, with diversity and cooperative spectrum sensing. We then derive the expressions for SNR walls and discussed the effect of diversity and cooperative spectrum sensing on the SNR walls. The analysis was then extended to the channel with Nakagami fading and it was shown that in this scenario, the SNR wall increases significantly. All the derived expressions were validated using Monte Carlo simulations.

Above works were carried out by considering narrowband sensing. Our next

work involved detection techniques for wideband spectrum sensing. Two new detection algorithms, namely, ranked square law combining (R-SLC) and ranked square law selection (R-SLS), were proposed that make use of diversity. Complete theoretical analysis was provided for these algorithms considering Nakagami fading. The proposed algorithms outperform the ranked channel detection algorithm when used without diversity. The theoretical analysis was then validated using Monte Carlo simulations. Also, the effects of different parameters on the detection performance was studied.

In our next work, a novel detection algorithm for cooperative wideband spectrum sensing was proposed using hard combining. The complete theoretical analysis was provided for the proposed algorithm which is validated using Monte Carlo simulations. It was shown that the proposed algorithm outperforms the ranked channel detection algorithm. By choosing appropriate number of cooperating secondary users, the proposed algorithm performs better than both R-SLC and R-SLS. The effects of different parameters on the detection performance was also studied.

7.2 Future Research Directions

This thesis has presented theoretical analysis of existing narrowband spectrum sensing algorithms considering practical scenarios and few novel detection algorithms for wideband spectrum sensing. In the process of this work, however, we identified related problems that one may consider worth pursuing. These are briefly described as below.

- *Analysis of other detection techniques under generalized fading* :
  In Chapter 3, we have analyzed the performance of energy detection based spectrum sensing under general fading model. This analysis can be extended for other spectrum sensing techniques available in literature, namely, matched filter detection, cyclostationary detection, eigenvalue based detection, covariance based detection, etc.

- *Machine learning techniques for spectrum sensing*:

In Chapters 3 and 4, we addressed the problem of spectrum sensing where it is assumed that primary users transmit at single power level. Recently, a new multiple primary transmit power (MPTP) scenario has been proposed in [66], where PU could work under more than one discrete power levels while the task of spectrum sensing is not only to detect the status of PU, but also to recognize PU's transmit power level. This can be addressed as a classification problem with multiple classes. Machine learning techniques can be applied to solve this problem. The machine learning techniques can also be applied to the traditional scenario where PU transmits at a single power level which can be considered as a problem of binary classification.

- *Analysis of proposed algorithms in practical scenarios*:
  In Chapter 5, we proposed detection algorithms that use SLC and SLS diversity and the analysis was given considering Nakagami fading. One can extend the same to more general system models consisting of varying channel bandwidths, SNR levels across channels, fading, noise uncertainty, etc. The problem can be formulated in an optimization frame work to find the optimal thresholds when different priorities, and different occupancy probabilities are considered for PU channels.

- *Use of soft combining for cooperative wideband spectrum sensing*:
  In Chapter 6, we addressed the problem of cooperative wideband spectrum sensing where we use hard combining at the fusion center. We know that the soft combining gives better performance when compared to hard combining. Hence, the soft combining can be used for solving the problem we considered for cooperative wideband spectrum sensing. However, the use of soft combining require higher control channel bandwidth. One can use quantized soft combining in order to reduce the required control channel bandwidth.

- *Combining antenna diversity and cooperative spectrum sensing for performance improvement*:
  In all our works where we use cooperative spectrum sensing, we consider

that all the cooperating secondary users have single receive antenna. One can consider the scenario where cooperating secondary users have multiple antennas. In this case, one can get improved performance since it takes advantages of both antenna diversity and CSS. The major problem with this kind of scheme is the computational complexity. One can use quantized cooperative spectrum sensing to reduce the complexity.

References

[1] A. Abdi and M. Kaveh. K distribution: an appropriate substitute for rayleigh-lognormal distribution in fading-shadowing wireless channels. *Electronics Letters*, 34(9):851–852, Apr 1998. ISSN 0013-5194. doi: 10.1049/el:19980625.

[2] M. Abramovitz and I. A. stigan. *eds.,Handbook of Mathematical Functions. New York*. NY: Dover, 1970.

[3] I. F. Akyildiz, B. F. Lo, and R. Balakrishnan. Cooperative spectrum sensing in cognitive radio networks: A survey. *Physical Communication*, 4(1):40 – 62, 2011. ISSN 1874-4907. doi: https://doi.org/10.1016/j.phycom.2010.12.003. URL http://www.sciencedirect.com/science/article/pii/S187449071000039X.

[4] O. Alhussein, A. A. Hammadi, P. C. Sofotasios, S. Muhaidat, J. Liang, M. Al-Qutayri, and G. K. Karagiannidis. Performance analysis of energy detection over mixture gamma based fading channels with diversity reception. In *2015 IEEE 11th International Conference on Wireless and Mobile Computing, Networking and Communications (WiMob)*, pages 399–405, Oct 2015. doi: 10.1109/WiMOB.2015.7347990.

[5] A. Ali and W. Hamouda. Advances on spectrum sensing for cognitive radio networks: Theory and applications. *IEEE Communications Surveys Tutorials*, 19(2):1277–1304, Secondquarter 2017. ISSN 1553-877X. doi: 10.1109/COMST.2016.2631080.

[6] T. An, I. Song, S. Lee, and H. K. Min. Detection of signals with observations in multiple subbands: A scheme of wideband spectrum sensing

for cognitive radio with multiple antennas. *IEEE Transactions on Wireless Communications*, 13(12):6968–6981, Dec 2014. ISSN 1536-1276. doi: 10.1109/TWC.2014.2349938.

[7] G. B. Arfken and H. J. Weber. *Mathematical Methods for Physicists*. Elsevier Academic Press, San Diego, 6th ed. edition, 2005.

[8] D. Arianandа and G. Leus. Compressive wideband power spectrum estimation. *IEEE Transactions on Signal Processing,*, 60(9):4775–4789, Sept 2012. ISSN 1053-587X. doi: 10.1109/TSP.2012.2201153.

[9] D. Arianandа, G. Leus, and Z. Tian. Multi-coset sampling for power spectrum blind sensing. In *17th International Conference on Digital Signal Processing (DSP),*, pages 1–8, July 2011. doi: 10.1109/ICDSP.2011.6005003.

[10] A. Assra, J. Yang, and B. Champagne. An EM approach for cooperative spectrum sensing in multiantenna CR networks. *IEEE Transactions on Vehicular Technology*, 65(3):1229–1243, March 2016. ISSN 0018-9545. doi: 10.1109/TVT.2015.2408369.

[11] S. Atapattu, C. Tellambura, and H. Jiang. Energy detection of primary signals over η-μ fading channels. In *International Conference on Industrial and Information Systems (ICIIS),*, pages 118–122, Dec 2009. doi: 10.1109/ICIINFS.2009.5429879.

[12] S. Atapattu, C. Tellambura, and H. Jiang. Performance of an energy detector over channels with both multipath fading and shadowing. *IEEE Transactions on Wireless Communications,*, 9(12):3662–3670, December 2010. ISSN 1536-1276. doi: 10.1109/TWC.2010.100110.091042.

[13] S. Atapattu, C. Tellambura, and H. Jiang. Spectrum sensing via energy detector in low SNR. In *2011 IEEE International Conference on Communications (ICC)*, pages 1–5, June 2011. doi: 10.1109/icc.2011.5963316.

[14] A. Bagheri, P. C. Sofotasios, T. A. Tsiftsis, K. Ho-Van, M. I. Loupis, S. Freear, and M. Valkama. Energy detection based spectrum sensing

over enriched multipath fading channels. In *2016 IEEE Wireless Communications and Networking Conference*, pages 1–6, April 2016. doi: 10.1109/WCNC.2016.7565141.

[15] V. R. S. Banjade, C. Tellambura, and H. Jiang. New asymptotics for performance of energy detector. In *IEEE Global Communications Conference (GLOBECOM)*, pages 4020–4024, 2014.

[16] V. R. S. Banjade, C. Tellambura, and H. Jiang. Performance of p -norm detector in AWGN, fading, and diversity reception. *IEEE Transactions on Vehicular Technology*, 63(7):3209–3222, Sept 2014. ISSN 0018-9545. doi: 10.1109/TVT.2014.2298395.

[17] V. R. S. Banjade, C. Tellambura, and H. Jiang. Approximations for performance of energy detector and p-norm detector. *IEEE Communications Letters*, 19(10):1678–1681, Oct 2015. ISSN 1089-7798. doi: 10.1109/LCOMM.2015.2466105.

[18] A. A. A. Boulogeorgos, N. D. Chatzidiamantis, and G. K. Karagiannidis. Energy detection spectrum sensing under rf imperfections. *IEEE Transactions on Communications*, 64(7):2754–2766, July 2016. ISSN 0090-6778. doi: 10.1109/TCOMM.2016.2561294.

[19] D. Cabric, S. M. Mishra, and R. W. Brodersen. Implementation issues in spectrum sensing for cognitive radios. In *Conference Record of the Thirty-Eighth Asilomar Conference on Signals, Systems and Computers, 2004.*, volume 1, pages 772–776 Vol.1, Nov 2004. doi: 10.1109/ACSSC.2004.1399240.

[20] K. M. Captain and M. V. Joshi. Performance of wideband spectrum sensing under fading channel. In *2015 Seventh International Workshop on Signal Design and its Applications in Communications (IWSDA)*, pages 170–174, Sept 2015. doi: 10.1109/IWSDA.2015.7458397.

[21] K. M. Captain and M. V. Joshi. Energy detection based spectrum sensing over η-λ-μ fading channel. In *8th International Conference on Com-*

munication Systems and Networks (COMSNETS), pages 1–6, Jan 2016. doi: 10.1109/COMSNETS.2016.7439989.

[22] K. M. Captain and M. V. Joshi. Square law selection diversity for wideband spectrum sensing under fading. In *2016 IEEE 84th Vehicular Technology Conference (VTC-Fall)*, pages 1–6, Sept 2016. doi: 10.1109/VTCFall.2016.7881235.

[23] K. M. Captain and M. V. Joshi. Performance improvement in wideband spectrum sensing under fading: Use of diversity. *IEEE Transactions on Vehicular Technology*, 66(9):8152–8162, Sept 2017. ISSN 0018-9545. doi: 10.1109/TVT.2017.2679282.

[24] K. M. Captain and M. V. Joshi. SNR wall for cooperative spectrum sensing using generalized energy detector. In *Accepted for Publication at 10th International Conference on Communication Systems and Networks (COMSNETS)*, Jan 2018.

[25] D. Chen, J. Li, and J. Ma. Cooperative spectrum sensing under noise uncertainty in cognitive radio. In *2008 4th International Conference on Wireless Communications, Networking and Mobile Computing*, pages 1–4, Oct 2008. doi: 10.1109/WiCom.2008.295.

[26] H. S. Chen, W. Gao, and D. G. Daut. Spectrum sensing using cyclostationary properties and application to IEEE 802.22 wran. In *IEEE Global Telecommunications Conference (GLOBECOM)*, pages 3133–3138, Nov 2007. doi: 10.1109/GLOCOM.2007.593.

[27] X. Chen, W. Xu, Z. He, and X. Tao. Spectral correlation-based multi-antenna spectrum sensing technique. In *2008 IEEE Wireless Communications and Networking Conference*, pages 735–740, March 2008. doi: 10.1109/WCNC.2008.135.

[28] Y. Chen. Improved energy detector for random signals in Gaussian noise. *IEEE Transactions on Wireless Communications*, 9(2):558–563, February 2010. ISSN 1536-1276. doi: 10.1109/TWC.2010.5403535.

[29] Y. Chu and S. Liu. Hard decision fusion based cooperative spectrum sensing over nakagami-m fading channels. In *2012 8th International Conference on Wireless Communications, Networking and Mobile Computing*, pages 1–4, Sept 2012. doi: 10.1109/WiCOM.2012.6478534.

[30] D. Cohen and Y. Eldar. Sub-Nyquist sampling for power spectrum sensing in cognitive radios: A unified approach. *IEEE Transactions on Signal Processing*, 62(15):3897–3910, Aug 2014. ISSN 1053-587X. doi: 10.1109/TSP.2014.2331613.

[31] C. Cordeiro, K. Challapali, D. Birru, and S. S. N. IEEE 802.22: An introduction to the first wireless standard based on cognitive radios. *Journal of Communications*, 1:38–47, April 2006.

[32] A. V. Dandawate and G. B. Giannakis. Statistical tests for presence of cyclostationarity. *IEEE Transactions on Signal Processing*, 42(9):2355–2369, Sep 1994. ISSN 1053-587X. doi: 10.1109/78.317857.

[33] M. Derakhtian, F. Izedi, A. Sheikhi, and M. Neinavaie. Cooperative wideband spectrum sensing for cognitive radio networks in fading channels. *IET Signal Processing*, 6(3):227–238, May 2012. ISSN 1751-9675. doi: 10.1049/iet-spr.2011.0097.

[34] M. Derakhtian, F. Izedi, A. Sheikhi, and M. Neinavaie. Cooperative wideband spectrum sensing for cognitive radio networks in fading channels. *IET Signal Processing,*, 6(3):227–238, May 2012. ISSN 1751-9675. doi: 10.1049/iet-spr.2011.0097.

[35] N. Devroye and V. Tarokh. *Fundamental Limits of Cognitive Radio Networks*, pages 327–351. Springer Netherlands, Dordrecht, 2007. ISBN 978-1-4020-5979-7. doi: 10.1007/978-1-4020-5979-7_17.

[36] Y. Dhungana and C. Tellambura. New simple approximations for error probability and outage in fading. *IEEE Communications Letters*, 16(11):1760–1763, November 2012. ISSN 1089-7798. doi: 10.1109/LCOMM.2012.092112.121280.

[37] F. Digham, M.-S. Alouini, and M. K. Simon. On the energy detection of unknown signals over fading channels. *IEEE Transactions on Communications*,, 55(1):21–24, Jan 2007. ISSN 0090-6778. doi: 10.1109/TCOMM.2006.887483.

[38] F. F. Digham, M. S. Alouini, and M. K. Simon. On the energy detection of unknown signals over fading channels. In *IEEE International Conference on Communications*, volume 5, pages 3575–3579, May 2003. doi: 10.1109/ICC.2003.1204119.

[39] S. E. El-Khamy, M. S. El-Mahallawy, and E. N. S. Youssef. Improved wideband spectrum sensing techniques using wavelet-based edge detection for cognitive radio. In *2013 International Conference on Computing, Networking and Communications (ICNC)*, pages 418–423, Jan 2013. doi: 10.1109/ICCNC.2013.6504120.

[40] B. Farhang-Boroujeny. Filter bank spectrum sensing for cognitive radios. *IEEE Transactions on Signal Processing*, 56(5):1801–1811, May 2008. ISSN 1053-587X. doi: 10.1109/TSP.2007.911490.

[41] FCC. Spectrum policy task force report (ET Docket no. 02-135). Nov 2002.

[42] FCC. Spectrum policy task force report (ET Docket no. 02-155). Nov 2002.

[43] FCC. Notice of proposed rule making and order (ET Docket no. 03-322). Dec 2003.

[44] Y. Feng and X. Wang. Adaptive multiband spectrum sensing. *IEEE Wireless Communications Letters*, 1(2):121–124, April 2012. ISSN 2162-2337. doi: 10.1109/WCL.2012.022012.110230.

[45] W. A. Gardner. Signal interception: a unifying theoretical framework for feature detection. *IEEE Transactions on Communications*, 36(8):897–906, Aug 1988. ISSN 0090-6778. doi: 10.1109/26.3769.

[46] W. A. Gardner. Exploitation of spectral redundancy in cyclostationary signals. *IEEE Signal Processing Magazine*, 8(2):14–36, April 1991. ISSN 1053-5888. doi: 10.1109/79.81007.

[47] A. Ghasemi and E. Sousa. Impact of user collaboration on the performance of sensing-based opportunistic spectrum access. In *Vehicular Technology Conference, 2006. VTC-2006 Fall. 2006 IEEE 64th*, pages 1–6, Sept 2006. doi: 10.1109/VTCF.2006.268.

[48] A. Ghasemi and E. S. Sousa. Collaborative spectrum sensing for opportunistic access in fading environments. In *First IEEE International Symposium on New Frontiers in Dynamic Spectrum Access Networks, 2005. DySPAN 2005.*, pages 131–136, Nov 2005. doi: 10.1109/DYSPAN.2005.1542627.

[49] M. Ghaznavi and A. Jamshidi. Efficient method for reducing the average control bits in a distributed cooperative sensing in cognitive radio system. *IET Communications*, 7(9):867–874, June 2013. ISSN 1751-8628. doi: 10.1049/iet-com.2012.0574.

[50] I. S. Gradshteyn and I. M. Ryzhik. *Table of Integrals, Series and Products*. CA: Academic, San Diego, 6th ed. edition, 2000.

[51] Y. Gwon, H. T. Kung, and D. Vlah. Compressive sensing with optimal sparsifying basis and applications in spectrum sensing. In *Global Communications Conference (GLOBECOM)*, pages 5386–5391, Dec 2012. doi: 10.1109/GLOCOM.2012.6503977.

[52] K. Hamdi, X. N. Zeng, A. Ghrayeb, and K. B. Letaief. Impact of noise power uncertainty on cooperative spectrum sensing in cognitive radio systems. In *2010 IEEE Global Telecommunications Conference (GLOBECOM)*, pages 1–5, Dec 2010. doi: 10.1109/GLOCOM.2010.5683357.

[53] G. Hattab and M. Ibnkahla. Multiband spectrum access: Great promises for future cognitive radio networks. *Proceedings of the IEEE*, 102(3):282–306, March 2014. ISSN 0018-9219. doi: 10.1109/JPROC.2014.2303977.

[54] V. Havary-Nassab, S. Hassan, and S. Valaee. Compressive detection for wide-band spectrum sensing. In *2010 IEEE International Conference on Acoustics, Speech and Signal Processing*, pages 3094–3097, March 2010. doi: 10.1109/ICASSP.2010.5496101.

[55] V. Havary-Nassab, S. Hassan, and S. Valaee. Compressive detection for wide-band spectrum sensing. In *IEEE International Conference on Acoustics Speech and Signal Processing (ICASSP),*, pages 3094–3097, March 2010. doi: 10.1109/ICASSP.2010.5496101.

[56] S. Haykin. Cognitive radio: brain-empowered wireless communications. *IEEE Journal on Selected Areas in Communications*, 23(2):201–220, Feb 2005. ISSN 0733-8716. doi: 10.1109/JSAC.2004.839380.

[57] S. Haykin, D. J. Thomson, and J. H. Reed. Spectrum sensing for cognitive radio. *Proceedings of the IEEE*, 97(5):849–877, May 2009. ISSN 0018-9219. doi: 10.1109/JPROC.2009.2015711.

[58] S. P. Herath, N. Rajatheva, and C. Tellambura. Energy detection of unknown signals in fading and diversity reception. *IEEE Transactions on Communications*, 59(9):2443–2453, September 2011. ISSN 0090-6778. doi: 10.1109/TCOMM.2011.071111.090349.

[59] S. S. Kalamkar and A. Banerjee. On the performance of generalized energy detector under noise uncertainty in cognitive radio. In *National Conference on Communications (NCC)*, pages 1–5, Feb 2013. doi: 10.1109/NCC.2013.6487927.

[60] S. S. Kalamkar, A. Banerjee, and A. K. Gupta. SNR wall for generalized energy detection under noise uncertainty in cognitive radio. In *2013 19th Asia-Pacific Conference on Communications (APCC)*, pages 375–380, Aug 2013. doi: 10.1109/APCC.2013.6765974.

[61] V. Kapinas, S. Mihos, and G. Karagiannidis. On the monotonicity of the generalized marcum and nuttall Q -functions. *Information Theory, IEEE Transactions on*, 55(8):3701–3710, Aug 2009. ISSN 0018-9448. doi: 10.1109/TIT.2009.2023710.

[62] S. Kay. *Fundamentals of Statistical Signal Processing: Detection theory*. Prentice Hall Signal Processing Series. Prentice-Hall PTR, 1998. ISBN 9780135041352.

[63] K. Kim, I. A. Akbar, K. K. Bae, J. S. Um, C. M. Spooner, and J. H. Reed. Cyclostationary approaches to signal detection and classification in cognitive radio. In *2007 2nd IEEE International Symposium on New Frontiers in Dynamic Spectrum Access Networks*, pages 212–215, April 2007. doi: 10.1109/DYSPAN.2007.35.

[64] M. Kim and J. i. Takada. Efficient multi-channel wideband spectrum sensing technique using filter bank. In *2009 IEEE 20th International Symposium on Personal, Indoor and Mobile Radio Communications*, pages 1014–1018, Sept 2009. doi: 10.1109/PIMRC.2009.5450175.

[65] V. Kostylev. Energy detection of a signal with random amplitude. In *IEEE International Conference on Communications (ICC 2002).*, volume 3, pages 1606–1610 vol.3, 2002. doi: 10.1109/ICC.2002.997120.

[66] J. Li, F. Gao, T. Jiang, and W. Chen. A new spectrum sensing strategy when primary user has multiple power levels. In *2014 IEEE Global Communications Conference*, pages 840–845, Dec 2014. doi: 10.1109/GLOCOM.2014.7036913.

[67] Y. Li and Z. Ding. Arma system identification based on second-order cyclostationarity. *IEEE Transactions on Signal Processing*, 42(12):3483–3494, Dec 1994. ISSN 1053-587X. doi: 10.1109/78.340782.

[68] Z. Li, F. R. Yu, and M. Huang. A cooperative spectrum sensing consensus scheme in cognitive radios. In *IEEE INFOCOM 2009*, pages 2546–2550, April 2009. doi: 10.1109/INFCOM.2009.5062184.

[69] M. Lin and A. P. Vinod. Progressive decimation filter banks for variable resolution spectrum sensing in cognitive radios. In *2010 17th International Conference on Telecommunications*, pages 857–863, April 2010. doi: 10.1109/ICTEL.2010.5478757.

[70] J. Lunden, V. Koivunen, A. Huttunen, and H. V. Poor. Spectrum sensing in cognitive radios based on multiple cyclic frequencies. In *2007 2nd International Conference on Cognitive Radio Oriented Wireless Networks and Communications*, pages 37–43, Aug 2007. doi: 10.1109/CROWNCOM.2007.4549769.

[71] A. López-Parrado and J. Velasco-Medina. Cooperative wideband spectrum sensing based on sub-nyquist sparse fast fourier transform. *IEEE Transactions on Circuits and Systems II: Express Briefs*, 63(1):39–43, Jan 2016. ISSN 1549-7747. doi: 10.1109/TCSII.2015.2483278.

[72] J. Ma and Y. G. Li. Soft combination and detection for cooperative spectrum sensing in cognitive radio networks. In *IEEE GLOBECOM 2007 - IEEE Global Telecommunications Conference*, pages 3139–3143, Nov 2007. doi: 10.1109/GLOCOM.2007.594.

[73] J. Ma, G. Zhao, and Y. Li. Soft combination and detection for cooperative spectrum sensing in cognitive radio networks. *IEEE Transactions on Wireless Communications*, 7(11):4502–4507, November 2008. ISSN 1536-1276. doi: 10.1109/T-WC.2008.070941.

[74] J. Ma, G. Y. Li, and B. H. Juang. Signal processing in cognitive radio. *Proceedings of the IEEE*, 97(5):805–823, May 2009. ISSN 0018-9219. doi: 10.1109/JPROC.2009.2015707.

[75] Y. Ma, Y. Gao, Y. C. Liang, and S. Cui. Efficient blind cooperative wideband spectrum sensing based on joint sparsity. In *2016 IEEE Global Communications Conference (GLOBECOM)*, pages 1–6, Dec 2016. doi: 10.1109/GLOCOM.2016.7841772.

[76] K. Maeda, A. Benjebbour, T. Asai, T. Furuno, and T. Ohya. Recognition among ofdm-based systems utilizing cyclostationarity-inducing transmission. In *2007 2nd IEEE International Symposium on New Frontiers in Dynamic Spectrum Access Networks*, pages 516–523, April 2007. doi: 10.1109/DYSPAN.2007.74.

[77] A. Mariani, A. Giorgetti, and M. Chiani. SNR wall for energy detection with noise power estimation. In *2011 IEEE International Conference on Communications (ICC)*, pages 1–6, June 2011. doi: 10.1109/icc.2011.5963367.

[78] O. Mehanna and N. D. Sidiropoulos. Frugal sensing: Wideband power

spectrum sensing from few bits. *IEEE Transactions on Signal Processing*, 61 (10):2693–2703, May 2013. ISSN 1053-587X. doi: 10.1109/TSP.2013.2252171.

[79] M. Mishali and Y. C. Eldar. Blind multiband signal reconstruction: Compressed sensing for analog signals. *IEEE Transactions on Signal Processing*, 57 (3):993–1009, March 2009. ISSN 1053-587X. doi: 10.1109/TSP.2009.2012791.

[80] M. Mishali and Y. C. Eldar. Blind multiband signal reconstruction: Compressed sensing for analog signals. *IEEE Transactions on Signal Processing*, 57 (3):993–1009, March 2009. ISSN 1053-587X. doi: 10.1109/TSP.2009.2012791.

[81] J. Mitola. Cognitive radio for flexible mobile multimedia communications. In *Mobile Multimedia Communications, 1999. (MoMuC '99) 1999 IEEE International Workshop on*, pages 3–10, 1999. doi: 10.1109/MOMUC.1999.819467.

[82] J. Mitola. Software radio architecture: a mathematical perspective. *IEEE Journal on Selected Areas in Communications*, 17(4):514–538, Apr 1999. ISSN 0733-8716. doi: 10.1109/49.761033.

[83] J. Mitola and G. Q. Maguire. Cognitive radio: making software radios more personal. *IEEE Personal Communications*, 6(4):13–18, Aug 1999. ISSN 1070-9916. doi: 10.1109/98.788210.

[84] F. Moghimi, A. Nasri, and R. Schober. Adaptive l_p-norm spectrum sensing for cognitive radio networks. *IEEE Transactions on Communications*, 59(7):1934–1945, July 2011. ISSN 0090-6778. doi: 10.1109/TCOMM.2011.051311.090588.

[85] S. Nallagonda, S. D. Roy, A. Chandra, and S. Kundu. Performance of cooperative spectrum sensing in hoyt fading channel under hard decision fusion rules. In *2012 5th International Conference on Computers and Devices for Communication (CODEC)*, pages 1–4, Dec 2012. doi: 10.1109/CODEC.2012.6509221.

[86] S. Nallagonda, S. D. Roy, and S. Kumdu. Performance of cooperative spectrum sensing in fading channels. In *2012 1st International Conference on Re-*

cent Advances in Information Technology (RAIT), pages 202–207, March 2012. doi: 10.1109/RAIT.2012.6194506.

[87] S. Nallagonda, S. K. Bandari, S. D. Roy, and S. Kundu. Performance of cooperative spectrum sensing with soft data fusion schemes in fading channels. In *2013 Annual IEEE India Conference (INDICON)*, pages 1–6, Dec 2013. doi: 10.1109/INDCON.2013.6725924.

[88] S. Nallagonda, A. Chandra, S. Roy, S. Kundu, P. Kukolev, and A. Prokes. Detection performance of cooperative spectrum sensing with hard decision fusion in fading channels. *International Journal of Electronics*, 103(2):297–321, 2016. doi: 10.1080/00207217.2015.1036369. URL https://doi.org/10.1080/00207217.2015.1036369.

[89] E. Neasmith and N. Beaulieu. New results on selection diversity. *IEEE Transactions on Communications,*, 46(5):695–704, May 1998. ISSN 0090-6778. doi: 10.1109/26.668745.

[90] A. H. Nuttall. Some integrals involving the Q_M- function. Technical report, Naval Underwater Syst. Center (NUSC) Tech. Rep., May 1974.

[91] A. Papazafeiropoulos and S. Kotsopoulos. The η-λ-μ: A general fading distribution. In *IEEE Global Telecommunications Conference, GLOBECOM 2009.*, pages 1–5, Nov 2009. doi: 10.1109/GLOCOM.2009.5425777.

[92] A. Papoulis and S. Pillai. *Probability, Random Variables, and Stochastic Processes*. McGraw-Hill series in electrical engineering: Communications and signal processing. Tata McGraw-Hill, 2002. ISBN 9780070486584. URL https://books.google.co.in/books?id=g6eUoWOlcQMC.

[93] E. C. Y. Peh, Y. C. Liang, Y. L. Guan, and Y. Zeng. Optimization of cooperative sensing in cognitive radio networks: A sensing-throughput tradeoff view. *IEEE Transactions on Vehicular Technology*, 58(9):5294–5299, Nov 2009. ISSN 0018-9545. doi: 10.1109/TVT.2009.2028030.

[94] Y. Polo, Y. Wang, A. Pandharipande, and G. Leus. Compressive wide-band spectrum sensing. In *IEEE International Conference on Acoustics, Speech and Signal Processing (ICASSP),*, pages 2337–2340, April 2009. doi: 10.1109/ICASSP.2009.4960089.

[95] R. V. Prasad, P. Pawlczak, J. A. Hoffmeyer, and H. S. Berger. Cognitive functionality in next generation wireless networks: standardization efforts. *IEEE Communications Magazine*, 46(4):72–78, April 2008. ISSN 0163-6804. doi: 10.1109/MCOM.2008.4481343.

[96] Z. Quan, S. Cui, H. V. Poor, and A. H. Sayed. Collaborative wideband sensing for cognitive radios. *IEEE Signal Processing Magazine*, 25(6):60–73, November 2008. ISSN 1053-5888. doi: 10.1109/MSP.2008.929296.

[97] Z. Quan, S. Cui, A. H. Sayed, and H. V. Poor. Optimal multiband joint detection for spectrum sensing in cognitive radio networks. *IEEE Transactions on Signal Processing*, 57(3):1128–1140, March 2009. ISSN 1053-587X. doi: 10.1109/TSP.2008.2008540.

[98] H. Sadeghi and P. Azmi. Cyclostationarity-based cooperative spectrum sensing for cognitive radio networks. In *International Symposium on Telecommunications (IST)*, pages 429–434, Aug 2008. doi: 10.1109/ISTEL.2008.4651341.

[99] A. Salarvan and G. K. Kurt. Multi-antenna spectrum sensing for cognitive radio under rayleigh channel. In *2012 IEEE Symposium on Computers and Communications (ISCC)*, pages 000780–000784, July 2012. doi: 10.1109/ISCC.2012.6249394.

[100] A. Singh, M. R. Bhatnagar, and R. K. Mallik. Optimization of cooperative spectrum sensing with an improved energy detector over imperfect reporting channels. In *2011 IEEE Vehicular Technology Conference (VTC Fall)*, pages 1–5, Sept 2011. doi: 10.1109/VETECF.2011.6092887.

[101] A. Singh, M. R. Bhatnagar, and R. K. Mallik. Cooperative spectrum sensing in multiple antenna based cognitive radio network using an improved en-

ergy detector. *IEEE Communications Letters*, 16(1):64–67, January 2012. ISSN 1089-7798. doi: 10.1109/LCOMM.2011.103111.111884.

[102] P. Sofotasios, E. Rebeiz, L. Zhang, T. Tsiftsis, D. Cabric, and S. Freear. Energy detection based spectrum sensing over κ -μ and κ -μ extreme fading channels. *Vehicular Technology, IEEE Transactions on*, 62(3):1031–1040, March 2013. ISSN 0018-9545. doi: 10.1109/TVT.2012.2228680.

[103] J. Song, Z. Feng, P. Zhang, and Z. Liu. Spectrum sensing in cognitive radios based on enhanced energy detector. *IET Communications*, 6(8):805–809, May 2012. ISSN 1751-8628. doi: 10.1049/iet-com.2010.0536.

[104] A. Sonnenschein and P. M. Fishman. Radiometric detection of spread-spectrum signals in noise of uncertain power. *IEEE Transactions on Aerospace and Electronic Systems*, 28(3):654–660, Jul 1992. ISSN 0018-9251. doi: 10.1109/7.256287.

[105] S. Srinu and S. L. Sabat. Cooperative wideband spectrum sensing in suspicious cognitive radio network. *IET Wireless Sensor Systems*, 3(2):153–161, June 2013. ISSN 2043-6386. doi: 10.1049/iet-wss.2012.0044.

[106] G. Stüber. *Principles of Mobile Communication*. Kluwer Academic, Norwell, 2nd edition edition, 2001. ISBN 9780792379980.

[107] H. Sun, W.-Y. Chiu, J. Jiang, A. Nallanathan, and H. Poor. Wideband spectrum sensing with sub-Nyquist sampling in cognitive radios. *IEEE Transactions on Signal Processing*, 60(11):6068–6073, Nov 2012. ISSN 1053-587X. doi: 10.1109/TSP.2012.2212892.

[108] H. Sun, W. Y. Chiu, J. Jiang, A. Nallanathan, and H. V. Poor. Wideband spectrum sensing with sub-Nyquist sampling in cognitive radios. *IEEE Transactions on Signal Processing*, 60(11):6068–6073, Nov 2012. ISSN 1053-587X. doi: 10.1109/TSP.2012.2212892.

[109] H. Sun, A. Nallanathan, C. X. Wang, and Y. Chen. Wideband spectrum sens-

ing for cognitive radio networks: a survey. *IEEE Wireless Communications*, 20(2):74–81, April 2013. ISSN 1536-1284. doi: 10.1109/MWC.2013.6507397.

[110] H. Sun, A. Nallanathan, S. Cui, and C.-X. Wang. Cooperative wideband spectrum sensing over fading channels. *IEEE Transactions on Vehicular Technology*, PP(99):1–1, 2015. ISSN 0018-9545. doi: 10.1109/TVT.2015.2407700.

[111] H. Sun, A. Nallanathan, S. Cui, and C. X. Wang. Cooperative wideband spectrum sensing over fading channels. *IEEE Transactions on Vehicular Technology*, 65(3):1382–1394, March 2016. ISSN 0018-9545. doi: 10.1109/TVT.2015.2407700.

[112] Z. Sun and J. Laneman. Performance metrics, sampling schemes, and detection algorithms for wideband spectrum sensing. *IEEE Transactions on Signal Processing,*, 62(19):5107–5118, Oct 2014. ISSN 1053-587X. doi: 10.1109/TSP.2014.2332979.

[113] Z. Sun and J. N. Laneman. Sampling schemes and detection algorithms for wideband spectrum sensing. In *2014 IEEE International Symposium on Dynamic Spectrum Access Networks (DYSPAN)*, pages 541–552, April 2014. doi: 10.1109/DySPAN.2014.6817837.

[114] P. D. Sutton, J. Lotze, K. E. Nolan, and L. E. Doyle. Cyclostationary signature detection in multipath rayleigh fading environments. In *2007 2nd International Conference on Cognitive Radio Oriented Wireless Networks and Communications*, pages 408–413, Aug 2007. doi: 10.1109/CROWNCOM.2007.4549833.

[115] P. D. Sutton, K. E. Nolan, and L. E. Doyle. Cyclostationary signatures for rendezvous in ofdm-based dynamic spectrum access networks. In *2007 2nd IEEE International Symposium on New Frontiers in Dynamic Spectrum Access Networks*, pages 220–231, April 2007. doi: 10.1109/DYSPAN.2007.37.

[116] R. Tandra and A. Sahai. SNR walls for signal detection. *IEEE Journal of Selected Topics in Signal Processing*, 2(1):4–17, Feb 2008. ISSN 1932-4553. doi: 10.1109/JSTSP.2007.914879.

[117] Z. Tian and G. B. Giannakis. A wavelet approach to wideband spectrum sensing for cognitive radios. In *2006 1st International Conference on Cognitive Radio Oriented Wireless Networks and Communications*, pages 1–5, June 2006. doi: 10.1109/CROWNCOM.2006.363459.

[118] Z. Tian and G. B. Giannakis. Compressed sensing for wideband cognitive radios. In *2007 IEEE International Conference on Acoustics, Speech and Signal Processing - ICASSP '07*, volume 4, pages IV–1357–IV–1360, April 2007. doi: 10.1109/ICASSP.2007.367330.

[119] Z. Tian, Y. Tafesse, and B. M. Sadler. Cyclic feature detection with sub-Nyquist sampling for wideband spectrum sensing. *IEEE Journal of Selected Topics in Signal Processing*, 6(1):58–69, Feb 2012. ISSN 1932-4553. doi: 10.1109/JSTSP.2011.2181940.

[120] M. A. Torad, A. El-Kassas, and H. El-Hennawy. Cooperative wideband spectrum sensing over rician and nakagami fading channels. In *2015 IEEE International Symposium on Signal Processing and Information Technology (ISSPIT)*, pages 180–185, Dec 2015. doi: 10.1109/ISSPIT.2015.7394324.

[121] J. A. Tropp, J. N. Laska, M. F. Duarte, J. K. Romberg, and R. G. Baraniuk. Beyond Nyquist: Efficient sampling of sparse bandlimited signals. *IEEE Transactions on Information Theory*, 56(1):520–544, Jan 2010. ISSN 0018-9448. doi: 10.1109/TIT.2009.2034811.

[122] J. Unnikrishnan and V. V. Veeravalli. Cooperative sensing for primary detection in cognitive radio. *IEEE Journal of Selected Topics in Signal Processing*, 2(1):18–27, Feb 2008. ISSN 1932-4553. doi: 10.1109/JSTSP.2007.914880.

[123] H. Urkowitz. Energy detection of unknown deterministic signals. *Proceedings of the IEEE*, 55(4):523–531, April 1967. ISSN 0018-9219. doi: 10.1109/PROC.1967.5573.

[124] R. Venkataramani and Y. Bresler. Perfect reconstruction formulas and bounds on aliasing error in sub-Nyquist nonuniform sampling of multi-

band signals. *IEEE Transactions on Information Theory*, 46(6):2173–2183, Sep 2000. ISSN 0018-9448. doi: 10.1109/18.868487.

[125] E. Visotsky, S. Kuffner, and R. Peterson. On collaborative detection of tv transmissions in support of dynamic spectrum sharing. In *First IEEE International Symposium on New Frontiers in Dynamic Spectrum Access Networks, 2005. DySPAN 2005.*, pages 338–345, Nov 2005. doi: 10.1109/DYSPAN.2005.1542650.

[126] H. Wang, Y. Xu, X. Su, and J. Wang. Cooperative spectrum sensing in cognitive radio under noise uncertainty. In *2010 IEEE 71st Vehicular Technology Conference*, pages 1–5, May 2010. doi: 10.1109/VETECS.2010.5494009.

[127] Y. Wang, A. Pandharipande, Y. L. Polo, and G. Leus. Distributed compressive wide-band spectrum sensing. In *Information Theory and Applications Workshop, 2009*, pages 178–183, Feb 2009. doi: 10.1109/ITA.2009.5044942.

[128] I. Wolfram Research. *Mathematica*. Wolfram Research, Inc., Champaign, Illinois, version 10.1 edition, 2015.

[129] R. T. Yazicigil, T. Haque, M. R. Whalen, J. Yuan, J. Wright, and P. R. Kinget. Wideband rapid interferer detector exploiting compressed sampling with a quadrature analog-to-information converter. *IEEE Journal of Solid-State Circuits*, 50(12):3047–3064, Dec 2015. ISSN 0018-9200. doi: 10.1109/JSSC.2015.2464708.

[130] C.-P. Yen, Y. Tsai, and X. Wang. Wideband spectrum sensing based on sub-Nyquist sampling. *IEEE Transactions on Signal Processing*, 61(12):3028–3040, June 2013. ISSN 1053-587X. doi: 10.1109/TSP.2013.2251342.

[131] T. Yucek and H. Arslan. A survey of spectrum sensing algorithms for cognitive radio applications. *IEEE Communications Surveys Tutorials*, 11(1):116–130, First 2009. ISSN 1553-877X. doi: 10.1109/SURV.2009.090109.

[132] F. Zeng, C. Li, and Z. Tian. Distributed compressive spectrum sensing in cooperative multihop cognitive networks. *IEEE Journal of Selected*

Topics in Signal Processing, 5(1):37–48, Feb 2011. ISSN 1932-4553. doi: 10.1109/JSTSP.2010.2055037.

[133] J. Zeng and X. Su. On SNR wall phenomenon under cooperative energy detection in spectrum sensing. In *2015 10th International Conference on Communications and Networking in China (ChinaCom)*, pages 53–60, Aug 2015. doi: 10.1109/CHINACOM.2015.7497910.

[134] Y. Zeng and Y. C. Liang. Covariance based signal detections for cognitive radio. In *2007 2nd IEEE International Symposium on New Frontiers in Dynamic Spectrum Access Networks*, pages 202–207, April 2007. doi: 10.1109/DYSPAN.2007.33.

[135] Y. Zeng and Y. C. Liang. Maximum-minimum eigenvalue detection for cognitive radio. In *2007 IEEE 18th International Symposium on Personal, Indoor and Mobile Radio Communications*, pages 1–5, Sept 2007. doi: 10.1109/PIMRC.2007.4394211.

[136] Y. Zeng and Y. C. Liang. Spectrum-sensing algorithms for cognitive radio based on statistical covariances. *IEEE Transactions on Vehicular Technology*, 58 (4):1804–1815, May 2009. ISSN 0018-9545. doi: 10.1109/TVT.2008.2005267.

[137] Y. Zeng and Y. C. Liang. Eigenvalue-based spectrum sensing algorithms for cognitive radio. *IEEE Transactions on Communications*, 57(6):1784–1793, June 2009. ISSN 0090-6778. doi: 10.1109/TCOMM.2009.06.070402.

[138] Y. Zeng, C. L. Koh, and Y. C. Liang. Maximum eigenvalue detection: Theory and application. In *2008 IEEE International Conference on Communications*, pages 4160–4164, May 2008. doi: 10.1109/ICC.2008.781.

[139] Y. Zeng, Y. C. Liang, A. T. Hoang, and E. C. Y. Peh. Reliability of spectrum sensing under noise and interference uncertainty. In *2009 IEEE International Conference on Communications Workshops*, pages 1–5, June 2009. doi: 10.1109/ICCW.2009.5208033.

[140] W. Zhang and K. B. Letaief. Cooperative spectrum sensing with transmit and relay diversity in cognitive radio networks - [transaction letters]. *IEEE Transactions on Wireless Communications*, 7(12):4761–4766, December 2008. ISSN 1536-1276. doi: 10.1109/T-WC.2008.060857.

[141] W. Zhang, R. K. Mallik, and K. B. Letaief. Optimization of cooperative spectrum sensing with energy detection in cognitive radio networks. *IEEE Transactions on Wireless Communications*, 8(12):5761–5766, December 2009. ISSN 1536-1276. doi: 10.1109/TWC.2009.12.081710.

CHAPTER A

Appendix for Chapter 4

A.1 Derivation for $\bar{P}_{D,plc}$ in Eq. (4.25)

To derive $\bar{P}_{D,plc}$, we require the following result

$$\lim_{N\to\infty} Q\left(a\sqrt{N}\right) = \begin{cases} 0, & \text{if } a > 0, \\ 1, & \text{if } a < 0, \\ 0.5 & \text{if } a = 0. \end{cases} \tag{A.1}$$

Applying limit $N \to \infty$ to Eq. (4.23) and using Eq. (A.1), we get

$$\bar{P}_{D,plc} = \int_{a_1}^{b_1}\int_{a_2}^{b_2} \mathcal{H}\left[G_p\left((1+\tilde{\gamma}_1 x)^{\frac{p}{2}} + (1+\tilde{\gamma}_2 y)^{\frac{p}{2}}\right) - 2\lambda\,(xy)^{\frac{p}{2}}\right] \frac{25}{L_1 L_2\left(\ln(10)\right)^2 xy} dydx \tag{A.2}$$

where, $\mathcal{H}(x)$ represents the Heaviside function defined as

$$\mathcal{H}(x) = \begin{cases} 0, & \text{if } x < 0, \\ \frac{1}{2}, & \text{if } x = 0, \\ 1 & \text{if } x > 0. \end{cases} \tag{A.3}$$

Applying the change of variables as $z = \ln(z)$ and $w = \ln(w)$, we get

$$\bar{P}_{D,plc} = C_1 \int_{-c}^{c} \int_{-d}^{d} \mathcal{H}\left[G_p\left((1+e^{z}\tilde{\gamma}_1)^{\frac{p}{2}} + (1+e^{w}\tilde{\gamma}_2)^{\frac{p}{2}}\right) - 2\lambda e^{\frac{zp}{2}} e^{\frac{wp}{2}}\right] dwdz, \quad \text{(A.4)}$$

where, $c = \ln(b_1)$, $d = \ln(b_2)$ and $C_1 = 100/L_1L_2p^2\ln(10)^2$.

We will evaluate this integral for three ranges of λ. First, we evaluate $\bar{P}_{D,plc}$ for

$$\lambda \leq \frac{G_p}{2}\left\{\left(\tilde{\gamma}_1 + e^{-c}\right)^{\frac{p}{2}} + \left(\tilde{\gamma}_2 + e^{-d}\right)^{\frac{p}{2}}\right\} \quad \text{(A.5)}$$

In this range, the argument of $\mathcal{H}[\cdot]$ in Eq. (A.4) is > 0 for any $z < c$ or $w < d$. Hence, we get $\bar{P}_{D,plc}$ as

$$\bar{P}_{D,plc} = C_1 \int_{-c}^{c} \int_{-d}^{d} (1)\, dwdz = 1 \quad \text{(A.6)}$$

The next range of λ is considered as

$$\lambda \geq \frac{G_p}{2}\left\{(\tilde{\gamma}_1 + e^{c})^{\frac{p}{2}} + \left(\tilde{\gamma}_2 + e^{d}\right)^{\frac{p}{2}}\right\} \quad \text{(A.7)}$$

In this range, the argument of $\mathcal{H}[\cdot]$ in Eq. (A.4) is < 0 for $z > -c$ or $w > -d$. Hence, we get $\bar{P}_{D,plc}$ as

$$\bar{P}_{D,plc} = C_1 \int_{-c}^{c} \int_{-d}^{d} (0)\, dwdz = 0. \quad \text{(A.8)}$$

Finally, we consider the range of λ as

$$\frac{G_p}{2}\left\{\left(\tilde{\gamma}_1 + e^{-c}\right)^{\frac{p}{2}} + \left(\tilde{\gamma}_2 + e^{-d}\right)^{\frac{p}{2}}\right\} < \lambda < \frac{G_p}{2}\left\{(\tilde{\gamma}_1 + e^{c})^{\frac{p}{2}} + \left(\tilde{\gamma}_2 + e^{d}\right)^{\frac{p}{2}}\right\} \quad \text{(A.9)}$$

Here, we can find the integration range of w in terms of z for which the argument

of $\mathcal{H}[\cdot]$ is > 0. After some mathematical simplifications, we get this condition as

$$w < -\ln\left[\left\{A - \left(e^{-z} + \tilde{\gamma}_1\right)^{\frac{p}{2}}\right\}^{\frac{2}{p}} - \tilde{\gamma}_2\right], \tag{A.10}$$

where $A = 2\lambda/G_p$. This will be the upper limit of w for which $\mathcal{H}(\cdot)$ in Eq. (A.4) becomes 1. Note that, we need to make sure that the upper limit does not go beyond d and below $-d$. Hence, the upper limit for w can be written as

$$U_1 = \max\left[\min\left\{d, -\ln\left[\left\{A - \left(e^{-z} + \tilde{\gamma}_1\right)^{\frac{p}{2}}\right\}^{\frac{2}{p}} - \tilde{\gamma}_2\right]\right\}, -d\right] \tag{A.11}$$

Using this, we can write $\bar{P}_{D,plc}$ as

$$\bar{P}_{D,plc} = C_1 \int_{-c}^{c}\int_{-d}^{U_1} (1)\, dw dz = C_1 \underbrace{\int_{-c}^{c} U_1 dz}_{I_1} + 2cd. \tag{A.12}$$

The integration limit of I_1 in Eq. (A.12) can be split into two parts as

$$I_1 = \underbrace{\int_{-c}^{U_2} (d)\, dz}_{I_{11}} + \underbrace{\int_{U_2}^{c} \max\left[R_2(-z), -d\right] dz}_{I_{12}} \tag{A.13}$$

where $R_2(z) = -\ln\left(\left(A - (e^x + \tilde{\gamma}_2)^{\frac{p}{2}}\right)^{\frac{2}{p}} - \tilde{\gamma}_1\right)$ and $U_2 = \max\left[-c, R_2(-d)\right]$. The I_{11} in Eq. (A.13) is reduced as

$$I_{11} = dU_2 + dc \tag{A.14}$$

Now, the integration limit of I_{12} in Eq. (A.13) can again split into two parts as

$$I_{12} = \int_{U_2}^{U_3} -\ln\left[\left\{A - \left(e^{-z} + \tilde{\gamma}_1\right)^{\frac{p}{2}}\right\}^{\frac{2}{p}} - \tilde{\gamma}_2\right] dz + \int_{U_3}^{c} (-d)\, dz, \tag{A.15}$$

where U_3 is given as $U_3 = \min\left[c, R_2\left(d\right)\right]$.

It is mathematically too involved to integrate the first integral in Eq. (A.15) and hence we approximate the $\ln(x)$ term by using the approximation $\ln(x+1) \approx x$ for small x. Using this approximation, we can write I_{12} as

$$I_{12} \approx -\int_{U_2}^{U_3} \left\{ A - \left(e^{-z} + \tilde{\gamma}_1\right)^{\frac{p}{2}} \right\}^{\frac{2}{p}} dz + \int_{U_2}^{U_3} \tilde{\gamma}_2 + 1 dz + \int_{U_3}^{c} (-d)\, dz. \tag{A.16}$$

Since it is mathematically involved to integrate the first integral in Eq. (A.16), we first approximate its integrand using asymptotic analysis. Using the Taylor series expansion of a function $f(t)$, we can write [36]

$$f(z) = aaz^q + aa_1 z^{q+1} + O(z^{q+2}) \text{ as } z \to 0^+. \tag{A.17}$$

Here, aa, aa_1 and q represent real constants and $O(t^{q+2})$ is the error term as $t \to 0^+$. Using Eq. (A.17), the authors in [36] propose the approximation as

$$f(z) \approx aaz^q e^{-\alpha z}, \text{ as } z \to 0^+, \tag{A.18}$$

where $\alpha = -\frac{aa_1}{aa}$. The Taylor series expansion of integrand of first integral in Eq. (A.16) can be obtained as

$$f(z) = \left(A - (1+\tilde{\gamma}_1)^{\frac{p}{2}}\right)^{\frac{2}{p}} + (1+\tilde{\gamma}_1)^{\frac{p}{2}-1} \left(A - (1+\tilde{\gamma}_1)^{\frac{p}{2}}\right)^{\frac{2}{p}-1} z + O\left(z^2\right), \tag{A.19}$$

as $z \to 0^+$. On comparing Eq. (A.19) with Eq. (A.18) we get $aa = \left(A - (1+\tilde{\gamma}_1)^{\frac{p}{2}}\right)^{\frac{2}{p}}$, $aa_1 = (1+\tilde{\gamma}_1)^{\frac{p}{2}-1} \left(A - (1+\tilde{\gamma}_1)^{\frac{p}{2}}\right)^{\frac{2}{p}-1}$, $\alpha = \frac{-aa_1}{aa}$ and $q = 0$. Using this approximation, we can write I_{12} as

$$I_{12} \approx -\int_{U_2}^{U_3} aa\, e^{-\alpha z} dz + \int_{U_2}^{U_3} (\tilde{\gamma}_2 + 1)\, dz + \int_{U_3}^{c} (-d)\, dz, \tag{A.20}$$

After performing the integration I_{12} can be reduced as

$$I_{12} \approx \frac{aa}{\alpha}\left[e^{-\alpha U_3} - e^{-\alpha U_2}\right] + (\tilde{\gamma}_2 + 1)(U_3 - U_2) - d(c - U_3). \tag{A.21}$$

Substituting I_{11} and I_{12} from Eq. (A.14) and Eq. (A.21), respectively, into Eq. (A.13) gives us the reduced expression for I_1. Using this I_1 in Eq. (A.12), we get the reduced expression for $\bar{P}_{D,plc}$ for the final range of λ. This expression combined with Eq. (A.6) and Eq. (A.8) gives us the expression given in Eq. (4.25).

A.2 Derivation for $\bar{P}_D^{Nak}$ in Eq. (4.73)

After applying the change of variable as $w = \ln(x)$ in Eq. (4.72) and applying limit $N \to \infty$, using Eq. (A.3), the $\bar{P}_D^{Nak}$ can be written as

$$\bar{P}_D^{Nak} = \int_0^{\infty} \int_{\ln(a)}^{\ln(b)} \mathcal{H}\left(G_p\left(1 + \bar{\gamma}e^w z\right)^{\frac{p}{2}} - \lambda e^{\frac{wp}{2}}\right) \frac{5m^m z^{m-1} e^{-mz}}{L\ln(10)\,\Gamma(m)} dw dz \tag{A.22}$$

The range of w in terms of z for which argument of $\mathcal{H} > 0$ can be found as

$$w < -\ln\left[\left(\frac{\lambda}{G_p}\right)^{\frac{2}{p}} - z\bar{\gamma}\right]. \tag{A.23}$$

Using this, we can write $\bar{P}_D^{Nak}$ as

$$\bar{P}_D^{Nak} = \frac{5\, m^m}{L\ln(10)\,\Gamma(m)} \int_0^{\infty} \int_{\ln(a)}^{U4} \frac{z^{m-1}}{e^{mz}} dw dz = \frac{5}{L\ln(10)} \left[\underbrace{\int_0^{\infty} U_4 \frac{m^m z^{m-1}}{\Gamma(m) e^{mz}} dz}_{I_1} - \underbrace{\ln(a) \int_0^{\infty} \frac{m^m z^{m-1}}{\Gamma(m) e^{mz}} dz}_{I_2}\right], \tag{A.24}$$

where, U_4 is given as

$$U_4 = \max\left[\min\left[\ln(b), -\ln\left[\left(\frac{\lambda}{G_p}\right)^{\frac{2}{p}} - z\bar{\gamma}\right]\right], \ln(a)\right] \tag{A.25}$$

The integral I_1 in Eq. (A.24), can be written as

$$I_1 = \underbrace{\int_0^{U_5} \frac{\ln(a)\, m^m z^{m-1}}{\Gamma(m) e^{mz}} dz}_{I_{11}} + \underbrace{\int_{U_5}^{U_6} -\ln\left(\frac{\lambda}{G_p} - z\bar{\gamma}\right) \frac{m^m z^{m-1}}{\Gamma(m) e^{mz}} dz}_{I_{12}} + \underbrace{\int_{U_6}^{\infty} \frac{\ln(b)\, m^m z^{m-1}}{\Gamma(m) e^{mz}} dz}_{I_13}, \tag{A.26}$$

where we use $R_3(z) = \left(\frac{1}{\bar{\gamma}}\left(\frac{\lambda}{G_p}\right)^{\frac{2}{p}} - \frac{1}{z\bar{\gamma}}\right)$, $U_5 = \max[0, R_3(a)]$ and $U_6 = \max[0, R_3(b)]$.

The I_{11} and I_{13} in Eq. (A.26) can be reduced as

$$I_{11} = \frac{\ln(a)}{m^m} P(m, m\, U_5) \text{ and } I_{13} = \frac{\ln(b)}{m^m} Q(m, m\, U_6), \tag{A.27}$$

where $P(a,z) = \frac{\gamma(a,z)}{\Gamma(a)}$ and $Q(a,z) = \frac{\Gamma(a,z)}{\Gamma(a)}$ are the regularized lower and upper incomplete Gamma functions.

Using the approximation $\ln(x+1) = x$ for small x, we can derive approximate I_{12} in Eq. (A.26) as

$$I_{12} \approx \left(1 - \left(\frac{\lambda}{G_p}\right)^{\frac{2}{p}}\right) [P(m, m\, U_6) - P(m, m\, U_5)] + \bar{\gamma} [P(m+1, m\, U_6) - P(m+1, m\, U_5)] \tag{A.28}$$

Substituting I_{11}, I_{12} and I_{13} from Eq. (A.27) and Eq. (A.28) Eq. (A.26) we get I_1. The I_2 in Eq. (A.24) can be reduced as $I_2 = \ln(a)$. Using I_1 and I_2 in Eq. (A.24) and carrying out few simplifications, we get $\bar{P}_D^{Nak}$ given in Eq. (4.73).

A.3 Derivation for $\bar{P}_{D,plc}^{Nak}$ in Eq. (4.77)

Using transformation of random variable as $t = \ln(x)$ and $u = \ln(y)$ in Eq. (4.76) and applying limit $N \to \infty$ we get

$$\bar{P}_{D,plc}^{Nak} = \frac{25m^{2m}}{L_1 L_2 \left(\ln(10)\right)^2} \int_0^{\infty}\int_0^{\infty}\int_{-c}^{c}\int_{-d}^{d} z^{m-1}e^{-mz}w^{m-1}e^{-mw} \mathcal{H}\left[G_p\left(\frac{\left(1+\bar{\gamma}_1 e^t z\right)^{\frac{p}{2}}}{e^{\frac{-up}{2}}} + \frac{\left(1+\bar{\gamma}_2 e^u w\right)^{\frac{p}{2}}}{e^{\frac{-tp}{2}}}\right) - \frac{2\lambda}{e^{\frac{-(t+u)p}{2}}}\right] dudtdzdw \quad \text{(A.29)}$$

Here, we can find the integration limit of u in terms of t, z and w for which the argument of $\mathcal{H}(\cdot)$ is > 0. After few mathematical simplifications, we get upper limit of u as

$$u < -\ln\left[\left(\frac{2\lambda}{G_p} - \left(\bar{\gamma}_1 z + e^{-t}\right)^{\frac{p}{2}}\right)^{\frac{2}{p}} - \bar{\gamma}_2 w\right] \quad \text{(A.30)}$$

Once again, we need to make sure that, the upper limit do not go beyond d and below $-d$. Hence, we can write the upper limit of u as

$$U7 = \max\left[\min\left[-\ln\left[\left(\frac{2\lambda}{G_p} - \left(\bar{\gamma}_1 z + e^{-t}\right)^{\frac{p}{2}}\right)^{\frac{2}{p}} - \bar{\gamma}_2 w, d\right]\right], -d\right] \quad \text{(A.31)}$$

Hence, we can write $\bar{P}_{D,plc}^{Nak}$ in Eq. (A.29) as

$$\bar{P}_{D,plc}^{Nak} = \frac{25m^{2m}}{L_1 L_2 \left(\ln(10)\right)^2} \int_0^{\infty}\int_0^{\infty}\int_{-c}^{c}\int_{-d}^{U7} z^{m-1}e^{-mz}w^{m-1}e^{-mw} dudtdzdw \quad \text{(A.32)}$$

After carrying out the integration with respect to u, we get the expression for $\bar{P}_{D,plc}^{Nak}$ given in Eq. (4.77). These are the steps for reducing the expression to three integrals from four integrals. We can continue in this fashion to derive the final expression but the final expression will be too lengthly. Hence, we keep the expression that is reduced to three integrals.

CHAPTER B

Appendix for Chapter 5

B.1 Derivation of pdf in Eq. (5.11)

The pdf of sum of two independent random variables X and Y. i.e., $Z = X + Y$, can be obtained by convolving the marginal pdfs of X and Y, which can be obtained as

$$f_Z(z) = \int_{-\infty}^{\infty} f_X(x) f_Y(z-x) dx. \tag{B.1}$$

First we derive the pdf of decision statistic under SLC diversity for $H_m = 1$. After substituting pdf from Eq. (5.11) under $H_m = 1$ into Eq. (B.1), we obtain

$$f_Z(z) = a^2 e^{-\alpha z} \int_0^z x^q (z-x)^q dx, \tag{B.2}$$

After performing the convolution, we obtain the pdf of decision statistic under SLC diversity with two diversity branches. It is given as

$$f_Z(z) = \frac{a^2 \Gamma(1+q)^2 z^{2q+1} e^{-\alpha z}}{\Gamma(2q+2)}. \tag{B.3}$$

The pdf of decision statistic under SLC diversity with three diversity branches can be obtained by convolving pdf in Eq. (B.3) with Eq. (5.11) under $H_m = 1$. Following the similar procedure of convolution as done for two diversity case,

the pdf for the case of three diversity branch can be obtained as

$$f_z(z) = \frac{a^3\Gamma(1+q)^3 z^{3q+2} e^{-\alpha z}}{\Gamma(3q+3)}. \tag{B.4}$$

Looking at the pattern in Eq. (B.3) and Eq. (B.4), we can write the pdf of decision statistic under SLC diversity with P diversity branches as

$$f_{T_m}(t) = \frac{a^P\Gamma(1+q)^P t^{Pq+P-1} e^{-\alpha t}}{\Gamma(Pq+P)}. \tag{B.5}$$

The pdf of decision statistic under $H_m = 0$ follows chi-squared distribution. If $Y = X_1 + X_2 + \cdots + X_P$, where $X_1, X_2, \cdots, X_P$ are following chi-squared distribution with N degrees of freedom then Y follows chi-squared distribution with PN degrees of freedom. Hence, the pdf of decision statistic using SLC diversity under $H_m = 0$ with P diversity branches is given as

$$f_{T_m}(t) = \chi^2_{PN} = \frac{t^{P\cdot G-1} e^{-\frac{x}{2}}}{2^{P\cdot G}\Gamma(P\cdot G)}. \tag{B.6}$$

B.2 Theoretical analysis of R-SLC for $L = 3$

Consider the case when there are three channels in the partial band, i.e., $L = 3$ with $S_d = L_d = 1$, $I_d = 0$. Based on the number of ON channels, there are four cases, i.e., all channels OFF, only one channel ON, two channels ON and all the channels ON. First, let us consider that all the channels are OFF. In this case $PS^{Nak}_{000}(\tau)$ can be obtained as

$$PS(\tau|H_1, H_2, H_3 = 0) = PS^{Nak}_{000}(\tau) = Pr\left\{T_{min} < \tau\right\}. \tag{B.7}$$

The pdf of T_{min}, i.e., $f_{T_{min}}(t)$, for this case can be obtained by using pdf under $H_m = 0$ from Eq. (5.12) in Eq. (5.16) and using $L = 3$. Once pdf of T_{min} is obtained, $PS^{Nak}_{000}(\tau)$ can be obtained by integrating $f_{T_{min}}(t)$ from 0 to τ. Since all the channels are ON, there is no chance of interference and hence the probability of interference opportunity is zero, i.e., $PI^{Nak}_{000}(\tau) = 0$.

We now consider the case when all the channels are ON. In this case $PI_{111}^{Nak}(\tau)$ can be obtained as

$$PI(\tau|H_1, H_2, H_3 = 1) = PI_{111}^{Nak}(\tau) = Pr\left\{T_{min} < \tau\right\}. \tag{B.8}$$

The $f_{T_{min}}(t)$ in this case can be obtained in a similar way corresponding to OFF case by using pdf under $H_m = 1$ from Eq. (5.12). $PS_{111}^{Nak}(\tau)$ is zero since all the channels are ON.

Next we consider the case of only one channel being ON. Assuming channels 1 and 2 as OFF and channel 3 as ON, $PS_{001}^{Nak}(\tau)$ can be obtained as

$$\begin{aligned}
&PS(\tau|H_1 = H_2 = 0, H_3 = 1) = PS_{001}^{Nak}(\tau) \\
&= Pr\left\{T_1 < (T_2, T_3), T_1 < \tau\right\} + Pr\left\{T_2 < (T_1, T_3), T_2 < \tau\right\} \\
&= \int_0^{\tau} \left[f_{T_1}(t_1) \left(\int_{t_1}^{\infty} f_{T_2}(t_2)\, dt_2 \right) \left(\int_{t_1}^{\infty} f_{T_3}(t_3)\, dt_3 \right) \right] dt_1 \\
&+ \int_0^{\tau} \left[f_{T_2}(t_2) \left(\int_{t_2}^{\infty} f_{T_1}(t_1)\, dt_1 \right) \left(\int_{t_2}^{\infty} f_{T_3}(t_3)\, dt_3 \right) \right] dt_2.
\end{aligned} \tag{B.9}$$

Since channels 1 and 2 are OFF, $f_{T_1}(t_1) = f_{T_2}(t_2) = f_T(t)$. Using this, $PS_{001}^{Nak}(\tau)$ reduces to

$$PS_{001}^{Nak}(\tau) = 2 \int_0^{\tau} f_T(t)\, \bar{F}_T(t)\, \bar{F}_{T_3}(t) dt. \tag{B.10}$$

where, $\bar{F}_T(t)$ and $\bar{F}_{T_3}(t)$ are the ccdfs for $f_T(t)$ and $f_{T_3}(t_3)$, respectively. The PI in this case can be obtained as

$$\begin{aligned}
PI(\tau|H_1,&H_2 = 0, H_3 = 1) = PI_{001}^{Nak}(\tau), \\
&= Pr\left\{T_3 < (T_1, T_2), T_3 < \tau\right\}, \\
&= \int_0^{\tau} f_{T_3}(t) \left(\bar{F}_T(t)\right)^2 dt.
\end{aligned} \tag{B.11}$$

Finally, we consider only one channel being OFF. Let us consider channel 1 as OFF

and channels 2 and 3 as ON. The PS is then obtained as

$$\begin{aligned} PS(\tau|H_1 = 0, H_2 = H_3 = 1) &= PS_{011}^{Nak}(\tau) \\ &= Pr\left\{T_1 < (T_2, T_3), T_1 < \tau\right\} \\ &= \int_0^{\tau} f_{T_1}(t)\left(\bar{F}_T(t)\right)^2 dt. \end{aligned} \tag{B.12}$$

Since channels 2 and 3 are ON, $f_{T_2}(t_2) = f_{T_3}(t_3) = f_T(t)$. Following a similar procedure, the PI in this case can be obtained as

$$PI_{011}^{Nak}(\tau) = 2\int_0^{\tau} f_T(t)\bar{F}_T(t)\bar{F}_{T_1}(t)dt. \tag{B.13}$$

Once PS and PI are known for all four cases, P_{ISO} and P_{EIO} can be obtained as

$$P_{ISO}^{Nak}(\tau) = 1 - \sum_{i=0}^{1}\sum_{j=0}^{1}\sum_{k=0}^{1}(1-p)^{L-i-j-k}p^{i+j+k}PS_{ijk}^{Nak}(\tau), \tag{B.14}$$

$$P_{EIO}^{Nak}(\tau) = \sum_{i=0}^{1}\sum_{j=0}^{1}\sum_{k=0}^{1}(1-p)^{L-i-j-k}p^{i+j+k}PI_{ijk}^{Nak}(\tau), \tag{B.15}$$

respectively.

In a similar way, the analysis can be done for any parameter setting. Note that when we consider L channels in the partial band, we need to find PS and PI considering $\binom{L}{1} + 1$ cases. For example, for $L = 4$, we need to consider five cases, i.e., all channels OFF, any one channel ON, any two channels ON, any three channels ON and all four channels ON.

List of Publications

Journal

- K. M. Captain and M. V. Joshi, "Performance Improvement in Wideband Spectrum Sensing under Fading: Use of Diversity," in IEEE Transactions on Vehicular Technology, Vol. 66, no. 9, pp. 8152-8162, Sept 2017.
- K. M. Captain and M. V. Joshi, "SNR Wall for Generalized Energy Detector in the Presence of Noise Uncertainty and Fading," submitted to Physical Communication (ELSEVIER).

International Conference Proceedings

- K. M. Captain and M. V. Joshi, "Novel Detection Algorithm for Cooperative Wideband Spectrum Sensing Using Hard Combining," submitted to IEEE Global Communications Conference (GLOBECOM-2018).
- K. M. Captain and M. V. Joshi, "Novel Detection Algorithm for Cooperative Wideband Spectrum Sensing," submitted to Mobile Computing and Networking (MobiCom-2018).
- K. M. Captain and M. V. Joshi, "SNR Wall for CSS Using GED in the Presence of Noise Uncertainty and Fading," submitted to International Conference on Signal Processing and Communications (SPCOM-2018).
- K. M. Captain and M. V. Joshi, "SNR Wall for Cooperative Spectrum Sensing Using Generalized Energy Detector," accepted at 10th International Conference on Communication Systems and Networks (COMSNETS), 2018.

- K. M. Captain and M. V. Joshi, "Square Law Selection Diversity for Wideband Spectrum Sensing under Fading," in IEEE 84th Vehicular Technology Conference (VTC-Fall), Sept 2016, pp. 1-6.

- K. M. Captain and M. V. Joshi, "Energy Detection Based Spectrum Sensing Over $\eta - \lambda - \mu$ Fading Channel," in 8th International Conference on Communication Systems and Networks (COMSNETS), 2016, pp. 1-6.

- K. M. Captain and M. V. Joshi, "Performance of Wideband Spectrum Sensing Over Fading Channel," in International Workshop on Signal Design and its Applications in Communications (IWSDA), Bangalore, India, 2015, pp. 190-194.